The immuno-inhibitory adaptor protein SLy2

A potential therapeutic target for pneumococcal infections

Dissertation

der Mathematisch-Naturwissenschaftlichen Fakultät
der Eberhard Karls Universität Tübingen
zur Erlangung des Grades eines
Doktors der Naturwissenschaften
(Dr. rer. nat.)

vorgelegt von
Fee Schmitt
aus Sindelfingen

Tübingen

2014

Tag der mündlichen Qualifikation:	3.12.2014
Dekan:	Prof. Dr. Wolfgang Rosenstiel
1. Berichterstatter:	PD Dr. Sandra Beer-Hammer
2. Berichterstatter:	Prof. Dr. Hans-Georg Rammensee

ABSTRACT

The present work describes the experimental investigation of the SH3 Lymphocyte protein 2 (SLy2) in the mammalian immune system. SLy2 is an adaptor protein which is physiologically expressed in hematopoietic tissues as well as in heart, brain and placenta. *SLy2* is located on human chromosome 21 and was reported to be amongst a particular group of genes, which were amplified in Down syndrome (DS) patients and which were proposed to contribute to DS phenotypes. Aside from congenital heart defects and mental retardation, susceptibility to infections with *Streptococcus pneumoniae* is a common immunological problem in DS patients. Notably, these infections represent the major cause of mortality in a Swedish DS cohort.

In this work, the immunological role of SLy2 was examined with the help of a tg-*SLy2* animal model, that over-expresses *SLy2* in B and T lymphocytes. The investigations unraveled a novel intracellular mechanism by which abundance of B-1 lymphocytes and their capacity to produce pneumococcal polysaccharide-specific antibodies were inhibited following *SLy2* over-expression, suggesting that *SLy2* amplification in human DS might contribute to a general susceptibility to *S. pneumoniae* infections. This hypothesis was supported by additional data from BALB/c and *SLy2*$^{-/-}$ mice. As previously reported, BALB/c mice were resistant to *S. pneumoniae* infections, and *SLy2*-deficient mice generally showed improved adaptive immunity. Here we proved that BALB/c mice share important immunological phenotypes with *SLy2*$^{-/-}$ mice, including a massive down-regulation of *SLy2* in splenic B cells and increased peritoneal B-1 cell abundance. In conclusion, the presented data strongly propose SLy2 as an immuno-inhibitory adaptor protein, which might represent a potential future therapeutic target for prevention of pneumococcal infections.

ZUSAMMENFASSUNG

Die vorliegende Arbeit beschreibt die experimentellen Untersuchungen zur Funktion des SH3 Lymphocyte protein 2 (SLy2) im Immunsystem von Maus und Mensch. SLy2 ist ein Adapterprotein, das physiologisch in hämatopoietischen Geweben, sowie im Herzen, im Gehirn und in der Plazenta exprimiert wird. *SLy2* ist auf dem humanen Chromosom 21 lokalisiert und gehört zu einer speziellen Gruppe von Genen, die bei Down Syndrom (DS) Patienten amplifiziert sind. Es wird vermutet, dass diese Gene grundlegend zum Phänotyp des Syndroms beitragen. Neben angeborenen Herzfehlern und mentaler Beeinträchtigung sind Infektionen mit *Streptococcus pneumoniae* ein weit verbreitetes immunologisches Problem bei DS Patienten. Bemerkenswerterweise stellen diese Infektionen die Haupttodesursache einer Schwedischen DS Kohorte dar.

In dieser Arbeit wurde die immunologische Rolle von SLy2 mit Hilfe eines tg-*SLy2* Mausmodells, welches *SLy2* in B und T Lymphozyten überexprimiert, untersucht. Die Forschungsarbeiten haben einen neuen intrazellulären Mechanismus aufgedeckt, über den die Anzahl von B-1 Zellen sowie ihre Fähigkeit Pneumokokken-Polysaccharid-spezifische Antikörper zu produzieren, durch eine Überexpression von *SLy2* gehemmt wird. Die Ergebnisse lassen vermuten, dass die Amplifikation von *SLy2* in DS Patienten zu einer generellen Anfälligkeit für *S. pneumoniae* Infektionen führt. Diese Hypothese wird durch zusätzliche Daten von BALB/c und *SLy2*$^{-/-}$ Mäusen unterstützt. Es ist bereits bekannt, dass BALB/c Mäuse resistent gegen *S. pneumoniae* Infektionen sind. Vor kurzem wurde auch für *SLy2*-defiziente Mäuse eine generell verbesserte adaptive Immunantwort gezeigt. Hier konnten wir zeigen, dass BALB/c Mäuse wichtige immunologische Phänotypen aufweisen, die sich mit denen von *SLy2*$^{-/-}$ Mäusen decken. Dazu gehören eine massiv verminderte Expression von *SLy2* in B Zellen aus der Milz und ein verstärktes Aufkommen von peritonealen B-1 Zellen. Zusammenfassend lässt sich sagen, dass die präsentierten Daten SLy2 als ein immunsupprimierendes Adapterprotein beschreiben, welches ein potenzielles zukünftiges Zielprotein bei der Prävention von Pneumokokken Infektionen darstellt.

CONTENTS

LIST OF TABLES

LIST OF FIGURES

ABBREVIATIONS

AD	Alzheimer's disease
AML	acute myeloid leukemia
ANOVA	analysis of variance
APC	antigen presenting cell
ASC	antibody secreting cell
BCR	B cell receptor
BSA	bovine serum albumin
CD	cluster of differentiation
cDNA	complementary DNA
CNS	central nervous system
CVID	common variable immune deficiency
CGG	chicken gamma globuline
DMEM	Dulbecco's Modified Eagle's Medium
DN	double negative
DNA	deoxyribonucleic acid
dNTP	deoxyribonucleotide triphosphate
DS	Down syndrome
EDTA	etylenediaminetetraacetic acid
ELISA	enzyme-linked immunosorbent assay
FACS	fluorescence activated cell sorting
FC	flow cytometry
FCS	fetal calf serum
fwd	forward
Gln	Glutamine
HA	hemagglutinine
HDAC1	histone deacetylase 1
hi	high
HRP	horseradish peroxidase
IB	immunoblot
Ig	immunoglobuline
IL	interleukin
int	intermediate
IP	immunoprecipitation
IPC	internal positive control
kDa	kilo Dalton
KO	*SLy2*$^{-/-}$
L	ligand
lo	low
LPS	lipopolysaccharide
MACS	magnetic activated cell sorting

MFI	mean fluorescence intensity
MHC	major histocompatibility complex
mRNA	messenger RNA
MZ	maginal zone
NES	nuclear export signal
NK	natural killer
NLS	nuclear localization signal
NRD	negative regulatory domain
OBF1	OCT2 binding factor 1
p	phospho
PBS	phosphate buffered saline
PCR	polymerase chain reaction
PCV	pneumococcal conjugate vaccine
PPV	pneumococcal polysaccharide vaccine
Pro	Proline
(p)PS	(pneumococcal) polysaccharide
R	receptor
rev	reverse
RNA	ribonucleic acid
RPMI	Roswell Park Memorial Institute
RT-PCR	real-time PCR
SA	streptavidine
SAM	sterile-alpha-motif
SAP30	Sin3A-associated protein 30
SASH1	SAM and SH3 domain containing protein 1
SD	standard deviation
SDS	sodium dodecyl sulfate
SEM	standard error of the mean
Ser	Serine
SH	src-homology
siRNA	small interfering RNA
SLy	SH3 lymphocyte protein
SNP	single nucleotide polymorphism
SPF	specific pathogen free
TAD	transactivating domain
TCR	T cell receptor
TD	T cell-dependent
TG	transgenic-SLy2
Thr	Threonine
TI	T cell-independent
TNP	trinitrophenyl
WHO	world health organization
WT	wild-type

CHAPTER 1

INTRODUCTION

1.1 The family of SLy adaptor proteins

Adaptor proteins are involved in regulatory mechanisms, thus representing one adjustable screw in cellular signaling pathways. Apart from enzymes, like phosphatases, proteases and kinases, adaptor proteins have no catalytic activity. Hence, adaptors are not able to activate or inactivate other proteins by phosphorylation, for example. However, *via* characteristic protein domains they exert protein-protein interactions, thereby stabilizing protein complexes and regulating signaling cascades in an indirect manner in their function as so-called scaffold proteins [71]. A multitude of adaptor proteins are known to particularly regulate B cell signaling through their interaction with protein tyrosine kinases and phosphatases. Such interactions are mediated by src-homology 2 (SH2) domains, that are able to recognize Tyrosine phosphorylation sites, or *via* SH3 domains, that preferably bind to Proline-rich peptide sequences [55]. The importance of scaffold proteins in immune cells was reviewed in detail by Shaw and Filbert, who reported about the critical functions of scaffolds during T cell activation, Ca^{2+}-signaling, activation of the inflammasome, Toll-like receptor (TLR) signaling, as well as formation of the immunological synapse [81].
An emerging family of adaptor proteins expressed in immune cells represents the SH3 Lymphocyte protein (SLy) family, including SLy1, SLy2 and the sterile-alpha-motif (SAM) and SH3 domain containing protein 1 (SASH1). In 2001, SLy1 was discovered as the first member of this family by Beer et al. [12]. In the same year, SLy2 (also termed HACS1, NASH1, SAMSN1) was described [18, 91], and two years later, the third member, SASH1, was published as a candidate tumor suppressor in breast cancer [103]. All members of the SLy family express an SH3 and an SAM domain. Based on the strong sequence similarity in their functional SH3 and SAM domains, SLy1, SLy2 and SASH1 were grouped into one family of adaptor proteins [18, 104]. Although it is known that SLy1 is required for adaptive immune responses in mice and is involved in marginal zone (MZ) B cell generation as well as thymocyte development [11, 75, 79], the underlying molecular mechanisms still remain enigmatic. Similarly, the specific roles for SASH1 and SLy2 in immune cells are under current investigation.

1.1.1 SH3 Lymphocyte protein 2 - SLy2

The extensive study of a protein's biochemical features, such as cellular localization, intracellular shuttling, phosphorylation status and of course its interactome, remains indispensable for understanding the mechanistic background of biological phenotypes. Murine *SLy2* is located on chromosome 16, encoding a protein composed of 364 amino acids [97]. SLy2 is composed of a bipartite nuclear localization signal (NLS) at the N-terminus and a specific phosphorylation site at Ser23 [14]. Furthermore, a nuclear export signal (NES) is predicted within the SAM domain, ranging from amino acid number 270 to 275. The SH3 and SAM domains, which are indicative of scaffolding functions, are located in the middle half and the C-terminal part of the protein [18]. The domain structure of SLy2 is schematically illustrated in *Fig. 1*.

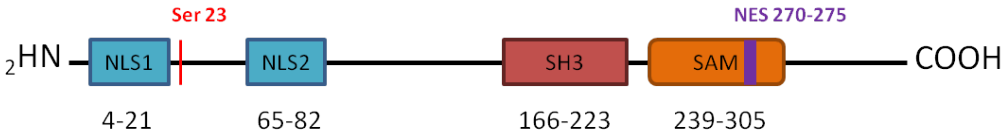

Figure 1: **Schematic illustration of the SLy2 protein.** Colored boxes represent functional domains, NLS, SH3 and SAM domain. Numbers stand for amino acids encoding the respective domains. Specific phosphorylation site Ser23 is highlighted in red. C-terminally located SAM domain incorporates a potential NES (colored in violet).

Recently, 14-3-3 proteins were demonstrated to represent important cytosolic binding partners of SLy2, which regulate its nucleo-cytoplasmic shuttling in an phosphorylation-dependent manner [14]. In the nucleus, SLy2 was shown to interact with the Sin3A-associated protein 30 (SAP30) and histone deacetylase 1 (HDAC1), forming a ternary complex that increases HDAC1 enzymatic activity [14]. The deacetylating activity of HDAC1 represents a major mechanism of epigenetic regulation of gene expression. Interestingly, the application of specific inhibitors of HDAC activity are currently investigated in therapies of human multiple myeloma as well as acute myeloid leukemia [29, 60], two hematopoietic malignancies where *SLy2* was found to be strongly expressed [18, 65].
Further investigations on SLy2 binding partners revealed Cbl-b, RN-tre, SLP-65, SLP-76, Gab-1, the intracellular domain of CD2, and cortactin to represent potential candidates [95]. Cortactin is an essential regulator of actin cytoskeleton rearrangements. Cell culture experiments indicated an SH3 domain-dependent translocation of SLy2 to F-actin structures, which are also targeted by cortactin in response to extracellular stimuli [95]. Interestingly, actin cytoskeleton rearrangements promote cell spreading and the formation of immunological synapses [7].
Together, these studies demonstrate that the biologically relevant functions of SLy2 strongly depend on its interactome, which is certainly cell type-specific and regulated by particular intrinsic signaling cascades.

SLy2 expression in humans

To get an idea of a protein's place of activity and to identify cell types in which the protein of interest may exert its biological functions, expression pattern analyses might be helpful. Human SLy2, which is conserved to its murine counterpart, was reported to be highly expressed in myeloma, acute myeloid leukemia, lymphoma, normal bone marrow, lymph nodes, spleen, and thymus, whereas lower levels were additionally found in the heart, brain, placenta, and the lung [18]. Due to its preferred expression in lymphoid tissues, SLy2 is proposed to have important immunological functions *in vivo*. In humans, *SLy2* is located on chromosome 21q11.2 and was found to be amongst a very particular group of amplified genes in lymphoblastoid cells derived from Down syndrome (DS) patients [3]. Immunological diseases are a major problem in DS patients, although congenital heart defects as well as mental retardation represent the most public ones. This is noteworthy as to the fact that *SLy2* is expressed in immune tissues as well as in heart and brain.

The role of SLy2 in the immune system

The expression of *SLy2* in activated immune cells was recently examined by RT-PCR analyses of stimulated human peripheral blood B cells and murine splenic B cells [104]. It was demonstrated, and confirmed by Western blotting, that SLy2 was up-regulated following IL-4 stimulation, and this effect was synergistically enhanced by co-stimulation with CD40L [104]. The authors concluded a role for SLy2 in B cell differentiation processes. Phenotype analyses of *Hacs1*$^{-/-}$ mice revealed an enhanced adaptive immunity in mice missing *SLy2*, predicting it to be an immuno-inhibitory adaptor protein [97]. In particular, *Hacs1*$^{-/-}$ mice showed increased humoral immune responses to Ficoll antigens, and increased B cell proliferation following B cell receptor (BCR) stimulation, as well as increased humoral T cell responses. Interestingly, cell population shifts were exclusively observed for peritoneal B-1a cells, which were more abundant in *Hacs1*$^{-/-}$ mice, whereas other hematopoietic subpopulations remained unchanged [97]. Similarly, a first phenotype analysis of tg-*SLy2* (TG) mice revealed that thymocyte development, peripheral T cell numbers, immature and mature B cells, MZ and germinal center B cells as well as plasma cells were unaltered following *SLy2* over-expression [95]. However, purified splenic B cells from TG mice showed reduced spreading on antigen-coated surfaces, emphasizing the role of SLy2 in actin cytoskeleton rearrangements through the interaction with the lymphocytic cortactin homolog HS1 [95]. Together, these studies proposed SLy2 to act as an inhibitor of adaptive immunity and hypothesized the association of SLy2 and the cortactin homolog HS1 to be one of the mechanisms behind the immuno-suppressive function of SLy2 *in vivo* [95, 97].
Although these studies revealed important immunologic functions for SLy2, a detailed cell type-specific mechanism, leading to the reported phenotypes of SLy2 mouse models, was so far not identified. Especially with regard to the fact that *SLy2* was over-expressed in DS

patients and predicted to contribute to specific DS phenotypes [3], the present work aimed to elucidate such a phenotype-genotype relation with the help of TG mice, over-expressing *SLy2* in lymphocytes. In the following sections, the immunological basics for the present study will be introduced systematically.

1.2 Humoral immune responses

Humoral components of the immune system include all non-cellular substances, such as complement factors, cytokines, and immunoglobulines (Igs). The entity of secreted Igs constitute a specific effector of the humoral immune system. Dependent on the antigen stimulus, Igs are produced and released from so-called antibody-secreting cells (ASCs) in order to rapidly neutralize incoming pathogens.

1.2.1 Classification of antigens

Antigens are classified into distinct types, due to their ability to induce different arms of immune responses. Two main classes of antigens can be distinguished, representing on the one hand T cell-independent (TI) antigens, and on the other hand T cell-dependent (TD) antigens. TI antigens are able to stimulate Ig production without the help of MHC class II-restricted T cells [61]. In contrast, TD antigens associate with MHC molecules on antigen-presenting cells (APCs) in order to activate T cells. As such, T cell activation is a prerequisite for the generation of a proper immune response to these types of antigens.

T cell-independent antigens

According to the mechanism a B cell is activated, two categories of TI antigens are discriminated. TI-1 antigens are B cell mitogens, that activate B cells independently of the BCR. The prototypic TI-1 antigen represents lipopolysaccharide (LPS), which activates B cells *via* TLR4.
Another route of B cell activation is induced by large polysaccharides (PS) derived from encapsulated bacteria, such as *Streptococcus pneumoniae* (*S. pneumoniae*). These PS are able to cross-link BCRs, which induces BCR signaling cascades. Such antigens are classically categorized as TI-2 antigens. In experimental medicine, the synthetic PS Ficoll is widely-used to study TI-2 antigen responses in model animals. TI-2 antigens mainly activate MZ B cells and B-1 cells, whereas TI-1 antigens recruit all subsets of naive and memory B cells [70]. *Fig. 2* depicts the activation of B cells through BCR cross-linking by large PS, leading to a differentiation to ASCs.

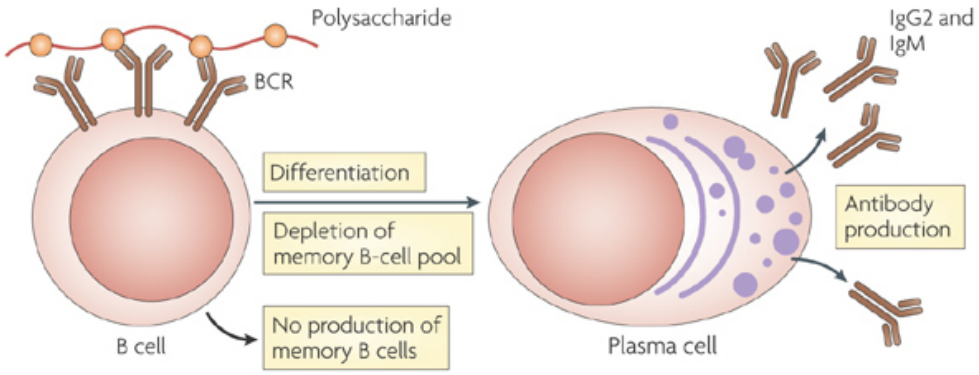

***Figure 2:* B cell receptor cross-linking by polysaccharides.** PS such as Ficoll or those derived from *S. pneumoniae* cause BCR cross-linking. This is followed by a rapid activation of B cells and leads to the differentiation to ASCs, such as plasma cells, which produce antibodies that target the PS antigen (adapted from [73]).

Taken together, the characteristic feature of TI antigens is their capacity to activate B cells without being presented by MHC molecules to the respective T cells, thus enabling a very rapid elimination of pathogens. However, TI responses basically don't induce the generation of memory B cells [61], and hence, omit the development of long-lasting immunity against specific pathogens.

T cell-dependent antigens

Another group of antigens, which is composed of proteins or small peptides, contribute to an activation of B cells with the help of T cells, and thus, are referred to as TD antigens. These antigens are presented to activated T cells *via* MHC molecules. Activated cognate B and T cells then meet at the interface between B and T cell areas in the spleen, and elicit a very specific and productive immune response [70]. In the present study, chicken gamma globuline (CGG) was selected to examine TD responses in mice. A great advantage of TD immune responses is the generation of highly-effective immune responses and the generation of memory B cells. Altogether, this type of immune reaction is comparatively slow, however long-lasting and more sustainable than TI responses.

Antigens derived from *Streptococcus pneumoniae*

A closer view to the individual antigens derived from *S. pneumoniae* indicates that infections always induce TI as well as TD responses. The encapsulated bacteria *S. pneumoniae* include a multitude of different antigens, which are recognized by immune cells and antagonized by humoral and cellular effectors. Protein antigens that elicit TD responses represent pneumolysine, pneumococcal surface proteins, and pneumococcal surface antigen for example [100]. Nevertheless, the most virulent antigens from *S. pneumoniae* are the capsular

pneumococcal polysaccharides (pPS), which are serotype-dependent antigens that elicit TI immune responses. Classically, pPS represent TI-2 antigens that activate B cells *via* BCR cross-linking. Yet, recent studies provided evidence that cross-linking *per se* was not sufficient to achieve an immune response at the highest level in mice [48]. It was shown that secondary signals from IL-4 and CD40L were additionally required for effective pPS-specific antibody production [47]. This finding clearly distinguishes pPS from the synthetic PS Ficoll, where CD40L signals did not improve the immune response [46]. Furthermore, this points out that Ficoll-based approaches are not inevitably sufficient to draw a general conclusion on TI-2 antigen responses in animal models.

1.2.2 Immunoglobuline production upon antigen encounter

Antigen-specific antibodies represent indispensable humoral effectors, which are released from ASCs, such as plasma cells. B lymphocytes are able to differentiate to plasma cells upon antigen-induced activation. The subclasses of antibodies released from ASCs strongly depend on the antigenic stimulus. In mice, IgG3 is the predominant subclass produced upon TI-1 and TI-2 antigen contact, whereas TD antigens induce a IgG1 dominant response [85]. Aside from the IgG isotypes, IgM antibodies are generally produced first following antigen encounter. Moreover, pre-existing IgM, which is measurable in the serum without any previous exposure to exogenous pathogens, plays an essential role in the innate immune system, as it provides a rapid and broadly specific defense. The characteristic features of this so-called natural IgM are outlined in the following paragraph.

Natural immunoglobuline M

Most of the existing basal serum antibodies are of the IgM isotype. This natural IgM is part of the innate immune system and causes delay of pathogen replication in a first line defense [10], owing to its features of being polyreactive to endogenous as well as exogenous antigens. Polyreactivity is partly provided by its pentameric structure (*Fig. 3*), that enables a stable antigen interaction, despite the low binding affinity [13]. Pre-existing soluble IgM exerts protective effects for influenza virus infection as well as for infections with *S. pneumoniae* [9, 16], and was shown to protect from cardiovascular events as well as autoimmune disease [22, 56]. Notably, the majority of natural IgM is produced by B-1a cells [10, 13, 58], which assigns these cells an important protective role for viral or bacterial infections.

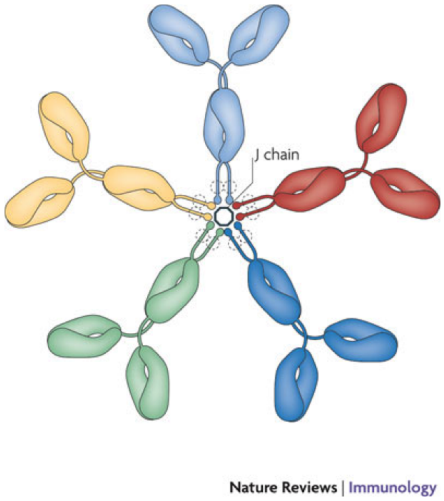

***Figure 3:* Pentameric structure of IgM.** Pentamer formation is mediated by the joining (J) chain (adapted from [26]).

1.3 B-1 cells in the innate and adaptive immune system

B-1 cells constitute a particular population amongst B lymphocytes, which was first described in 1983 as a spontaneously IgM-secreting splenic B cell population [38]. Apart from B-2 cells, which mainly include follicular B cells as well as MZ B cells, B-1 cells develop earlier in ontogeny and constitute the predominant B cell population in the pleural and peritoneal cavities [50, 37]. Moreover, these cells exert different effector functions as compared to conventional B-2 cells, which represent the most important effectors of adaptive immune responses. Although they are functionally diverse from B-2 cells, there is no distinct surface marker that allows unambiguous identification of B-1 cells. Instead, they have to be identified according to their function in addition to their surface marker expression pattern, which is $CD19^{hi}CD23^{-}CD43^{+}IgM^{hi}IgD^{var}$, and CD5 expression further segregates B-1a ($CD5^{int}$) and B-1b cells ($CD5^{-}$) [8]. Another surface molecule on B-1 cells represents the interleukin-5 receptor (IL-5R), which is also expressed by eosinophils and pre-plasmablasts [27].

1.3.1 Effector functions of B-1 cells

As indicated above, B-1 cells bear unique effector functions. Under steady state conditions bone marrow and splenic B-1 cells produce about 80 % of all natural serum IgM antibodies [10, 17]. The anti-inflammatory cytokine IL-10 is also B-1 cell-derived, which strongly argues for a tissue-protective role of B-1 cells during immune responses [69].
Following antigen-induced activation, peritoneal B-1 cells migrate to the spleen and peripheral lymph nodes, where they differentiate to specific IgM and IgA-producing plasma cells [34, 66, 101]. Moreover, B-1 cell-derived antibodies were found in the respiratory tract in response to influenza virus infection [16]. Notably, B-1a and B-1b cells have non-redundant functions and represent an essential effector population during *S. pneumoniae* infections

[35]. While B-1a cells were shown to protect from pneumococcal disease by the production of natural IgM, B-1b cells importantly contribute to an adequate specific antibody-response against capsular pPS.

1.3.2 B-1 cell development and self-replenishment

The question how B-1 cell abundance is regulated *in vivo* is still not fully clarified. Yet, two important mechanisms ensure the maintenance of B-1 cell pools, which include on the one hand *de novo* generation of B-1 cells from specific precursors, as shown in neonate as well as in adult mice [25, 30, 36, 39, 62], and on the other hand B-1 cell self-replenishment, representing a unique feature of this population [63, 86].

De novo generation of B-1 cells

B-2 cells are continuously re-generated from hematopoietic progenitors in the bone marrow, and recruited to secondary lymphoid organs. This is an accomplished and universally accepted basic concept in immunology. For B-1 cells, however, this mechanism only inadequately explains their abundance *in vivo*. A specific bone marrow progenitor was first described in 2006, and since, B-1 cells were thought to be mainly produced during fetal life [62]. The presence of a specific B-1 cell progenitor was supported in 2011, when Ghosn and colleagues found the latter in the adult mouse spleen [30]. Nevertheless, it is still a matter of discussion whether B-1 cells are generated from a single specific progenitor, or from a common B cell progenitor, that gives rise to either B-2 or B-1 cells, dependent on the environmental conditions. These two hypotheses are referred to as the 'lineage hypothesis' and the 'induced differentiation hypothesis', as extensively reviewed by Dorshkind and Montecino-Rodriguez [25].
Apart from the maturation of newly-generated B-1 cells, self-replenishment still represents a distinctive feature of mature peripheral B-1 cells [39]. This self-replenishment depends on the expression of specific B-1 cell-intrinsic factors that drive or impede cell proliferation. Amongst these, the cell-cycle regulator cyclinD2 represents a critical inducer of B-1 cell renewal [86], whereas siglecG was shown to be involved in the down-regulation of B-1 cell survival through inhibition of BCR-induced Ca^{2+} influx into B-1 cells [41]. Moreover, the cyclin-dependent kinase inhibitor p18 was reported to limit the size of the B-1a cell compartment in a dose-dependent manner [74]. Hence, these B-1 cell-intrinsic proteins are critically involved in B-1 cell homeostasis and might contribute to alterations in the size of B-1 cell pools.

IL-5Rα-dependent B-1 cell proliferation and differentiation

Another very important B-1 cell-specific regulator of cell proliferation and differentiation represents the IL-5Rα, which is constitutively expressed on B-1 cells and eosinophils, and a minority of 2-4 % of conventional splenic B cells [40, 90]. With the help of *IL-5*$^{-/-}$ mice and *IL-5R*$\alpha^{-/-}$ mice, the importance of the IL-5R for regulating B-1 cell numbers *in vivo* was unequivocally demonstrated [53, 102]. Moreover, the administration of a monoclonal antibody against IL-5, proved evidence for the involvement of IL-5 in homeostatic proliferation and survival of mature B-1 cells, and similarly *IL-5R*$\alpha^{-/-}$ mice showed impaired B-1 cell survival and proliferation [63]. Interestingly, the predominant expression of the IL-5Rα on eosinophils and B-1 cells was pointed out in *IL-5*$^{-/-}$ mice following oxazolone-induced contact sensitivity [44]. These mice exhibited no eosinophilic infiltration in the skin and produced no B-1 cell-derived oxazolone-specific IgM. In addition to its non-redundant role in IL-5-induced B-1 cell proliferation, IL-5Rα expression was reported to accelerate the ASC differentiation program in B cells [27]. Together, these studies prove substantial evidence, that the IL-5Rα is a master regulator of B-1 cell proliferation and differentiation. In turn, B-1 cell abundance as well as B-1 cell-specific antibody production strongly depend on IL-5Rα surface expression.

1.4 Regulation of IL-5Rα expression on B cells

A multitude of studies concern the IL-5Rα expression on murine eosinophils. Yet, the regulation of IL-5Rα on B cells, and particularly on B-1 cells, is to date comparably less well examined. Basically, the IL-5R consists of an α- and a β-chain. IL-4 was shown to induce the expression of the functionally important α-chain, whereas β-chain expression was promoted by cross-linking signals [98]. As to the fact that CD40L stimulation enhanced interleukin-4 receptor (IL-4R) expression and signaling in B cells [84], co-stimulation of IL-4 and CD40L synergistically enhanced IL-5Rα expression in murine B cells [27]. Thus, these two B cell mitogens efficiently contribute to the responsiveness of B lymphocytes to IL-5, whereas other mitogens were shown to be ineffective [4, 43], concluding that IL-5-induced enhancement of IgM production strongly depends on the B cell stimulus [43].

1.4.1 Transcriptional regulation of *IL-5R*α expression

An important B cell-specific transcription factor represents OCT2, which was recently shown to regulate *IL-5R*α expression in B cells, leading to B cell differentiation to ASCs [27]. OCT2 was previously reported to be required for serum Ig levels in naive mice as well as in animals immunized with TI antigens [19]. Furthermore, in mice reconstituted with *OCT2*$^{-/-}$ B cells, the abundance of B-1 cells was significantly reduced, pointing to the significance of OCT2 for B-1 cell maintenance [42].

OCT2 transactivating modifications and co-factors

The OCT2 protein is composed of an N-terminal Gln-rich region and a C-terminal Pro-, Ser-, and Thr-rich region, which were both shown to be required for optimal OCT2 activation, particularly through Ser-phosphorylation [88]. In addition, an N-terminal negative regulatory domain (NRD) was found in the OCT2.3 isoform, and differential phosphorylation was demonstrated to regulate OCT2 transcriptional activity in B lymphocytes [6]. Nevertheless, the unique indispensable features of the transcription factor OCT2 were reported to depend on its transactivation domain (TAD), C-terminally located to the protein's DNA binding domain (POU-domain) [20]. The domain organization of the transcription factor OCT2 is schematically represented in *Fig. 4*.

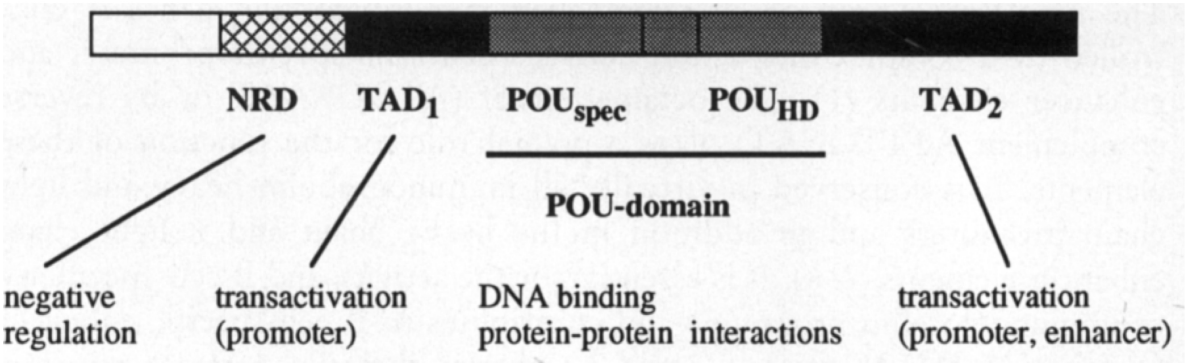

Figure 4: **Schematic OCT2 domain organization.** The N-terminal NRD was exclusively found in the OCT2.3 isoform, whereas the two TADs and the POU domain were commonly present, except from the isoforms OCT2.4 and OCT2.5 (adapted from [99]).

Aside from the transactivation of the transcription factor OCT2 by phosphorylation of functional protein domains, the protein-protein interaction of OCT2 with the B cell-specific co-factor OBF1 was reported to represent a molecular principle of OCT2 activation in B lymphocytes [99]. Together, cell-specific co-activation by OBF1 as well as the direct posttranslational modification of OCT2 govern the transcriptional activity of the latter in B cells, and hence, regulate the expression of OCT2 target genes, such as the *IL-5R*α.
Fig. 5 provides an illustration of how OCT2 is involved in B cell differentiation to ASC in a TD environment.

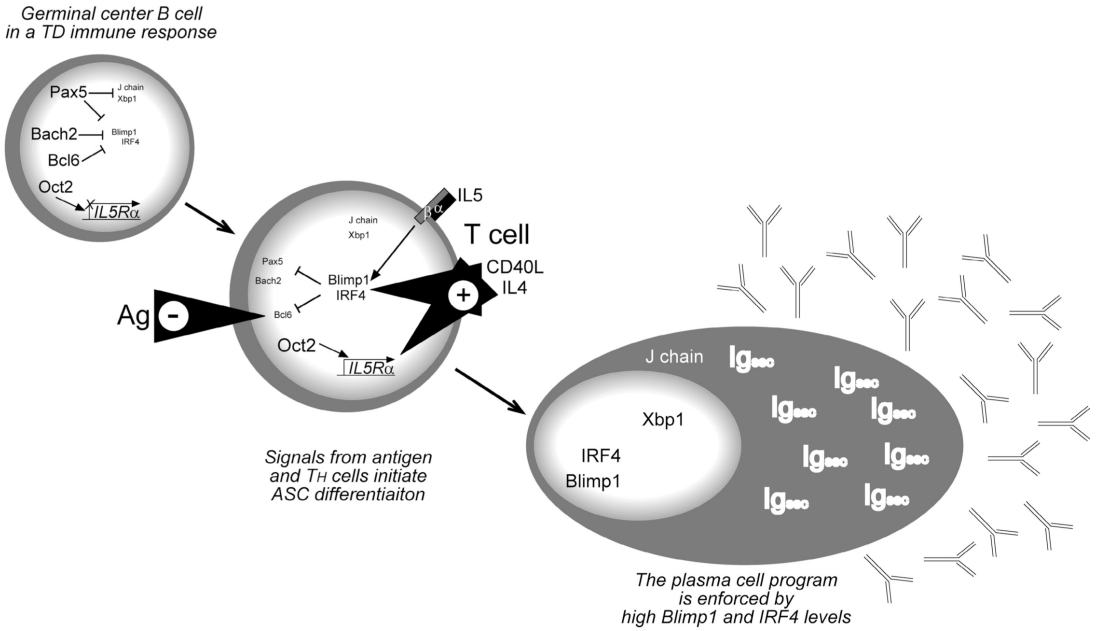

Figure 5: **Involvement of OCT2 in the regulation of ASC differentiation.** A germinal center B cell is activated by IL-4 and CD40L, which promote *IL-5Rα* expression *via* the transcription factor OCT2. Following surface expression of the IL-5Rα protein, IL-5 can induce a cell differentiation program through the expression of *Blimp1* and *IRF4*, leading to the production and secretion of antibodies (Ig_{sec}) (adapted from [27]).

1.5 Infections with *Streptococcus pneumoniae* in humans

Pneumonia represents the leading cause of death in children worldwide, according to the recently revised fact sheet, published by the world health organization (WHO). Pneumonia is caused by bacteria, viruses, or fungi, with *S. pneumoniae* being the most common cause of bacterial pneumonia. Beside malnutrition and environmental factors, pre-existing infections and a generally compromised immune system represent critical risk factors. The German Standing Vaccination Committee (STIKO) of the Robert Koch-Institute recommends pneumococcal vaccination for children under the age of 2 years in order to reduce morbidity of invasive pneumococcal disease and the resulting consequences [76]. Moreover, standard immunization with pneumococcal polysaccharide vaccines (PPV) is recommended for elderly people from the age of 60 years on. Children and young adults with pre-existing illnesses that affect the immune system, such as sickle cell anemia, HIV infections, respiratory diseases, metabolic diseases, as well as other acquired or innate immune defects are furthermore strongly recommended to be vaccinated with either a pneumococcal conjugate vaccine (PCV), or a PPV.

1.5.1 Host genetic risk factors for pneumococcal disease

Susceptibility to infections with *S. pneumoniae* strongly depends on environmental factors as well as on the health status of individuals. Yet, in the present era of genomics, more and more effort was put on studies to elucidate the genetic basis of susceptibility and resistance to infectious diseases. Although, some single nucleotide polymorphisms (SNP) were described to be associated with pneumococcal disease, no polymorphism has been shown to directly affect susceptibility in humans [15]. Alternative to human case-control studies, which are influenced by many disturbing factors, animal-based approaches were more efficient in uncovering host genetic factors that account for pneumococcal infections [49]. Comparison of different inbred mouse strains revealed that CBA/Ca mice were susceptible to *S. pneumoniae* D39, whereas BALB/c recovered from infections, and thus, were considered resistant [31, 49]. C57BL/6 mice were defined intermediate, showing a median survival time of 74 hours [31]. Genome-wide comparison of SNPs within the genome of CBA/Ca and BALB/c mice was recently performed [49], however, data on mouse strain-dependent gene expression profiles for individual cell types are lacking.

Susceptibility to *Streptococcus pneumoniae* along with Down syndrome

As mentioned above, recurrent infections are a common problem in DS patients and significantly contribute to increased morbidity and mortality. A recent study reported that infectious diseases including pneumonia represent the primary cause of death in a Swedish DS cohort [28]. Former investigations demonstrated that DS patients had significantly lower concentrations of serum IgM as compared to mentally retarded non-DS subjects [1]. Furthermore, DS patients mounted a significantly lower immune response to a 14-valent pneumococcal vaccine [67].
Aside from a general deficit of NK cells as well as T and B lymphocytes, T cell subpopulations such as helper T cells, and cytotoxic T cells, were particularly reduced in DS patients, and this was most pronounced in DS children up to 2 years of age [23]. Decreased overall lymphocyte counts may contribute to susceptibility to infectious diseases, however, cell-intrinsic defects could additionally account for immunosuppression in DS patients. This was suggested by a recent investigation, which showed that transitional and naive B cells were reduced in absolute and relative numbers in DS patients, accompanied by a disturbed humoral immune response [93]. However, to date there are no studies available that concern B lymphocyte functionality in DS patients. Especially with regard to DS, that represents a complex genetic disease, cell type-specific host genetic factors that contribute to a general susceptibility to infections, need to be investigated.

1.6 Aim of the present work

In due consideration of the significance of immunological problems in DS patients, and as to the fact that gene expression of the immuno-inhibitory adaptor *SLy2* was significantly enhanced in the latter, the present work focuses on the role of SLy2 in the mammalian immune system. In addition, given that *SLy2* was found to be expressed in acute myeloid leukemia and multiple myeloma, the investigation of the function of SLy2 in human diseases was further implicated. Therefore, the primary aim of this work was to examine the natural function of SLy2 in immune cells. For this purpose TG and KO mice were used as model organisms. TG mice, that over-express *SLy2* in T and B lymphocytes, and KO mice, that lack *SLy2* expression globally, were phenotypically analyzed by immunological and biochemical approaches. Although, previous work already described an immuno-inhibitory role for SLy2, detailed molecular mechanisms remained largely theoretical. Therefore, the present work aimed to clarify an intracellular mechanism, by which SLy2 exerts its immuno-inhibitory function *in vivo*. The identification of such a potential genotype-phenotype relation, and its validation for human beings was the desired goal of this study, in order to value the significance of *SLy2* dysregulation in human malignancies, and to spark interest in the investigation of the suitability of SLy2 as a future therapeutic target for immuno-modulatory strategies.

CHAPTER 2

MATERIALS

2.1 Laboratory equipment

Table 1: Laboratory equipment

Name	Manufacturer	Location
BD FACSCanto™II	BD Biosciences	Heidelberg, Germany
Centrifuge 5810 R	Eppendorf	Hamburg, Germany
Centrifuge 5430	Eppendorf	Hamburg, Germany
dry bath FB15103	Fisher Scientific	Schwerte, Germany
Gel Doc Device	Bio-Rad Laboratories	München, Germany
HERAcell incubator	Thermo Scientific	Schwerte, Germany
Heraeus Pico17	Thermo Scientific	Schwerte, Germany
HERAsafe clean bench	Thermo Scientific	Schwerte, Germany
LightCycler® 480 II	Roche	Mannheim, Germany
MACS Multi Stand	Miltenyi Biotec	Bergisch-Gladbach, Germany
Microscope PrimoVert	Zeiss	Oberkochen, Germany
MidiMACS™Separator	Miltenyi Biotec	Bergisch-Gladbach, Germany
MiniMACS™Separator	Miltenyi Biotec	Bergisch-Gladbach, Germany
NanoDrop Lite	Peqlab	Erlangen, Germany
peqSTAR 2X Gradient Thermocycler	Peqlab	Erlangen, Germany
QIAxcel	Qiagen	Hilden, Germany
Sunrise	Tecan	Crailsheim, Germany

2.2 Disposable materials

Disposable materials that are not listed in *Table 2*, were ordered from Sarstedt, Greiner, BD Biosciences, or Eppendorf.

Table 2: Disposable materials

Name	Manufacturer	Location
70 μm Cup Filcons	BD Biosciences	Heidelberg, Germany
96 well PCR-plate, white	Greiner	Frickenhausen, Germany
AMPLIseal™	Greiner	Frickenhausen, Germany
Cell Strainer 70 μm	BD Biosciences	Heidelberg, Germany
Costar 96 well EIA/RIA plate	Corning	Amsterdam, Netherlands
MACS® Separation Columns	Miltenyi Biotec	Bergisch-Gladbach, Germany
Micropipettes 10 μl	Brand	Wertheim, Germany
Microtainer® SST™ Tubes	BD Biosciences	Heidelberg, Germany
PCR 12er-SoftStrips	Biozym Biotech Trading	Vienna, Austria

2.3 Buffers, solutions and media

All solutions were prepared in water (Millipore quality), and pH was adjusted using NaOH or HCl.

Antibody dilution buffer
10 mM HEPES
0.5 M NaCl
1 % BSA (w/v)
0.2 % Tween20 (v/v)
0.02 % NaN_3 (w/v)

BBS (2x)
50 mM BES
280 mM NaCl
1.5 mM $Na_2HPO_4x2\,H_2O$
pH 6.95

Cell lysis buffer
50 mM Tris
150 mM NaCl
2 mM EDTA
5 % NP-40 (v/v)
Complete Mini (Protease inhibitor tablet)
PhosSTOP (Phosphatase inhibitor tablet)

ELISA blocking buffer	500 ml PBS 5 % BSA (w/v)
ELISA coating buffer	5 mM Na_2CO_3 45 mM $NaHCO_3$ pH 9.0
ELISA sample buffer	500 ml PBS 0.01 % BSA (w/v) 0.01 % $CaCl_2$ (w/v) 0.01 % $MgCl_2$ (w/v) 20 mM β-Mercaptoethanol
Erythrocyte lysis buffer	0.155 M NH_4Cl 0.01 M $KHCO_3$ 0.1 mM EDTA
HEK293T culture medium	500 ml DMEM High Glucose 10 % FCS (v/v) 5 ml Penicillin/Streptomycin (100x) 2 mM L-Glutamine
LB-agar (500 ml)	10 g LB-medium 7.5 g Agar-Agar autoclaved
LB-medium (500 ml)	10 g LB-medium autoclaved
MACS buffer	500 ml PBS 0.5 % BSA (w/v) 2.5 mM EDTA
SDS-running buffer (10x)	30.3 g Tris 144.2 g Glycin 10 g SDS 1000 ml H_2O pH 8.3-8.8
SDS-sample buffer (5x)	10 % SDS (w/v) 30 mM Tris at pH 6.8 0.1 % Bromphenolblue (w/v) 45 % Glycerin (v/v) 25 % β-Mercaptoethanol (v/v)

Separation gel buffer	0.75 M Tris 0.2 % SDS (w/v) pH 8.8
Separation gel (12 %)	9 ml Separation gel buffer 1.8 ml H_2O 7.2 ml Acrylamide 45 μl TEMED 135 μl 10 % APS
Stacking gel buffer	0.25 M Tris 0.2 % SDS (w/v) pH 6.8
Stacking gel (6 %)	4.5 ml Stacking gel buffer 3 ml H_2O 1.5 ml Acrylamide 8 μl TEMED 90 μl 10 % APS
Stimulation medium	500 ml RPMI 10 % FCS (v/v) 2 mM L-Glutamine 0.05 mM β-Mercaptoethanol (v/v)
TBS/T	50 mM Tris 150 mM NaCl 0.1 % Tween20 (v/v)
Tissue lysis buffer	500 mM KCl 100 mM Tris at pH 8.3 0.1 mg/ml Gelatine 1 % NP-40 (v/v) 1 % Tween20 (v/v) 500 μg/ml Proteinase K
Transfer buffer	SDS-running buffer 20 % Methanol

2.4 Chemicals and biological kits

Chemicals that are not listed in *Table 3*, were ordered in pro analysis quality from Merck, Roth, Serva, or Sigma-Aldrich.

Table 3: General chemicals

Name	Manufacturer	Location
Amersham Hybond™ Membranes	GE Healthcare	München, Germany
Annexin V	BD Biosciences	Mannheim, Germany
β-Mercaptoethanol 50mM	Gibco® Life technologies	Darmstadt, Germany
Cell Wall Polysaccharides	Statens Serum Institute	Copenhagen, Denmark
Complete Mini	Roche	Mannheim, Germany
DMEM High Glucose	GE Healthcare	München, Germany
FCS	GE Healthcare	München, Germany
Imject Alum	Themo Scientific	Schwerte, Germany
L-Glutamine 200mM	GE Healthcare	München, Germany
Mouse IL-5 Recombinant Protein	eBioscience	Frankfurt, Germany
NP-BSA	Biosearch Technologies	Novato, CA, USA
Nuclease-Free Water	Qiagen	Hilden, Germany
PBS	Gibco® Life technologies	Darmstadt, Germany
Penicillin/Streptomycin	GE Healthcare	München, Germany
PhosSTOP	Roche	Mannheim, Germany
Pneumococcal Polysaccharides	Statens Serum Institute	Copenhagen, Denmark
Pneumovax®23	Sanofi Pasteur	Leimen, Germany
Protein A Sepharose™	GE Healthcare	München, Germany
Recombinant Mouse IL-4	R&D Systems	Wiesbaden, Germany
RPMI	GE Healthcare	München, Germany
SA-HRP	BD Biosciences	Mannheim, Germany
SA-PerCP-Cy™5.5	BD Biosciences	Mannheim, Germany
TNP-CGG	Biosearch Technologies	Novato, CA, USA
TNP-Ficoll	Biosearch Technologies	Novato, CA, USA
TNP-LPS	Biosearch Technologies	Novato, CA, USA
TRI®Reagent	Sigma-Aldrich	Taufkirchen, Germany

Table 4: Commercially available biological kits

Kit	Description	Manufacturer
Amersham ECL Detection Reagents	Western blot detection Kit	GE Healthcare
B-1a cell isolation Kit	B-1a cell separation	Miltenyi Biotec
Bio-Rad DC™ Protein Assay	Protein estimation	Bio-Rad
BIOTAQ™DNA polymerase	Amplification of DNA in PCR	Bioline
BD™CompBeads	Compensation particles set	BD Biosciences
CD45R (B220) MicroBeads	B cell separation	Miltenyi Biotec
CD90.2 MicroBeads	T cell separation	Miltenyi Biotec
DuoSet® Economy Pack Mouse	IL4 and IL-5 ELISA	R&D Systems
EasyBlot IgG Kit	IB of precipitated proteins	GeneTex
High-Capacity cDNA Reverse Transcription Kit	cDNA synthesis	Applied Biosystems
High Pure RNA Isolation Kit	RNA isolation	Roche
NucleoBond® Xtra Maxi	DNA preparation	Macherey-Nagel
NucleoSpin® RNA	RNA isolation	Macherey-Nagel
OneShot®TOP10 Chemically Competent *E. coli*	Transformation of DNA	Invitrogen
SuperSignal West Femto Chemiluminescence Substrate	Western blot detection Kit	Thermo Scientific
SYBR Green I Master	qPCR reaction master mix	Roche
TMB Substrate Kit	ELISA detection Kit	Thermo Scientific
Transcription Factor Buffer Set	Intracellular FACS analysis	BD Biosciences
Transcriptor High Fidelity cDNA Synthesis Kit	cDNA synthesis	Roche

2.5 Oligonucleotides

All primers, that are listed in *Table 5*, were purchased from biomers.net, Ulm, Germany.
(Tm = melting temperature; Ta = annealing temperature)

Table 5: PCR primers

Target	Length [nu]	Sequence 5'-3'	Tm [°C]	Ta [°C]
ko neokana rev	23	gagaataggaacttcggaatagg	50.00	57.00
SLy2 fwd	22	ggatctcattgtgattccgtgg	56.00	57.00
SLy2 wt rev	22	gacttggagctgtcaatgtaac	48.00	57.00
tgSLy2 fwd	27	ctgaaggagactgtggttgagtggtgg	63.00	62.00
tgSLy2 rev	29	cttccatttgtcagttccctgtcatggac	64.00	62.00
cyclinD2 fwd	20	gctgtgcatttacaccgaca	52.00	60.00
cyclinD2 rev	20	acactaccagttcccactcca	51.00	60.00
IL-5 fwd	20	acattgaccgccaaaaagag	52.00	60.00
IL-5 rev	19	atccaggaaactgcctcgtc	51.00	60.00
IL-5Rα fwd	20	ggtcccggtatgcagttcta	52.00	60.00
IL-5Rα rev	21	ggaagaccctggttagatcctt	52.00	60.00
IPC fwd	20	caaatgttgcttgtctggtg	52.00	62.00
IPC rev	20	gtcagtcgagtgcacagttt	52.00	62.00
mβ-actin fwd	20	aaggccaaccgtgaaaagat	53.00	60.00
mβ-actin rev	21	gtggtacgaccagaggcatac	51.00	60.00
mSLy2 fwd	21	attgcagatccagaagacagg	51.00	60.00
mSLy2 rev	20	agaggcacggattccttttc	52.00	60.00
p18 fwd	21	aaatggatttgggagaactgc	52.00	60.00
p18 rev	22	aaattgggattagcacctctga	52.00	60.00
siglec-G fwd	21	tccgactaagagtggcctatg	51.00	60.00
siglec-G rev	22	gatgtgaaggattctcatgcaa	52.00	60.00
hβ-actin fwd	18	aaggccaaccgtgaaaagat	51.00	60.00
hβ-actin rev	20	gtggtacgaccagaggcatac	51.00	60.00
hSLy2 fwd	20	cctcttgtattcgccacaca	59.00	60.00
hSLy2 rev	20	aggaaagacacccaccttga	59.00	60.00

2.6 Antibodies

2.6.1 Purified antibodies

Table 6: Purified antibodies

Antigen	Manufacturer	Species	Clone
AKT	Cell Signaling	rabbit	C67E7
CD3	BD Biosciences	hamster	145-2C11
CD16/CD32	BioLegend	rat	93
CD40	BD Biosciences	hamster	HM40-3
ERK1/2	Cell Signaling	rabbit	137F5
HA-Tag	Cell Signaling	rabbit	C29F4
IgM	BD Biosciences	rat	R6-6O.2
IκBα	Cell Signaling	mouse	L35A5
Myc-Tag	Cell Signaling	rabbit	71D10
OCT2	Novus Biologicals	rabbit	polyclonal
pAKT	Cell Signaling	rabbit	D9E
pERK1/2	Cell Signaling	rabbit	D13.14.4E
pIκBα	Cell Signaling	mouse	5A5
pSer	Abcam	mouse	PSR-45

2.6.2 Conjugated antibodies

Table 7: Conjugated antibodies

Antigen	Manufacturer	Species	Application
CD4-Biotin	BD Biosciences	rat	FC
CD8a-Biotin	BD Biosciences	rat	FC
IgM-Biotin	BD Biosciences	rat	ELISA
IgG1-Biotin	BD Biosciences	rat	ELISA
IgG3-Biotin	BD Biosciences	rat	ELISA
IgG-HRP	Dianova	mouse	WB
IgG-HRP	Cell Signaling	rabbit	WB
TCR$\gamma\delta$-Biotin	BD Biosciences	hamster	FC

2.6.3 Fluorescently labeled antibodies

Table 8: Fluorescently labeled anti-mouse antibodies

Surface antigen	Fluorochrome	Species	Dilution	Manufacturer
B220	APC	rat	1:800	BD Biosciences
CD90.2	APC	rat	1:2500	BD Biosciences
BP-1 (Ly-51)	FITC	rat	1:200	BD Biosciences
CD4	FITC	rat	1:200	BD Biosciences
CD8a	FITC	rat	1:200	BD Biosciences
CD21/CD35	FITC	rat	1:200	BD Biosciences
CD125 (IL-5Rα)	FITC	rat	1:200	BD Biosciences
F4/80	FITC	rat	1:200	BioLegend
IgM	FITC	rat	1:200	BD Biosciences
Ly6G	FITC	rat	1:200	BD Biosciences
CD4	Pacific Blue	rat	1:800	BD Biosciences
CD5	Pacific Blue	rat	1:400	BD Biosciences
CD19	Pacific Blue	rat	1:600	BD Biosciences
CD44	Pacific Blue	rat	1:200	BD Biosciences
IgD	Pacific Blue	rat	1:100	BD Biosciences
CD11c	PE	rat	1:400	BD Biosciences
CD23	PE	rat	1:400	BD Biosciences
CD25	PE	rat	1:200	BD Biosciences
CD43	PE	rat	1:400	BD Biosciences
CD138	PE	rat	1:200	BD Biosciences
TCR$\gamma\delta$	PE	hamster	1:100	BD Biosciences
CD11b	PE-Cy7	rat	1:400	BD Biosciences
IgM	PE-Cy7	rat	1:200	BD Biosciences
CD5	PerCP-Cy^{TM}5.5	rat	1:100	eBioscience
CD8a	PerCP-Cy^{TM}5.5	rat	1:500	eBioscience
CD11b	PerCP-Cy^{TM}5.5	rat	1:100	eBioscience
Ly6G	PerCP-Cy^{TM}5.5	rat	1:100	eBioscience
Ter119	PerCP-Cy^{TM}5.5	rat	1:100	eBioscience

Table 9: Fluorescently labeled anti-human antibodies

Surface antigen	Fluorochrome	Species	Dilution	Manufacturer
CD19	APC	mouse	1:50	BioLegend
CD43	FITC	mouse	1:100	BioLegend
CD27	Pacific Blue	mouse	1:50	BioLegend
CD3	PE-Cy5	mouse	1:50	BioLegend
CD20	PerCP-Cy^{TM}5.5	mouse	1:50	BioLegend

2.7 Plasmid constructs

The pCG vector, expressing OCT2, was kindly provided by Prof. Winship Herr, University of Lausanne [88]. SLy2-pEF/myc/cyto constructs, expressing myc-tagged SLy2, were previously generated by Simone Brandt [14].

2.8 Animals

Gene-targeted *SLy2*$^{-/-}$ (KO) mice were recently generated from C57BL/6 mice by Max von Holleben [94]. The transgenic over-expressing mice tg-*SLy2* (TG) were generated by Miltenyi Biotec, as recently described in [95]. C57BL/6 and BALB/c mice were ordered from Charles River Laboratories.

CHAPTER 3

METHODS

3.1 Statistical analysis

Statistical evaluation was performed as indicated in the corresponding figure legends. Statistical analyses were performed with GraphPad Prism software. Graphics were generated with Corel PHOTO-PAINT, FlowJo, and GraphPad Prism softwares and figures were composed with Corel DRAW.

3.2 Human material

Peripheral venous blood was obtained from ten patients with DS (mean age: 8.4 years) and six non-DS-control subjects (mean age: 16.2 years). Serum IgM levels from DS patients were quantified during routine clinical visits. *SLy2* mRNA expression was assessed in a subgroup of six patients (mean age: 14.2 years) and six non-DS-controls (mean age: 16.2 years). This study was performed according to the recently revised Helsinki Protocol. All patients signed an informed consent form and the institutional ethical committee of the University of Tübingen approved these analyses.

3.3 Animal experiments

3.3.1 Breeding of gene targeted mice

WT, KO and TG mice were kept under specific pathogen free (SPF) conditions in open cages. Inbred offspring were backcrossed to their genetic background for at least six generations. C57BL/6 and BALB/c mice were bred by CharlesRiver Laboratories and ordered on demand.

3.3.2 Selection criteria

Mice were selected and pooled in groups according to their genotype, which was controlled by PCR. Experiments were performed with 9-14 weeks old mice. Age-matched WT animals were used as controls. All animal work was performed according to the German animal care regulations and approved by the local government (AZ 10.01.2012; PH5/11; PH6/12).

3.3.3 Preparation of lymphoid organs and sera

Mice were sacrificed by cervical dislocation after CO_2 or isoflurane-induced anesthesia and primary and secondary lymphoid organs were prepared. Peritoneal cells were obtained by peritoneal lavage using a 18 G needle and a 5 ml syringe. Spleen and thymus were carefully removed and homogenized using a 70 μm cell strainer. Spleen cells were centrifuged and resuspended in erythrocyte lysis buffer in order to get rid of erythrocytes. Lysis was carried out for 1 min at room temperature and stopped with 10 ml of ice cold PBS. Again cells were centrifuged and resuspended in an appropriate volume of PBS. All centrifugation steps were carried out at 4°C and 500 *g* for 5 min. Finally, bone marrow cells were washed out of tibia and femur using a 26 G needle and a 5 ml syringe and erythrocytes were depleted as described.
For serum preparation, mice were anesthetized by isofluran and blood was taken retro-orbitally with a 10 μl capillary. Blood was collected in Microtainer® SST™ tubes. Coagulation was awaited for 30 min at room temperature, then tubes were centrifuged at 11000 *g* for 2 min to spin down the clotted cells. Serum was carefully transferred into fresh tubes and stored at -20°C.

3.3.4 Immunization protocols

To study humoral immune responses to TI antigens, mice were immunized intraperitoneally with 100 μg TNP-Ficoll in 200 μl PBS, 50 μg TNP-LPS in 200 μl PBS, and 1 μg Pneumovax®23 in 200 μl PBS, respectively. TNP-CGG antigens were used to examine TD responses. To this end, for each animal 5 μg TNP-CGG were diluted in 100 μl PBS and precipitated with 100 μl of Imject Alum, according to the manufacturer's instructions. Sera were collected retro-orbitally before and 4, 7, 14, and 21 days after immunization.

3.4 Molecular Biology

3.4.1 Genotyping of mice

Earmarks were taken from three weeks old animals and tissue biopsies were subsequently lysed with tissue lysis buffer. Lysis was carried out for at least 1 h at 55°C. Thereafter, lysates were cleared by centrifuging for 3 min at 2500 *g*. PCR was performed with specific primers targeting the respective gene construct (*Table 5*). PCR products were subsequently separated using the QIAxcel DNA analyzer. The product identifying TG mice was detected at 578 bp, whereas WT samples showed no specific band. In addition, an internal positive control (IPC) gene was amplified to ensure that the PCR worked properly. The IPC product was detected in all samples at 220 bp.
Two PCR products from KO samples detected at 744 bp and 1015 bp identified a heterozygous genotype. The single lower band at 744 bp identified KO animals and the single upper band identified WT animals.

TG PCR run protocol

Initial denaturation: 5 min at 94°C
30 cycles: 30 sec denaturation at 94°C
40 sec primer annealing at 62°C
60 sec primer extension at 72°C
Final extension: 5 min at 72°C

Table 10: TG PCR reaction mix

Component	Volume	Final concentration
H_2O	17.8 μl	-
10x NH_4 Reaction Buffer	2.5 μl	1x
$MgCl_2$	1.0 μl	2 mM
dNTP-Mix	0.5 μl	2 mM
tgSLy2 fwd primer	0.5 μl	0.2 μM
tgSLy2 rev primer	0.5 μl	0.2 μM
IPC fwd primer	0.5 μl	0.2 μM
IPC rev primer	0.5 μl	0.2 μM
BIOTAQ^{TM} DNA polymerase	0.2 μl	1 Unit
DNA sample	1.0 μl	-

KO PCR run protocol

Initial denaturation: 5 min at 94°C
30 cycles: 30 sec denaturation at 94°C
40 sec primer annealing at 57°C
60 sec primer extension at 72°C
Final extension: 5 min at 72°C

Table 11: KO PCR reaction mix

Component	Volume	Final concentration
H_2O	18.3 μl	-
10x NH_4 Reaction Buffer	2.5 μl	1x
$MgCl_2$	1.0 μl	2 mM
dNTP-Mix	0.5 μl	2 mM
SLy2 fwd primer	0.5 μl	0.2 μM
SLy2 wt rev primer	0.5 μl	0.2 μM
ko neokana rev primer	0.5 μl	0.2 μM
BIOTAQ™ DNA polymerase	0.2 μl	1 Unit
DNA sample	1.0 μl	-

3.4.2 Quantitative real-time PCR

RNA isolation

Total cellular RNA was extracted using either an RNA purification Kit (Roche or Macherey-Nagel) for single cell suspensions and cultured cells, or TRI®Reagent and Chloroform/Isopropanol for whole tissue lysates, according to the manufacturer's instructions. Optical density at 260nm was measured to assess RNA concentration. Lambert-Beer equation was used for calculation.

cDNA synthesis

Reverse transcription of RNA was performed with the High-Capacity cDNA Reverse Transcription Kit for transcription of 0.5-2.0 μg RNA or the Transcriptor High Fidelity cDNA Synthesis Kit for the transcription of 50 ng - 0.5 μg RNA, according to the protocols provided.

qPCR

SYBR Green assays were applied for qPCR reactions. Specific primers were used for each target gene to be analyzed. For each reaction β-*actin* was used as a reference gene. An internal positive control sample was run side-by-side for each gene, and fold values were calculated for each sample. Primers were designed with the Universal ProbeLibrary Assay Design Center from Roche and qPCR data was analyzed with the LightCycler®480 software.

qPCR run protocol for SYBR Green assays

Initial denaturation: 5 min at 98°C
45 cycles: 10 sec denaturation at 98°C
10 sec primer annealing at 60°C
10 sec primer extension at 72°C
Final extension: 5 min at 72°C

Table 12: qPCR reaction mix

Component	Volume	Final concentration
H_2O	1.5 μl	-
2x SYBRMaster	5.0 μl	1x
fwd primer	0.4 μl	0.4 μM
rev primer	0.4 μl	0.4 μM
cDNA	2.5 μl	6.5 - 50 ng/μl

3.4.3 Amplification and preparation of plasmid DNA

To gain appropriate amounts of plasmid DNA for transient transfection of HEK293T cells, DNA had to be amplified with the help of competent bacteria.

Transformation of competent bacteria

OneShot®TOP10 competent *E. coli* were thawed on ice. Then, 5 μl of provided plasmid DNA was incubated with 25 μl of bacteria for 30 min on ice. Transformation was subsequently induced by 30 sec heat-shock incubation at 42°C, followed by 2 min incubation on ice. Transformed bacteria were then pre-incubated at 37°C in 200 μl SOC-medium in a bacterial shaker before they were streaked on pre-warmed LB-agar plates, containing 100 μg/ml ampicillin.

Plasmid preparation

Ampicillin-resistant single colonies were picked the other day and over-night cultures were inoculated. To this end, one single colony was added to 400 ml of LB-medium, supplemented with 100 μg/ml ampicillin to selectively culture transformed bacteria only. Bacteria were incubated at 37°C and 225 rpm over night in a bacterial shaker. Plasmid DNA was purified the next day using the NucleoBond®Xtra Maxi Kit according to the manufacturer's instructions.

3.5 Protein Biochemistry

3.5.1 HEK293T cell culture

HEK293T cells were stored in liquid nitrogen in 1 ml RPMI supplemented with 20 % FCS, and 10 % DMSO. Cells were quickly thawed on ice, washed with pre-warmed culture medium and plated on cell culture dishes for cultivation. HEK293T adherent cells were routinely split twice a week. To this end, medium was aspirated and cells were washed with fresh medium. Approximately 1x10^6 cells were resuspended in 10 ml fresh medium and plated on 10 cm dishes.

3.5.2 Transient transfection by calcium-phosphate

1x10^6 HEK293T cells were seeded in 10 ml on 10 cm dishes one day before transfection. 1 M $CaCl_2$ was diluted 1:5 in H_2O and 500 μl of dilution were prepared for each transfection. Then, 7-10 μg plasmid DNA were added and samples were mixed. Subsequently, 500 μl of 2x BBS were added in a drop-wise manner. Samples were mixed and incubated for 10 min at room temperature. Thereafter, medium of plated cells was refreshed and transfection mix was added in a drop-wise manner. Plates were rocked and incubated for 48 h, before protein lysates were prepared.

3.5.3 Lysis of primary and cultured cells

Cell lysis buffer was freshly supplemented with protease and phosphatase inhibitors. Primary murine immune cells were washed with ice cold PBS and lysed in 10 μl cell lysis buffer per 1x10^6 cells. Cultured cells were washed in PBS and were lysed in 500 μl cell lysis buffer per 10 cm dish. Lysis was carried out for 30 min on ice, then lysates were cleared by centrifuging at 13000 rpm and 4°C for 15 min. Protein lysates were stored at -20°C.

3.5.4 Protein determination and SDS sample preparation

Protein content of lysates was determined with the Bio-Rad DC™ Protein Assay Kit according to the standard protocol. Optical density was assessed with the Sunrise ELISA plate reader at 700 nm. BSA samples with a concentration ranging from 0 - 2 mg/ml were measured side-by-side for the calculation of a standard calibration curve. Protein content of lysates was adjusted to 10 - 50 μg per 20 μl, and samples were boiled with 5 μl 5x SDS-sample buffer for 10 min at 95°C.

3.5.5 Western blotting

SDS gels composed of a 6 % stacking gel and a 12 % separation gel were poured either freshly or in advance and stored at 4°C. Electrophoresis was run for 1 h at 60 V and then for an adequate period at 120 V in SDS-running buffer. Separated proteins were transferred on a Hybond™ nitrocellulose membrane by wet blotting. Transfer was carried out for 60-90 min and 100 mA per membrane at 4°C in transfer buffer. Membranes were subsequently washed in water to remove methanol residues, and then blocked for 1 h in either 5 % milkpowder in TBS/T or 5 % BSA in TBS/T. Thereafter, blocking reagent was removed by washing in TBS/T. Finally, membranes were incubated over night at 4°C with primary antibodies, diluted in antibody dilution buffer. Secondary HRP-linked antibodies were incubated the other day for 1 h at room temperature after washing the membrane three times in TBS/T. HRP reaction was induced with the ECL reagents or the SuperSignal West Femto Kit after washing again three times in TBS/T, and chemiluminescence was visualized using the Gel Doc Device. Pixel densities of bands were calculated using ImageJ software.

3.5.6 Immunoprecipitation

60 μl of Protein A Sepharose™ beads were washed three times with cell lysis buffer by inverting the tube. Beads were centrifuged at 500 *g* for 2 min in a pre-cooled centrifuge. 500 μg protein in 500 μl cell lysis buffer were used for precipitation. Protein lysates were incubated for 1 h at 4°C with specific antibodies for precipitation. Cell lysis buffer was used as negative control sample. Then, lysates were combined with prepared beads and incubated over night at 4°C. The other day, lysates and beads were loaded onto chromatography columns and supernatants were collected. Supernatants were stored at -20°C for further analyses. Beads were washed three times with cell lysis buffer and subsequently, precipitated proteins were eluted with 50 μl of 95°C pre-heated 2.5x SDS-sample buffer. Elution was repeated two additional times. Centrifuging between washing and elution steps was carried out at 500 *g* for 10 sec. Eluted proteins were finally analyzed by Western blotting. EasyBlot anti-Rabbit or anti-Mouse IgG Kit was used as a secondary reagent in order to mask the 50 kDa signal of the IgG heavy chain from the antibodies used for precipitation.

3.6 Cell Biology

3.6.1 Enzyme-linked immunosorbent assay (ELISA)

Basal IgM ELISA

Basal IgM levels were assessed in sera, supernatants of peritoneal wash outs, and splenic single cell suspensions. High binding 96-well plates were coated with 5 μg/ml purified anti-mouse IgM in coating buffer over night. The other day, the plate was washed and blocked for 1 hour with ELISA blocking buffer. Samples were diluted in ELISA sample buffer and incubated for 2 hours on coated plates. HRP reaction was induced with TMB and read out at 450 nm after detecting specifically bound mouse IgM with biotinylated anti-mouse IgM antibodies and SA-HRP conjugates.

TNP-specific immunoglobuline ELISA

TNP-specific Ig levels were assessed in sera of immunized mice. High binding 96-well plates were coated with 10 μg/ml purified NP-BSA in coating buffer over night. The other day, the plate was washed and blocked for 1 hour with ELISA blocking buffer. Samples were diluted in ELISA sample buffer and incubated for 2 hours on coated plates. HRP reaction was induced with TMB and read out at 450 nm after detecting specifically bound mouse Ig with biotinylated anti-mouse IgM, IgG3, and IgG1 antibodies and SA-HRP conjugates.

Polysaccharide-specific immunoglobuline ELISA

pPS-specific Ig levels were assessed in sera and peritoneal lavage supernatants of immunized mice. To this end, high binding 96-well plates were coated with 1 μg/ml purified pPS or 5 μg/ml Pneumovax®23 vaccine in coating buffer over night at 37°C. The other day, the plate was washed and blocked for 1 hour at 37°C with ELISA blocking buffer. Samples were diluted in ELISA sample buffer containing 10 μg/ml cell wall polysaccharides and incubated for 15 minutes at 37°C to capture cell wall-specific antibodies. Then, samples were pipetted onto coated plates and incubated for 2 hours at 37°C. HRP reaction was induced with TMB and read out at 450 nm after detecting specifically bound mouse Igs with biotinylated anti-mouse IgM, IgG3 antibodies and SA-HRP conjugates.

Cytokine ELISA

IL-4 and IL-5 cytokine ELISAs were performed with commercially available kits according to the manufacturer's instructions. To this end, T cells were stimulated as described above, and supernatants were analyzed.

3.6.2 Magnetic cell sorting (MACS)

Isolated spleen cells were homogenized and depleted of erythrocytes. Cells were labeled with CD90.2 MicroBeads to positively isolate T cells or B220 MicroBeads to positively select B cells, and separated with LS Columns according to standard protocols provided by the manufacturer. For specific isolation of peritoneal B-1a cells, peritoneal wash-outs of ten mice per genotype were pooled and B-1a cells were isolated in multiple steps using the B-1a cell Isolation Kit according to the protocol provided.

3.6.3 *Ex vivo* stimulation of primary lymphocytes

T cell receptor signaling

For Western blot analyses of TCR signaling, positively isolated splenic T cells from three mice per genotype were pooled. T cells were resuspended in 7.5 ml of ice-cold stimulation medium without FCS and three 15 ml tubes were prepared with 2.5 ml of cell suspension. Then, cells were either kept unstimulated or stimulated with 2.5 μg/ml anti-CD3 at 37°C for 5 min or for 5 h. Incubation was stopped with ice-cold PBS and cells were immediately lysed in 750 μl cell lysis buffer per sample.

T cell cytokine production and release

24-well plates were coated over night with 5 μg/ml of purified anti-CD3 in 500 μl PBS per well. Primary splenic T cells were isolated by MACS and resuspended in stimulation medium with 10 % FCS at a concentration of 4x10^6 cells per ml. 2x10^6 cells were seeded per well and incubated for 48 h at 37°C. Thereafter, cells were harvested and RNA was isolated. Supernatants were collected for cytokine ELISAs.

B cell signaling

For Western blot analyses of IL-4 and anti-CD40 signaling, positively isolated splenic B cells from three mice per genotype were pooled. B cells were resuspended in 7.5 ml of ice-cold stimulation medium without FCS and three 15 ml tubes were prepared with 2.5 ml of cell suspension. Then cells were either kept unstimulated or stimulated with 10 ng/ml IL-4 in combination with 2 μg/ml anti-CD40 at 37°C for 5 minutes or for 5 hours. Incubation was stopped with ice-cold PBS and cells were immediately lysed in 750 μl cell lysis buffer.

IL-5-induced IgM production and release from B cells

2x10^6 purified splenic B cells were stimulated in 24-well plates in a volume of 500 μl. To induce IgM production and release, cells were stimulated for 96 hours at 37°C with medium containing 10 ng/ml IL-4 plus 2 μg/ml anti-CD40 alone or in combination with 10 ng/ml IL-5. Additionally, unstimulated cells were incubated to assess FCS-mediated IgM production. After 96 hours, supernatants were collected and total IgM levels were measured by ELISA.

Stimulation of IL-5Rα expression on B-1 cells

To stimulate IL-5Rα expression on B-1 cells, peritoneal lavage cells or spleen cells were incubated for 48 hours at 37°C in stimulation medium containing 10 ng/ml IL-4 in combination with 2 μg/ml anti-CD40. To this end, half of all peritoneal cells or 2x10^6 splenocytes were stimulated in 500 μl in a 24-well plate. FACS analyses of IL-5Rα expression levels on B-1a and B-1b cells were performed before and 48 hours after stimulation, and fold values were calculated.

Stimulation of IgM production in B-1 cells

To measure intracellular IgM levels in B-1 cells, peritoneal lavage cells were incubated for 24 hours at 37°C in stimulation medium alone or in medium supplemented with 10 ng/ml IL-4 in combination with 10 ng/ml IL-5 and 2 μg/ml anti-CD40. To this end, half of all peritoneal cells were stimulated in 500 μl in a 24-well plate. FACS analyses of intracellular IgM levels in peritoneal B-1a and B-1b cells were performed 24 hours after stimulation.

3.6.4 Fluorescence activated cell sorting (FACS)

Fluorescence activated cell sorting was used as a standard method to analyze the abundance of hematopoietic cell populations and the expression levels of cell-type specific intracellular and surface proteins. All flow cytometry data were analyzed with FlowJo software.

Compensation controls

Flow cytometry using a BD FACSCanto™ II cytometer allows the simultaneous detection of fluorescence in eight different colors, also referred to as channels. Each color absorbs light within an individual range of wavelengths and accordingly emits like that. However, there is always a spill-over of emission into other channels causing false positive signals. After calibrating with single-colored samples, also referred to as compensation controls, the BD FACSDiva software automatically calculates a compensation that counterbalances false positive signals. For this purpose, BD™ CompBeads were applied according to the manufacturer's instructions.

Surface staining protocol

Following organ preparation, cells were routinely kept on ice in PBS. Per 1x10^6 cells usually 50 μl of 2x-concentrated staining master mix were prepared. Previous to fluorescent staining, 1x10^6 cells were resuspended in 50 μl of CD16/CD32 antibody dilution and incubated for 10 minutes on ice in order to block unspecific binding to FcRs. Subsequently, 2x-concentrated master mix was added and cells were stained for 15 min in the dark. Thereafter, cells were washed with 300 μl PBS and centrifuged at 4°C and 500 *g* for 5 minutes. Finally, 1x10^6 cells were resuspended in 150-200 μl PBS and flow cytometry was performed. For analysis of apoptotic cells, stained cells were washed and resuspended in 50 μl Annexin V (1:100). Then, cells were incubated for 15 minutes, before 200 μl PBS and 4 μl of propidium iodide were added in advance of cytometric analyses. *Table 13* shows the individual surface markers for lymphocyte subpopulations in the respective tissues.

Intracellular staining protocol

Cell surface antigens were stained as described above. Then, cells were fixed and permeabilized with the Transcription Factor Buffer Set according to the protocol provided. Intracellular staining of IgM was performed for 30 minutes at 4°C. Cells were thoroughly washed with the provided washing buffer, and subsequently analyzed by flow cytometry.

Table 13: Gating of cell populations

Tissue	Cell population	Gating
Human peripheral blood	Naive B cells	$CD19^+CD3^-CD20^+CD43^-CD27^-$
	'B-1' cells	$CD19^+CD3^-CD20^+CD43^+CD27^+$
	Memory B cells	$CD19^+CD3^-CD20^+CD43^-CD27^+$
	Pre-plasmablasts	$CD19^+CD3^-CD20^-CD43^+CD27^+$
Bone marrow	Pre-B cells	$CD43^{lo/-}IgM^-B220^+CD19^+$
	Late pro-B cells	$CD43^{hi}IgM^-B220^+CD19^+$
	Common lymphoid progenitor	$CD43^{hi}IgM^-B220^-CD19^-$
	Pre-pro-B cells	$CD43^{hi}IgM^-B220^+CD19^-$
	B-1 progenitors	$Lin^-CD43^-IgM^-B220^{lo}CD19^{hi}$
Peritoneal cavity	B-1a cells	$CD19^+CD43^+IgM^{hi}CD5^{int}$
	B-1b cells	$CD19^+CD43^+IgM^{hi}CD5^-$
Spleen	B cells	$B220^+$
	Mature B cells	$B220^+IgM^{hi}IgD^{lo}$
	Immature B cells	$B220^+IgM^{lo}IgD^{hi}$
	Marginal zone B cells	$B220^+CD21^+CD23^-$
	Germinal center B cells	$B220^+CD23^+PNA^+$
	Plasma cells	$CD4^-CD8^-CD21^-F4/80^-B220^+CD138^+$
	Granulocytes	$CD90^-CD19^-CD11b^+Ly6G^+$
	Monocytes	$CD90^-CD19^-CD11b^+Ly6G^-$
	Dendritic cells	$CD90^-CD19^-CD11c^+$
	Eosinophils	$CD90^-CD19^-CD11b^+SiglecF^+$
	B-1a cells	$CD19^+CD43^+IgM^{hi}CD5^{int}$
	B-1b cells	$CD19^+CD43^+IgM^{hi}CD5^-$
Thymus	DN1 cells	$CD90^+TCR\gamma\delta^-CD4^-CD8^-CD44^+CD25^-$
	DN2 cells	$CD90^+TCR\gamma\delta^-CD4^-CD8^-CD44^+CD25^+$
	DN3 cells	$CD90^+TCR\gamma\delta^-CD4^-CD8^-CD44^-CD25^-$
	DN4 cells	$CD90^+TCR\gamma\delta^-CD4^-CD8^-CD44^-CD25^+$
	Cytotoxic T cells	$CD90^+TCR\gamma\delta^-CD8^+$
	T helper cells	$CD90^+TCR\gamma\delta^-CD4^+$
	Double positive T cells	$CD90^+TCR\gamma\delta^-CD4^+CD8^+$
	Double negative T cells	$CD90^+TCR\gamma\delta^-CD4^-CD8^-$

CHAPTER 4

RESULTS

4.1 Immune inhibition by *SLy2* over-expression *in vivo*

Microarray analyses of human chromosome 21 transcripts revealed that *SLy2* was amongst a distinct group of genes, which are amplified in DS patients, and which are predicted to contribute to characteristic phenotypes of the syndrome [3]. Beside mental retardation and congenital heart defects, the immune system is severely affected in DS patients. Infections with *S. pneumoniae* are a major problem and represent the main cause of death in a Swedish DS population [28]. However, concrete genotype-phenotype correlations remain to be investigated. To get more insights into the relevance of *SLy2* over-expression in the mammalian immune system, the previously published tg-*SLy2* mouse model, where *SLy2* is over-expressed in B and T lymphocytes was analyzed in more detail [95]. The immune system of these mice was characterized on systemic, cellular and molecular levels in order to clarify the function of the adaptor protein SLy2, and its mechanism of action.

4.1.1 *SLy2* expression in peripheral blood from Down syndrome patients and tg-*SLy2* mice

To validate the microarray data which were obtained from lymphoblastoid cells derived from DS patients [3], peripheral blood samples from DS patients and age-matched controls were analyzed by RT-PCR. In parallel, *SLy2* expression was quantified in immune tissues of TG mice to confirm significant over-expression and to validate the mouse model. RT-PCR assays revealed average 4.2-fold higher *SLy2* mRNA levels in human DS patients, compared to their age-matched controls (*Fig. 6* A). The differences were statistically significant and confirmed the microarray data. Analysis of *SLy2* expression in primary immune tissues of TG mice revealed an average 23-fold over-expression in the bone marrow, and 4158-fold over-expression in the thymus compared to WT mice. In splenic B and T lymphocytes, over-expression of *SLy2* was by mean 104-fold and 649-fold, respectively (*Fig. 6* B). Together, these data were a prerequisite of the subsequent investigations, and were considered to be confirmatory and supportive of previously published findings [3, 95].

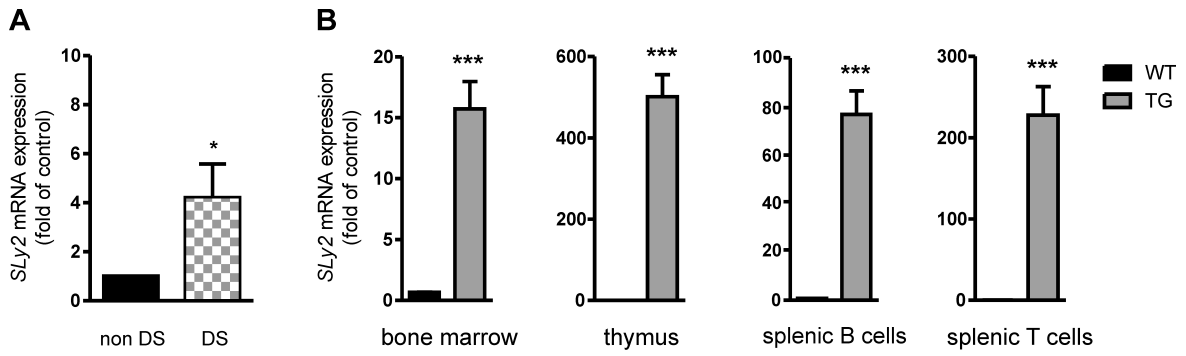

Figure 6: SLy2* mRNA expression in human peripheral blood and TG mice. (A)** RT-PCR analysis of human peripheral blood from DS patients and age-matched non-DS controls. Bars represent the means + SEM of n = 6 patients, presented as fold of non-DS control. Asterisk indicates statistical significance (* $p < 0.05$; Student's t-test). **(B)** RT-PCR analysis of bone marrow, thymus and splenic B and T cells from TG mice and WT animals. These data were analyzed together with Klaudia Buljovcic. Bars represent the means + SEM of n = 4-6 mice per genotype, presented as fold of an internal positive control. Asterisks indicate statistical significance ($p < 0.001$; Student's t-test).

4.1.2 Effect of *SLy2* over-expression on the specific humoral immune system

The humoral immune response is composed of unspecific and specific mediators. Unspecific mediators comprise complement factors, as well as cytokines and growth factors. Immunoglobulines (Igs) derived from ASCs represent specific mediators of the humoral immune system. Igs are present in the serum without any previous exposure to exogenous pathogens. These antibodies are so-called natural antibodies, which are constitutively produced from specific hematopoietic cell populations. Following invasion of exogenous pathogens, the serum Ig titers can elevate significantly. These Igs represent very specific high affinity antibodies that were produced from activated ASCs and that were able to neutralize incoming pathogens. The next presented results show the effects of *SLy2* over-expression on specific humoral immune responses following stimulation with different antigens.

Basal IgM levels in Down syndrome patients and tg-*SLy2* mice

Analysis of basal IgM titers of inpatient DS subjects was performed during routine clinical visits. Reference values for healthy individuals range from 40 - 170 mg/dl. *Fig. 7* A shows the serum IgM titers of individual DS patients, and the mean value of 34.3 mg/dl. This evaluation reveals that basal serum IgM levels in a group of inpatient DS children was lower by mean as compared to the reference values, which confirms published data [1]. In parallel,

basal serum IgM titers as well as IgM levels in peritoneal wash-outs were assessed in TG animals and WT controls. Serum IgM levels were significantly reduced by 50.5 % on average in TG mice (*Fig. 7* B, left panel). Also basal IgM concentrations in the peritoneal cavity were slightly reduced in TG mice, however, differences were statistically not significant (*Fig. 7* B, right panel). These data suggest a role for SLy2 in the regulation of basal serum IgM titers, that were maintained by innate B cells. Amongst these, B-1 cells, present in the peritoneal cavity and the spleen, produce the majority of this so called natural IgM [10].

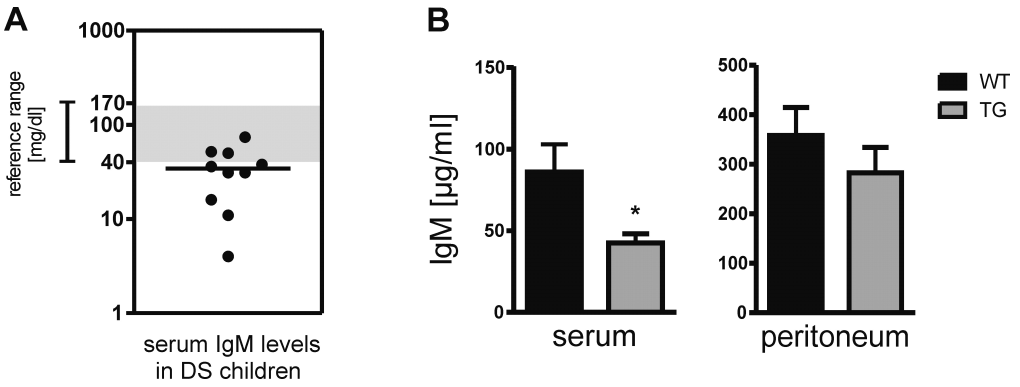

Figure 7: **Basal IgM levels in DS patients and TG mice. (A)** Serum IgM levels of inpatient DS children measured during routine clinical visits. Solid black line represents the mean of n = 10 patients. **(B)** Serum and peritoneal basal IgM levels of TG mice and WT controls, measured by ELISA. Peritoneal IgM levels were assessed in supernatants of peritoneal wash-outs in a volume of 3 ml. Bars represent the means + SEM of n = 6-7 mice per genotype. Asterisk indicates statistical significance (* $p < 0.05$; Student's t-test).

Immunoglobuline responses to T cell-dependent antigens

TD antibody production was investigated in WT and TG mice by immunization with CGG, a common TD antigen. Antigen-specific IgM and IgG1 levels were continuously assessed by ELISA before and 4, 7, 14, and 21 days following immunization. ELISA revealed that IgM production was impaired in TG mice, however, differences were statistically not significant when comparing all groups with pre-immune titers of WT mice (*Fig. 8* A, left plot). Yet, Student's t-test analyses of separate values of day 4 and 7 post-immmunization revealed significant reduction of 36 % by mean for serum IgM levels in TG mice at day 7 (*Fig. 8* A, right panel). Furthermore, IgG1 levels were assessed by ELISA and overall lower titers were found in TG mice (*Fig. 8* B, left plot). However, statistical significance was calculated exclusively for the separate values of day 21 when tested with Student's t-test. The mean difference in sera of TG mice was 56 % compared to WT controls (*Fig. 8* B, right panel). These data indicate, that SLy2 slightly inhibits TD immune responses *in vivo*, however, the effects were varying strongly amongst the individuals.

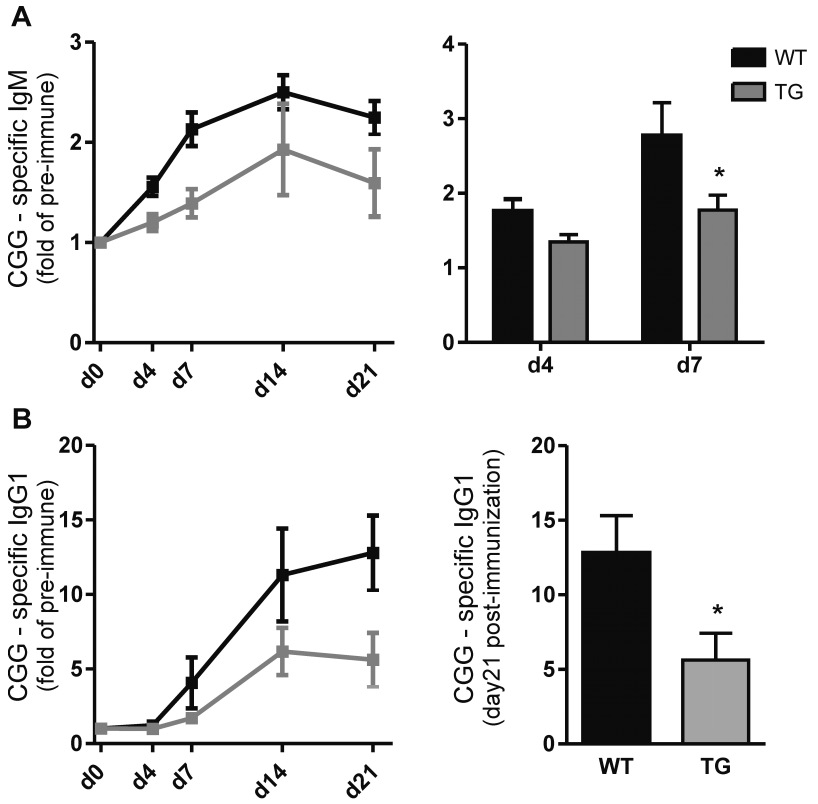

Figure 8: **T cell-dependent antibody responses in TG mice. (A)** CGG-specific serum IgM levels of WT and TG mice. Left plot depicts development of IgM titers followed over 21 days after immunization, shown as means ± SEM of n = 6-8 mice per group from two independent experiments. Statistical analysis was performed by ANOVA and Bonferroni posttests. Right plot shows the separate analysis of day 4 and day 7 values. Bars represent the means + SEM of n = 6-8 mice per genotype from two independent experiments. Asterisk indicates statistical significance (* $p < 0.05$; Student's t-test). **(B)** CGG-specific serum IgG1 levels of WT and TG mice. Left plot depicts development of IgG1 titers followed over 21 days, shown as means ± SEM of n = 6-8 mice per genotype from two independent experiments. Statistical analysis was performed by ANOVA and Bonferroni posttests. Right plot shows the separate analysis of day 21 values. Bars represent the means + SEM of n = 6-8 mice per genotype from two independent experiments. Asterisk indicates statistical significance (* $p < 0.05$; Student's t-test).

Immunoglobuline responses to T cell-independent antigens

TI antibody responses were assessed in WT and TG mice by immunization with the classical TI-1 antigen LPS, or the synthetic TI-2 antigen Ficoll. LPS induces a direct B cell activation *via* binding to TLR4, whereas the synthetic polysaccharide Ficoll activates B cells *via* BCR cross-linking. IgM and IgG3 courses, which were followed over 21 days, are shown in *Fig. 9*. LPS-specific IgM and IgG3 titers were not different between WT and TG animals (*Fig. 9* A, B). Moreover, Ficoll-specific IgM and IgG3 production were comparable in both groups (*Fig. 9* C, D). These results demonstrate that classical TI immune responses were not altered following *SLy2* over-expression *in vivo*, suggesting no direct function for the adaptor protein SLy2 in TLR4 and BCR-induced Ig production.

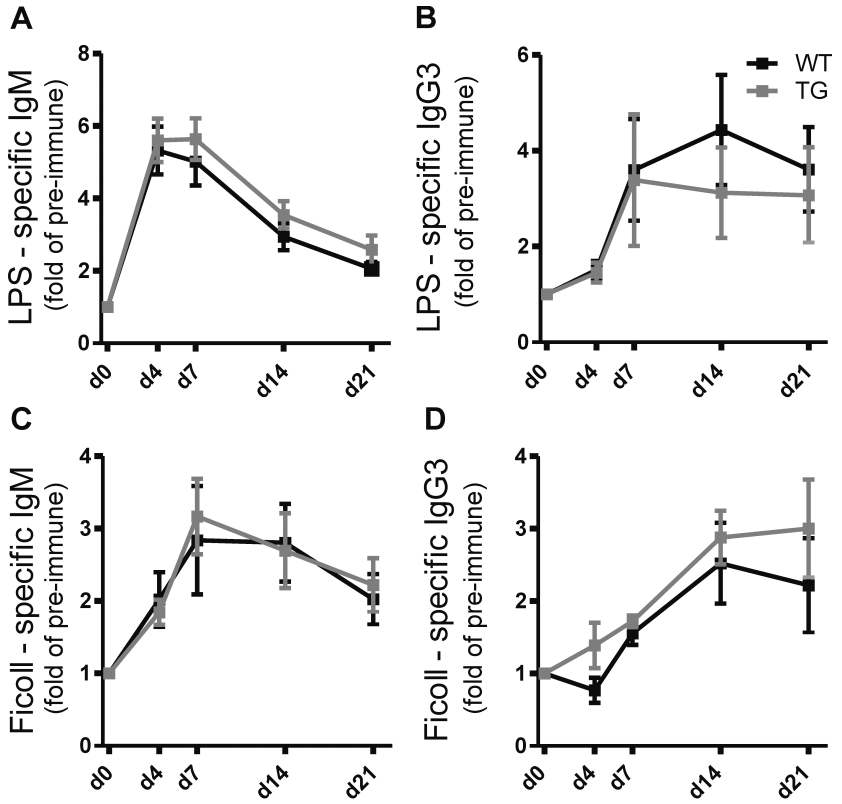

Figure 9: **T cell-independent antibody responses in TG mice.** **(A)** LPS-specific serum IgM levels of WT and TG mice, followed over 21 days after intraperitoneal immunization. Presented as means ± SEM of n = 6-8 mice per group from two independent experiments. **(B)** LPS-specific serum IgG3 levels of WT and TG mice, followed over 21 days after immunization. Presented as means ± SEM of n = 6-8 mice per group from two independent experiments. **(C)** Ficoll-specific IgM and **(D)** IgG3 courses following immunization, presented as means ± SEM of n = 6-8 mice per genotype from two independent experiments. Statistical analyses were performed by ANOVA and Bonferroni posttests.

Immunoglobuline responses to Pneumovax® vaccine

Pneumovax®23 (P23) is a 23-valent pPS vaccine, composed of pPS from 23 different serotypes of *S. pneumoniae*. Classically, pPS belong to the group of TI-2 antigens, which activate B cells *via* BCR cross-linking. However, pPS antigens are distinct to Ficoll antigens, as pPS additionally require T cell-derived IL-4 and CD40L to induce a proper antibody response [46]. Therefore, total Pneumovax®-specific IgM responses were measured in the sera of immunized WT and TG mice. TG mice exhibited severely impaired antibody-responses compared to WT animals, which were statistically significant from day 14 on (*Fig. 10* A, left plot). Separate *t*-test analysis of day 4 and day 7 values, also revealed a significant 28.6 % reduction of IgM levels at day 7 post-immunization (*Fig. 10* A, right panel). In addition to total P23-specific IgM production, courses of single pPS6B, pPS19F, and pPS4-specific IgM levels were examined (*Fig. 10* B, C). No differences between WT and TG animals were observed for pPS6B-specific IgM levels, and pPS19F-specific levels were only slightly lower in TG mice. However, pPS4-specific IgM responses were significantly reduced in TG mice, as depicted in *Fig. 10* C. According to P23-specific values, separate *t*-test analysis

of day 7, also revealed a significant 42 % reduction of pPS4-specific IgM concentrations (*Fig. 10* C, right panel). Moderate differences were also observed in peritoneal wash-outs at day 21 post-immunization, indicating that peritoneal IgM-producing cells were involved in pPS-specific antibody responses (*Fig. 10* D). IgG3 levels specific for pPS4 were comparable between WT and TG animals (*Fig. 10* E), which suggests a specific role for SLy2 in the production and release of IgM following pPS antigen contact.

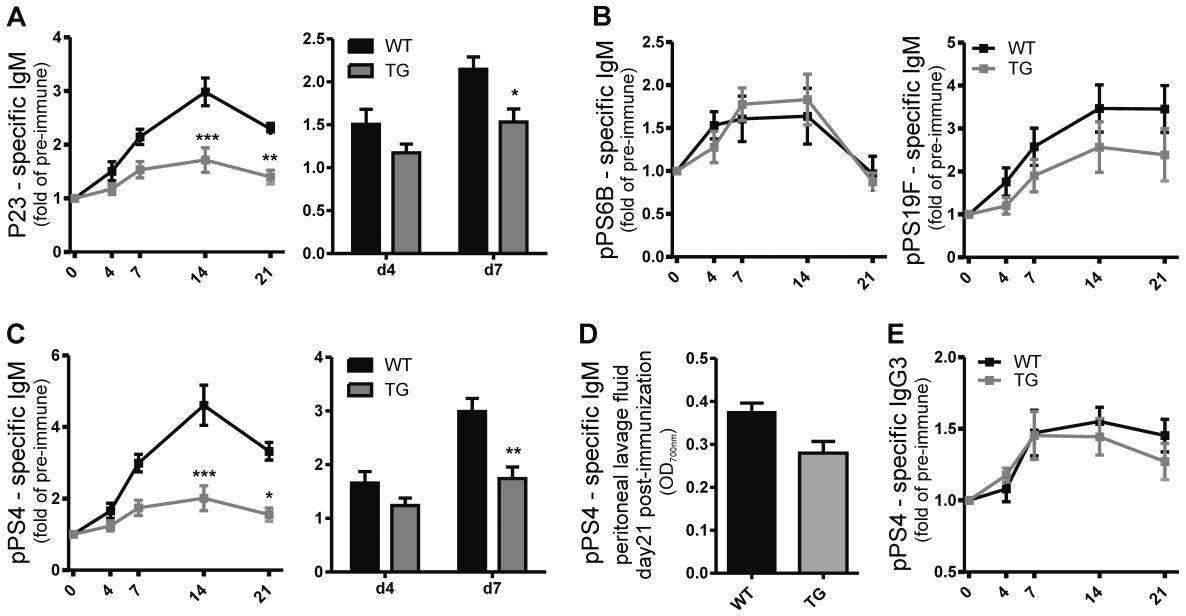

Figure 10: **Pneumovax® 23-induced immune responses in TG mice.** **(A)** Left plot: P23-specific serum IgM levels of WT and TG mice, followed over 21 days after intraperitoneal immunization. Presented as means ± SEM of *n* = 6-8 mice per group from two independent experiments. Asterisks indicate statistical significance (** $p < 0.01$; *** $p < 0.001$; ANOVA; Bonferroni posttests). Right panel: Separate analysis of day 4 and day 7 values. Bars represent means + SEM of *n* = 6-8 mice per genotype from two independent experiments. Asterisk indicates statistical significance (* $p < 0.05$; Student's *t*-test). **(B)** Serum levels of pPS6B-specific (left plot) and pPS19F-specific (right plot) IgM of WT and TG mice, followed over 21 days after intraperitoneal immunization. Presented as means ± SEM of *n* = 6-8 mice per group from two independent experiments. **(C)** Left plot: pPS4-specific serum IgM levels of WT and TG mice, followed over 21 days after intraperitoneal immunization. Presented as means ± SEM of *n* = 6-8 mice per group from two independent experiments. Asterisks indicate statistical significance (* $p < 0.05$; *** $p < 0.001$; ANOVA; Bonferroni posttests). Right panel: Separate analysis of day 4 and day 7 values. Bars represent means + SEM of *n* = 6-8 mice per genotype from two independent experiments. Asterisks indicate statistical significance (** $p < 0.01$; Student's *t*-test). **(D)** Peritoneal pPS4-specific IgM levels were assessed in supernatants of peritoneal wash-outs in a volume of 3 ml at day 21 post-immunization. Bars represent the means + SEM of *n* = 7 mice per genotype from two independent experiments. **(E)** pPS4-specific serum IgG3 levels of WT and TG mice, followed over 21 days after intraperitoneal immunization. Presented as means ± SEM of *n* = 6-8 mice per group from two independent experiments. All immunoglobulin titers were assessed by ELISA.

Altogether, investigations of specific humoral immune responses in WT and TG mice demonstrated an inhibitory function for SLy2 in pPS-specific immune responses, whereas classical TI antibody production *via* TLR4 and BCR activation remained unaffected. Moreover, TD antibody production was impaired, which might be indicative for a potential involvement of SLy2 in IL-4 and CD40L signaling, two important TD factors which essentially contribute to proper pPS-specific responses [46].

4.1.3 Influence of *SLy2* over-expression on hematopoietic cell populations

In order to clarify the reasons for the observed deficits in IgM production in TG mice, the abundance of cell populations of the hematopoietic system was analyzed by flow cytometry measurements. A variety of immune cell populations of primary and secondary immune tissues from WT and TG mice were examined. *Table 14* lists all populations that were quantified. B and T cell precursors were examined in bone marrow and thymus, representing the primary immune tissues. Mature B cell subpopulations as well as granulocytes, dendritic cells and monocytes were examined in the spleen, representing a secondary immune organ. All populations that were analyzed were comparable between WT and TG animals, concluding that *SLy2* over-expression does not influence their abundance *in vivo*.

Table 14: **Hematopoietic cell populations in WT and TG mice.** FACS analysis of selected cell populations in primary and secondary immune tissues of WT and TG mice. Values represent the means ± SD of *n* = 4-5 mice per genotype.

Tissue	Cell population	WT	TG
Thymus	DN1 cells	6.2 ± 3.0	4.7 ± 1.6
	DN2 cells	1.5 ± 0.9	1.4 ± 1.0
	DN3 cells	20.6 ± 9.4	20.4 ± 7.2
	DN4 cells	71.7 ± 11.3	72.4 ± 8.6
	Cytotoxic T cells	3.9 ± 1.2	3.6 ± 1.2
	Helper T cells	9.5 ± 1.8	8.5 ± 1.9
	Double positive T cells	83.7 ± 3.0	85.4 ± 3.2
	Double negative T cells	2.9 ± 0.3	2.6 ± 0.4
Spleen	B cells	54.3 ± 7.9	57.1 ± 6.2
	Mature B cells	18.2 ± 4.8	20.5 ± 4.0
	Immature B cells	65.5 ± 4.4	64.1 ± 4.5
	Marginal zone B cells	9.6 ± 1.5	9.2 ± 2.6
	Germinal center B cells	60.7 ± 14.4	64.5 ± 11.1
	Plasma cells	5.9 ± 2.0	5.9 ± 1.6
	Granulocytes	13.1 ± 2.9	14.6 ± 5.5
	Monocytes	18.6 ± 4.6	20.2 ± 2.9
	Dendritic cells	10.6 ± 1.8	12.7 ± 2.4
	Eosinophils	0.8 ± 0.1	0.6 ± 0.1
Bone marrow	Pre-B cells	40.3 ± 12.0	47.5 ± 5.7
	Late pro-B cells	9.8 ± 1.7	6.5 ± 2.5
	Common lymphoid progenitors	39.8 ± 12.4	36.6 ± 8.7
	Pre-pro-B cells	43.2 ± 10.4	35.8 ± 6.0
	$BP1^+$ pre-B cells	2.8 ± 1.0	1.9 ± 0.9

Peritoneal B-1 cells in tg-*SLy2* mice

Having shown that there were no shifts in hematopoietic leukocytes and conventional B-2 cell subpopulations in TG mice, we next addressed the abundance of B-1 cells. These cells were of special interest, due to their characteristic feature of being the major source of natural IgM as well as pneumococcal-specific IgM [10, 35]. Therefore, B-1 cell pools were analyzed by flow cytometry in the peritoneal cavities and the spleens of WT and TG animals (*Fig. 11* A). Peritoneal and splenic B-1 cells were defined in the fraction of singlet lymphocytes as the $CD19^{+}CD43^{+}IgM^{hi}$-expressing population. CD5-expression further separates B-1 cells into $CD5^{int}$ B-1a cells, and $CD5^{-}$ B-1b cells [51]. Analysis of flow cytometry data revealed by mean a 26 % significantly smaller proportion of B-1a cells in the peritoneal cavities of TG mice compared to WT controls (*Fig. 11* B, left panel), whereas B-1b cells remained unchanged (*Fig. 11* B, right panel). In the spleen, B-1a cells were comparable in WT and TG mice (*Fig. 11* C, left panel). B-1b cells were slightly reduced in spleens of TG animals, however, differences were statistically not significant (*Fig. 11* C, right panel). These findings indicate a function for SLy2 in down-regulating peritoneal B-1a cell abundance, which might be one possible explanation for the significantly lower basal serum IgM levels, and the impaired IgM responses to pPS vaccination.

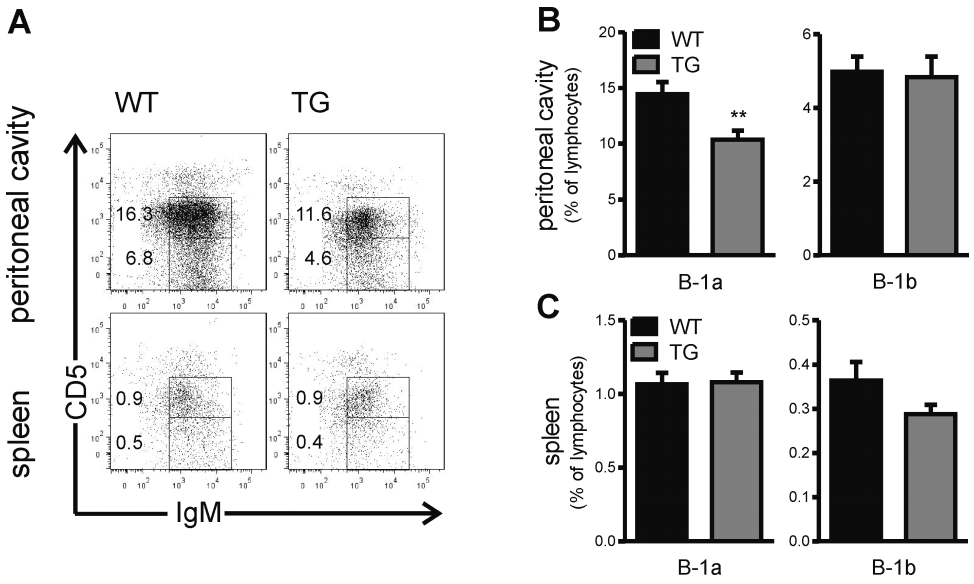

Figure 11: **B-1 cell analysis in TG mice. (A)** Flow cytometry analysis of peritoneal and splenic B-1a cells ($CD5^{int}IgM^{hi}$) and B-1b cells ($CD5^{-}IgM^{hi}$) in the fraction of $CD19^{+}CD43^{+}$ lymphocytes of one representative individual per genotype, presented as percentages of B-1 cells relative to singlet lymphocytes. **(B)** Mean percentages + SEM of peritoneal B-1a and B-1b cells relative to singlet lymphocytes of $n = 8$ mice per genotype from three independent experiments. Asterisks display statistical significance (* $p < 0.05$; ** $p < 0.01$; Student's *t*-test). **(C)** Mean percentages + SEM of splenic B-1a and B-1b cells relative to singlet lymphocytes of $n = 8$ mice per genotype from three independent experiments.

B cell populations in DS patients

Interestingly, $CD20^+CD27^+CD43^+$-expressing human B cells were claimed to represent the analogs of murine B-1 cells, and these cells appeared to be involved in constitutive IgM production as well as pPS-specific antibody responses in humans [32]. Although this cell population shares some features with murine B-1 cells, the question whether these cells are indeed the corresponding human B-1 cells still remains under debate [32, 92, 21]. A more recent publication suggested human pre-plasmablasts to be the ”better” analogs of murine B-1 cells [92]. Having shown that B-1 cells were reduced in *SLy2* over-expressing TG mice, we wondered about the abundance of the predicted B-1 cells in DS patients. To this end, we analyzed human peripheral blood samples of one DS patient and one non-DS control by flow cytometry. Selected B lymphocyte subpopulations including the two candidate B-1 cell populations were analyzed according to a recently published gating strategy [21]. Naive and $CD19^+$ B cells were clearly reduced in the DS patient, which confirms published data [93] and validates our random samples (*Fig. 12*, left panel). Analysis of B-1 cells, memory B cells, and pre-plasmablasts, however, was never examined in DS subjects before and our preliminary result demonstrated a clear reduction, compared to the age-matched non-DS subject (*Fig. 12*, right panel). This finding might be indicative for a potential involvement of SLy2 in the characteristic immunological phenotypes of DS patients.

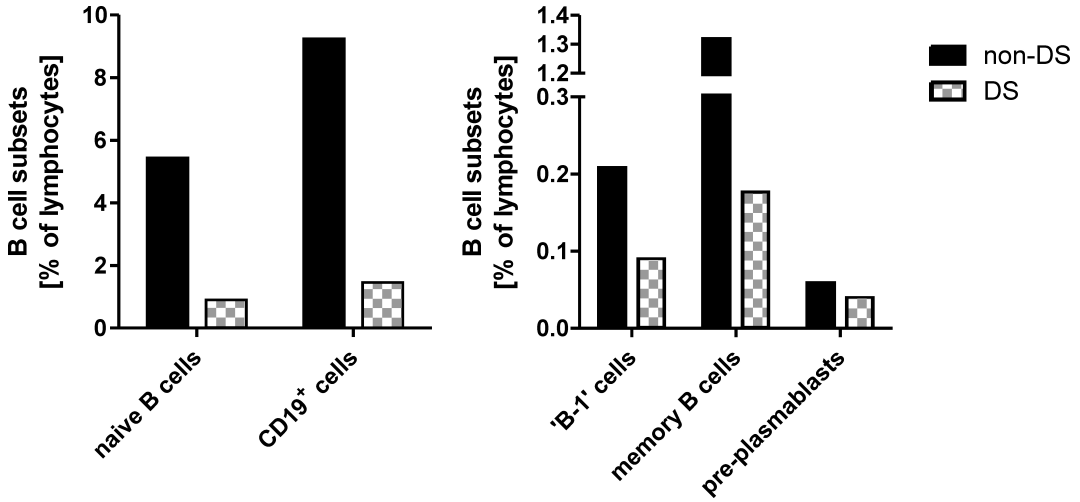

Figure 12: **B cell analysis in human peripheral blood.** Left panel: Flow cytometry analysis of naive B cells ($CD19^+CD3^-CD20^+CD43^-CD27^-$) and $CD19^+$ cells in human peripheral blood of one individual per group. Right panel: Flow cytometry analysis of B-1 cells ($CD19^+CD3^-CD20^+CD43^+CD27^+$), memory B cells ($CD19^+CD3^-CD20^+CD43^-CD27^+$), and pre-plasmablasts ($CD19^+CD3^-CD20^-CD43^+CD27^+$) in human peripheral blood of one individual per group.

4.1.4 Maturation and apoptosis of B-1 cells in *SLy2* over-expressing mice

In the TG mouse model we next addressed the reasons for the reduced peritoneal B-1a cell population. Basically, an initial pool of B-1 cells is produced in the fetal liver [62]. In adult mice the population maintains itself in the peritoneal cavity mainly by self-replenishment. Nevertheless, specific precursors in the bone marrow and spleen additionally give rise to mature B-1 cells in adult mice [30]. These precursors were defined as $IgM^{-}CD43^{-}B220^{lo}CD19^{hi}$-expressing cells within the fraction of lineage negative lymphocytes [30]. To find out whether SLy2 directly inhibits *de novo* maturation of B-1 cells from specific bone marrow progenitors, the abundance of B-1 precursors in the bone marrow was assessed by flow cytometry. The gating strategy for precursors is shown in *Fig. 13* A. Analysis of flow cytometry data revealed no significant differences when comparing WT and TG mice (*Fig. 13* B), demonstrating that SLy2 has no direct influence on *de novo* maturation of B-1 cells from specific bone marrow progenitors.

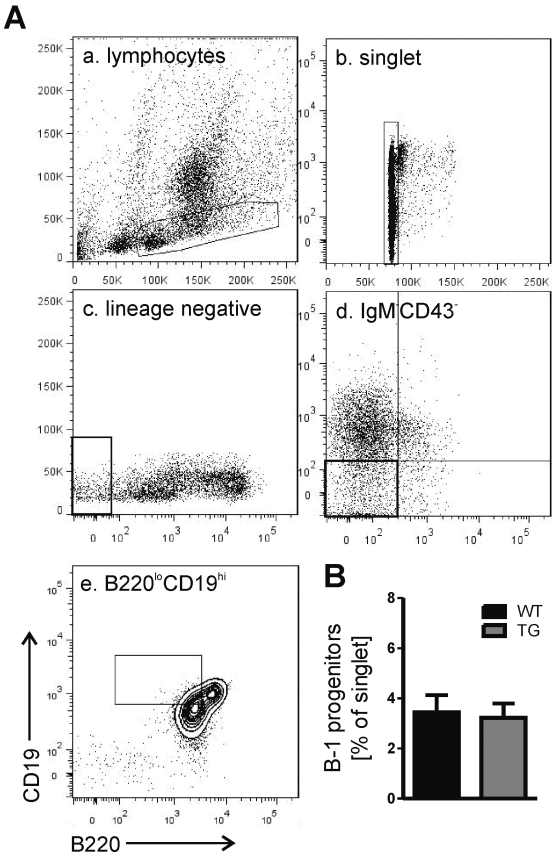

Figure 13: **B-1 cell bone marrow progenitors. (A)** Gating strategy of bone marrow progenitors depicted for one representative individual. **(B)** Analysis of bone marrow B-1 cell progenitors relative to singlet lymphocytes, presented as means + SEM of *n* = 5 mice per genotype from two independent experiments.

To exclude that SLy2 promotes apoptosis of mature B-1 cells in the peritoneal cavity, thereby contributing to reduced B-1a cell abundance *in vivo*, percentages of live, apoptotic, and necrotic B-1a cells were additionally assessed in WT and TG mice by Annexin V and propidium iodide staining. Analysis of flow cytometry data revealed no differences between the two genotypes, when calculating the relative distribution of peritoneal B-1a cells into live cells, cells in apoptosis stage I and II, and necrotic cells (*Fig. 14* A). Discrimination of different apoptosis stages by Annexin V and propidium iodide staining is demonstrated in *Fig. 14* B. The result of this flow cytometry-based experiment indicates that SLy2 is not directly involved in B-1 cell apoptosis.

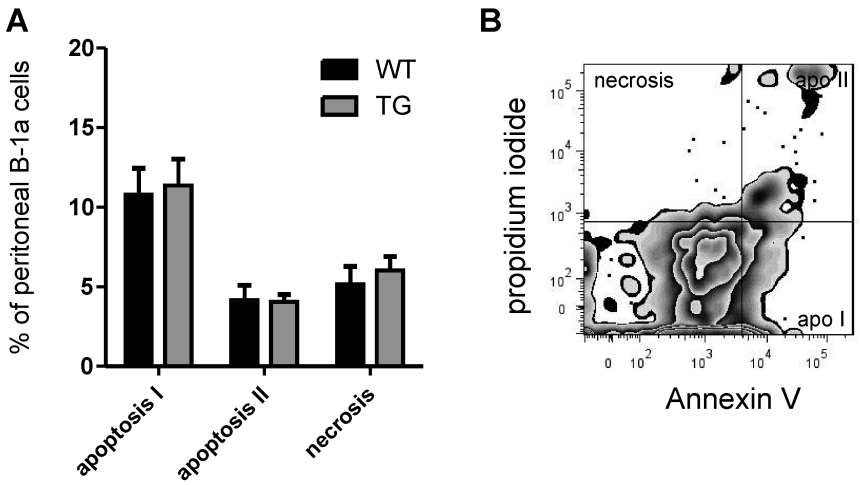

Figure 14: **B-1 cell apoptosis in the peritoneal cavity. (A)** Flow cytometry analysis of apoptotic and necrotic peritoneal B-1a cells. Mean percentages of n = 4-5 mice per genotype + SEM from two independent experiments are shown. **(B)** Annexin V and propidium iodide gating of peritoneal B-1a cells in apoptosis stage I or II, and necrotic cells of one representative individual.

Together, from the investigations on maturation and apoptosis of B-1a cells, we exclude a direct role for SLy2 in down-regulating *de novo* generation of B-1 cells or increasing cell degradation *in vivo*. Aside from these two important mechanisms regulating cell numbers *in vivo*, B-1 cells are unique amongst the lymphocytes, as they are able to maintain their population by self-replenishment with the help of multiple B-1 cell-extrinsic and B-1 cell-intrinsic growth factors. In the following subsection these factors were therefore examined in immune cells derived from WT and TG animals.

4.1.5 The role of SLy2 in B-1 cell growth factor production

As mentioned before, B-1 cells are able to proliferate without preceding BCR stimulation. This so called self-replenishment is mainly induced by T cell-derived cytokines, such as IL-5 [63], which signals through the IL-5Rα-chain, expressed on B-1 cells as well as on eosinophils. The expression of IL-5Rα in turn depends on IL-4 and CD40L stimulation of B-1 cells [27]. Notably, IL-4 and CD40L were shown to be indispensable for proper immune responses to pPS [47]. Therefore, production, release, and signaling of the B-1 cell-extrinsic growth factors IL-5, IL-4, and CD40L were addressed in the following experiments. First, T cell-receptor (TCR)-induced phosphorylation of downstream signaling proteins was investigated by Western blot analyses of isolated splenic T lymphocytes following stimulation with anti-CD3. The TCR-induced signaling cascade leads to differentiation of T cells and production of cytokines. Two important molecules were selected for phosphorylation analysis, namely the protein kinase AKT and the downstream protein IκBα (*Fig. 15*). To this end, WT and TG T cells were lysed without stimulation or following stimulation for 5 minutes or 5 hours. Evaluation of Western blots revealed no differential phosphorylation of these signaling proteins, indicating that TCR signaling was not essentially affected by *SLy2* overexpression.

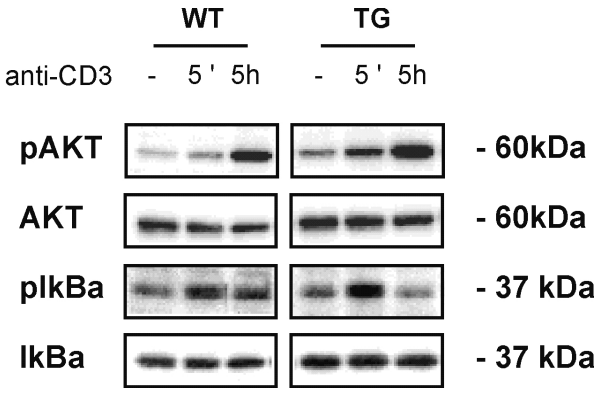

Figure 15: **anti-CD3-induced phosphorylation in T cells.** Western blot analysis of unstimulated and anti-CD3 stimulated splenic T cells. AKT and IκBα phosphorylation and protein levels in lysates of one representative experiment from two independent assays. T cells from three animals per genotype were pooled for one assay.

Subsequent investigations addressed IL-4 release from T cells, and IL-4 and CD40L signaling in B cells. To this end, IL-4 concentrations were assessed by ELISA in supernatants of anti-CD3-stimulated purified splenic T cells from WT and TG mice. Evaluation of IL-4 cytokine ELISA yielded comparable concentrations in both supernatants (*Fig. 16* A). Furthermore, IL-4 and anti-CD40-induced phosphorylation of downstream kinases in purified splenic B cells were analyzed by Western blotting. To this end, purified splenic B cells from WT and TG animals were either lysed unstimulated or following stimulation with IL-4 and anti-CD40 for 5 minutes or 5 hours. The two important downstream kinases AKT and ERK1/2 were selected for Western blot analyses (*Fig. 16* B). Yet, evaluation of specific phospho-

protein bands showed again no significant differences between WT and TG mice. These data indicate, that SLy2 has no critical influence on IL-4 and CD40L signaling.

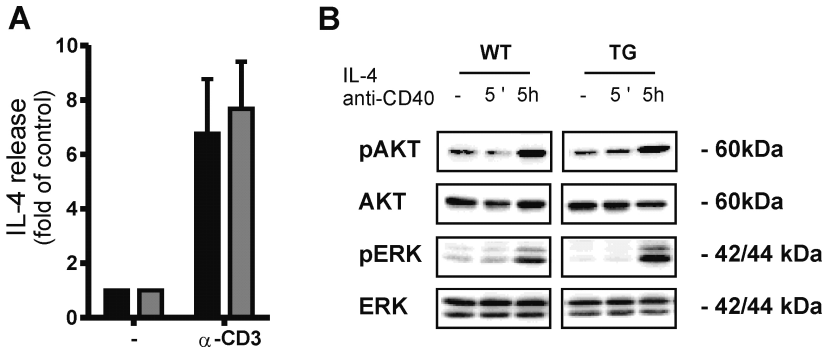

Figure 16: **IL-4 release and signaling in T and B cells. (A)** IL-4 ELISA of supernatants from unstimulated and anti-CD3-stimulated splenic T cells of *n* = 6 mice per genotype + SEM from four independent experiments, presented as fold of unstimulated controls. **(B)** Western blot analysis of unstimulated and IL-4+anti-CD40-stimulated splenic B cells. AKT and ERK phosphorylation and protein levels in lysates of one representative experiment from two independent assays. B cells from three animals per genotype were pooled for one assay.

The last remaining and most important B-1 cell-extrinsic growth factor was IL-5. Hence, the production of the latter as well as its release from T cells was extensively studied. To this end, basal and TCR-induced *IL-5* mRNA expression was assessed in purified splenic T cells from WT and TG animals (*Fig. 17* A). Although basal *IL-5* mRNA levels (left panel) were slightly reduced in TG mice, the differences were statistically not significant. Moreover, TCR-induced *IL-5* mRNA expression following stimulation with anti-CD3 for 48 hours was not changed in TG mice, compared to WT animals (right panel). Accordingly, IL-5 releases from purified splenic T cells were comparable, as measured in T cell culture supernatants following 48 hours of TCR stimulation with anti-CD3 (*Fig. 17* B).

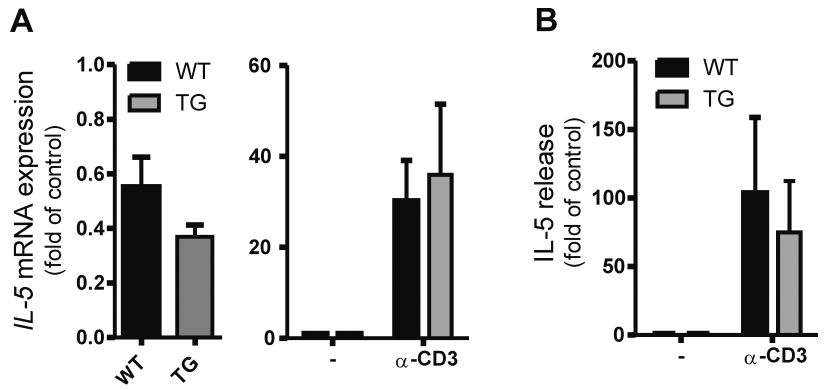

Figure 17: **IL-5 production and release of splenic T cells. (A)** Left panel: RT-PCR of purified splenic T cells from *n* = 8 mice per genotype + SEM, presented as fold of an internal positive control. Right panel: RT-PCR of purified splenic T cells following 48 hours of stimulation with anti-CD3. Values of *n* = 5 mice per genotype + SEM from four independent experiments are shown as fold of unstimulated controls. **(B)** IL-5 ELISA of supernatants from unstimulated and anti-CD3-stimulated splenic T cells of *n* = 8 mice per genotype + SEM from five independent experiments, presented as fold of unstimulated controls.

These data further localize the site of action of the adaptor protein SLy2. Production and release of IL-4 and IL-5 do not seem to be affected by *SLy2* over-expression. Furthermore, IL-4 and CD40L signaling remained unaltered. Hence, differential regulation of extrinsic B-1 cell growth factors was not the cause of the observed B-1 cell population shifts and hampered B-1 cell functionality in TG mice.

4.1.6 B-1 cell-intrinsic alterations following *SLy2* over-expression

Having shown that B-1 cell-extrinsic growth signals from T lymphocytes and IL-4 and CD40L signaling in B cells were unaffected in *SLy2* over-expressing TG mice, B-1 cell-intrinsic factors that control proliferation and differentiation were analyzed in more detail. The next experiments aimed to clarify the mechanism behind reduced peritoneal B-1a cell numbers and impaired immune responses to pPS vaccination.

Expression of B-1 cell-specific survival and proliferation genes

A variety of factors are known to control survival, proliferation, and differentiation specifically in B-1 cells. The expression levels of three cell cycle regulators, namely *cyclinD2*, *siglecG*, and *p18* [41, 86, 74], were examined by RT-PCR in purified peritoneal B-1a cells from WT and TG animals (*Fig. 18* A). RNA was extracted from a pool of peritoneal B-1a cells of ten mice per genotype. Analysis of data revealed no significant changes in mRNA expression levels of these genes, demonstrating that SLy2 does not significantly influence B-1 cell cycle through transcriptional regulation of *cyclinD2*, *siglecG*, and *p18*.
Yet, IL-5 still represents the major B-1 cell-extrinsic growth factor, as mentioned in the previous subsection. This T cell-derived cytokine specifically binds to the IL-5Rα on B-1 cell surfaces to induce cell proliferation or differentiation [63, 27]. Therefore, *IL-5R*α expression in purified B-1a cells was additionally assessed. Evaluation of RT-PCR yielded a clear reduction of 90.6 % by mean in B-1a cells from TG mice compared to those of WT controls (*Fig. 18* B). This finding reveals a possible explanation for the distinct B-1 cell numbers and B-1 cell functionality in TG mice.

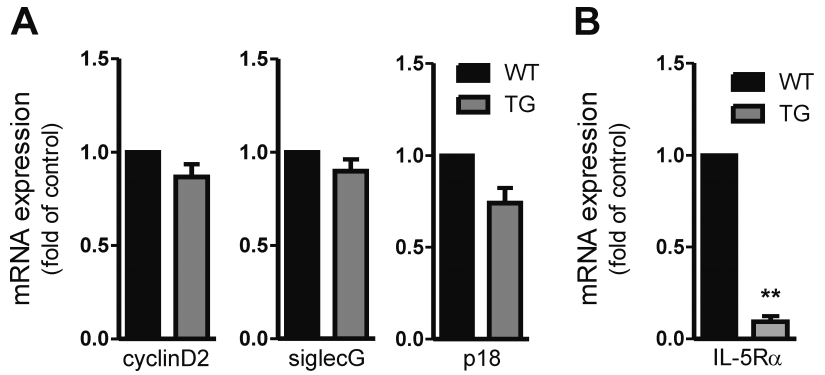

Figure 18: **Expression analysis of B-1 cell growth factors. (A)** RT-PCR analysis of *cyclinD2*, *siglecG*, and *p18* in a pool of purified peritoneal B-1a cells, washed out of ten mice per genotype. Bars represent the mean + SEM of three independent RT-PCR assays, presented as fold of WT control. **(B)** RT-PCR analysis of *IL-5Rα* in a pool of purified peritoneal B-1a cells, washed out of ten mice per genotype. Bars represent the mean + SEM of three independent RT-PCR assays, presented as fold of WT control. Asterisk indicates statistical significance (* $p < 0.05$; Student's *t*-test).

Stimulation-induced expression of the IL-5Rα on B-1 cells

Previous results demonstrated a significant reduction of basal *IL-5Rα* mRNA transcription in peritoneal B-1a cells. However, reduced transcription of genes is not stringently followed by reduced protein levels on cell surfaces. Therefore, IL-5Rα (also referred to as CD125) protein levels on B-1a cell surfaces were addressed in the next presented experiments. As described before, *IL-5Rα* expression is promoted by stimulation with IL-4 and CD40L [27]. Hence, single cell suspensions from peritoneal wash-outs and splenocytes were prepared from WT and TG animals, and IL-5Rα expression was induced by *ex vivo* stimulation with IL-4 and anti-CD40 for 48 hours. Thereafter, cells were analyzed by flow cytometry and IL-5Rα levels were compared to those of unstimulated cells, measured two days before. Histograms of FITC fluorescence intensity, which correlates with IL-5Rα (CD125) expression levels, show a left-shift for peritoneal and splenic B-1a cells of the TG mouse as compared to a WT control (*Fig. 19* A). The mean fluorescence intensity (MFI) of CD125-FITC in the gate of B-1a cells was assessed for stimulated and unstimulated samples, and induction of IL-5Rα expression was calculated. Analysis of data revealed a significantly reduced up-regulation of 12.8 % by mean on peritoneal B-1a cells, and on average 23.9 % less expression of IL-5Rα on splenic B-1a cells (*Fig. 19* B).

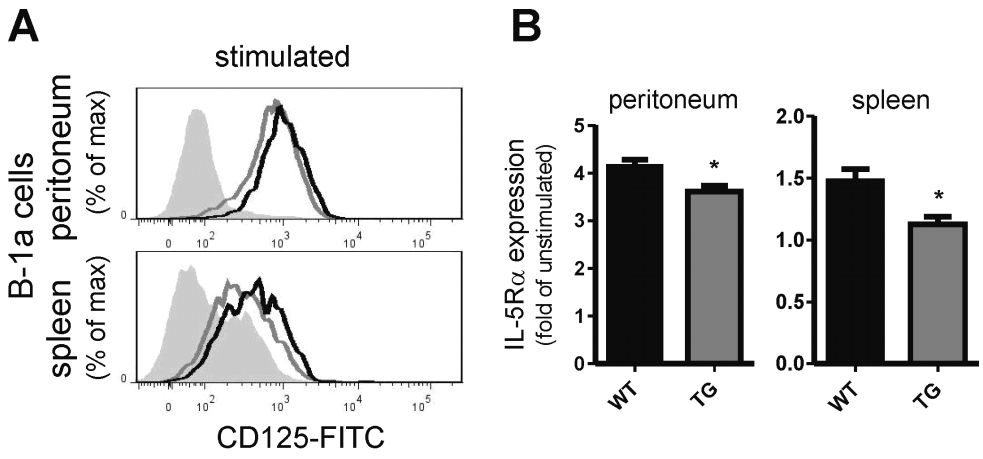

Figure 19: **B-1a cell surface expression of the IL-5Rα. (A)** Flow cytometry analysis of IL-5Rα expression on stimulated peritoneal and splenic B-1a cells. Solid black lines show histograms of CD125-FITC fluorescence intensity of one representative WT animal, solid grey lines represent those of one TG animal, and filled histograms depict isotype controls. **(B)** Analysis of FITC MFI of stimulated cells normalized to unstimulated controls of n = 7-9 mice per genotype + SEM from three independent experiments. Asterisk displays statistical significance (* $p < 0.05$; Student's t-test).

This finding proves that reduced transcription of *IL-5Rα* in B-1a cells from *SLy2* over-expressing TG mice results in compromised up-regulation of surface receptor levels following stimulation with IL-4 and anti-CD40. The next experiments were performed to confirm the functional consequences and to point out the relevance of this novel mechanism during Pneumovax®23 immunizations.

IL-5-induced IgM release from B cells

In brief, so far the most important findings were that basal and pPS-induced humoral IgM responses were reduced in *SLy2* over-expressing TG mice, and the expression of the receptor for the B-1 cell growth and differentiation factor IL-5 was impaired. Translationally, this suggests that biological effects of T cell-derived IL-5 were impaired following *SLy2* over-expression. To examine the functional consequences of differential regulation of the IL-5Rα on peritoneal and splenic B-1a cells, IL-5-induced IgM release from purified B cells was investigated. To this end, B220$^+$ cells were purified from WT and TG spleens and stimulated for 96 hours with IL-4 and anti-CD40 alone or in combination with IL-5. ELISA-based analysis of cell culture supernatants apparently proved that IgM levels increased by stimulation when compared to unstimulated samples, which were kept in stimulation medium supplemented with FCS only (*Fig. 20* A). Overall, TG mice produced less IgM in response to both stimulations, however differences were statistically not significant. To assess the sole effect of IL-5 stimulation, IL-5-induced IgM release was additionally calculated by normalizing values from IL-5-stimulated samples to those of IL-4 and anti-CD40 stimulated samples (*Fig. 20* B).

These results provide evidence that IL-5-induced IgM production was significantly reduced by average 21.7 % in samples from TG mice, confirming the functional defects that result from reduced IL-5Rα expression levels on B-1a cells.

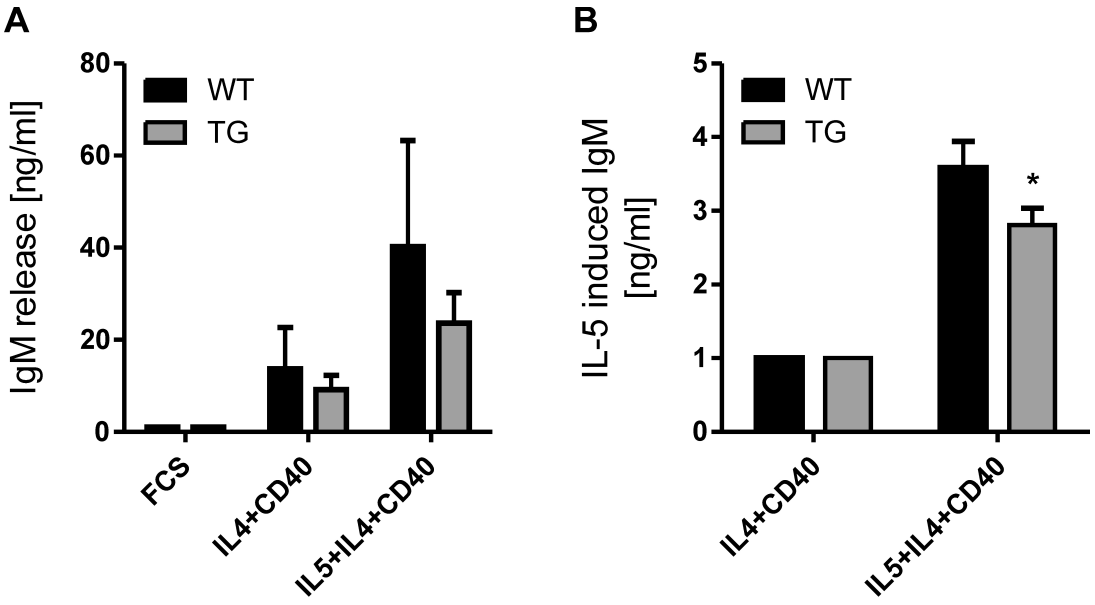

Figure 20: **IgM release of purified splenic B cells.** **(A)** IgM ELISA of supernatants from purified B cells, stimulated with FCS, IL-4 and anti-CD40, or IL-5, IL-4 and anti-CD40. Bars represent the means + SEM of *n* = 5 mice per genotype + SEM from three independent experiments. **(B)** Analysis of IL-5-induced IgM release of *n* = 5 mice per genotype. Bars represent the means + SEM, normalized to IL-4 and anti-CD40 stimulated samples, from three independent experiments. Asterisk displays statistical significance (* $p < 0.05$; Student's *t*-test).

Due to the limited abundance of B-1 cells, this experiment was performed with total splenic B cells, including a large amount of B-2 cells, which are also capable to produce IgM. Although IL-5Rα is a characteristic marker of B-1 cells, there was still lack of evidence that the measured IgM was derived from B-1 cells only. In order to attest that IL-5-induced IgM production was impaired in B-1 cells in particular, subsequent experiments were carried out.

IgM levels in B-1 cells following Pneumovax® immunization

Although IL-4 and CD40L were reported to be essential for a proper immune response to pPS [46], and these factors promote IL-5Rα expression on B-1 cells [27], a direct relationship between IL-5 signaling and B-1 cell-derived pPS-induced IgM production was still missing. In order to clarify this missing link in the presented novel relationship between *SLy2* overexpression and impaired pPS-specific humoral immune responses, intracellular IgM levels were analyzed particularly in peritoneal B-1 cells following *ex vivo* stimulation with IL-5 and following immunization of WT and TG mice with Pneumovax®23. First, we wanted to attest that reduced IL-5-induced IgM production, as demonstrated in *Fig. 20*, was based on defective B-1 cells. To this end, peritoneal cells were stimulated for 24 hours with IL-4, IL-5,

and anti-CD40. Flow cytometry analyses of intracellular IgM levels in B-1a and B-1b cells revealed average 15.7 % lower IgM levels in B-1a and 24.2 % lower levels in stimulated B-1b cells derived from TG mice as compared to WT controls (*Fig. 21* A). This finding proved evidence that B-1 cells in particular were the source of IL-5-induced IgM releases, which were shown to be impaired in TG mice (*Fig. 21*), concluding that compromised IL-5Rα expression results in lower humoral IgM responses when *SLy2* is over-expressed.

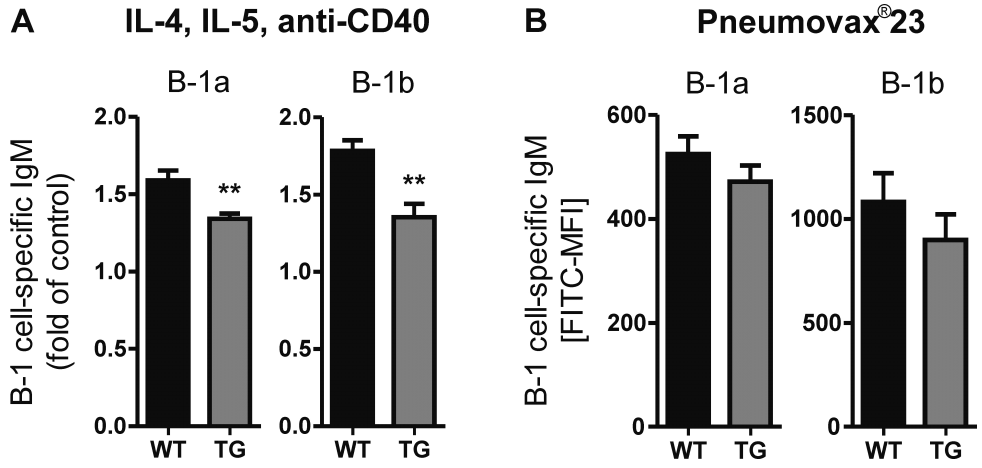

Figure 21: **IL-5 and P23-induced intracellular IgM in peritoneal B-1 cells. (A)** Flow cytometry analysis of intracellular IgM of peritoneal B-1a and B-1b cells, stimulated *ex vivo* with IL-4, IL-5, and anti-CD40 for 24 hours to induce IgM production. Bars represent the means + SEM of n = 5 mice per genotype + SEM from three independent experiments, presented as fold of unstimulated controls. Asterisks display statistical significance (** $p < 0.01$; Student's t-test). **(B)** Flow cytometry analysis of intracellular IgM of peritoneal B-1a and B-1b cells at day 3 following intraperitoneal vaccination of WT and TG animals with Pneumovax®23. Bars represent the means + SEM of n = 6 mice per genotype + SEM from two independent experiments, presented as IgM-FITC MFI.

Given that B-1 cells essentially contribute to pPS-specific immunoglobuline titers [35], we attributed the defective Pneumovax®23 responses observed in TG mice to the presented B-1 cell-intrinsic functional alterations of IL-5Rα expression. Nevertheless, also other cell types might be involved in mounting a pPS-specific immune response. To prove that defective B-1 cells in TG mice were the basis of this special phenotype, intracellular IgM levels were measured by flow cytometry in peritoneal B-1 cells at day 3 post-immunization with Pneumovax®23 (*Fig. 21* B). Analysis of data revealed slightly, however not significantly, reduced IgM production in peritoneal B-1a and B-1b cells of TG mice. Since it is known that *in vivo* activated peritoneal B-1 cells migrate to the spleen where they differentiate to ASCs [34, 101], B-1 cell-specific IgM in isolated splenocytes from immunized animals was additionally assessed. Analysis of MFI in splenic B-1a and B-1b cells clearly showed that cells from TG mice contained significantly less intracellular IgM, than those of WT animals (*Fig. 22* A). IgM in B-1a cells was 11.6 % lower by mean in TG mice, and IgM in B-1b cells

was 19.1 % lower by mean as compared to WT controls. Histograms of FITC MFI in splenic B-1a and B-1b cells of one representative individual per genotype are presented as an overlay diagram (*Fig. 22* B).

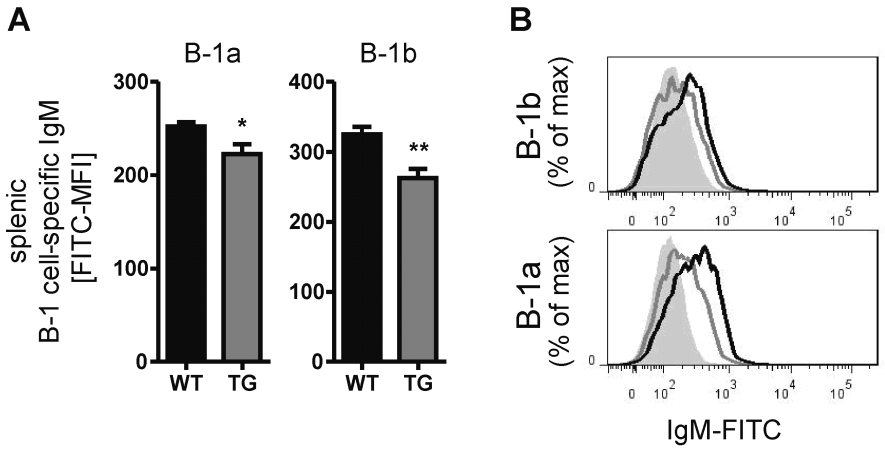

Figure 22: **P23-induced intracellular IgM in splenic B-1 cells. (A)** Flow cytometry analysis of intracellular IgM of splenic B-1a and B-1b cells at day 3 following intraperitoneal vaccination of WT and TG animals with Pneumovax®23. Bars represent the means + SEM of n = 6 mice per genotype + SEM from two independent experiments, presented as IgM-FITC MFI. Asterisks display statistical significance (* $p < 0.05$; ** $p < 0.01$; Student's t-test). **(B)** Overlay of histograms representing IgM-FITC fluorescence intensity of B-1a and B-1b cells of one individual animal per genotype. Solid black lines represent the WT animal, solid grey lines represent one TG animal, and filled histograms depict isotype controls.

In summary, so far the presented data clearly show, that *SLy2* over-expression results in reduced basal and Pneumovax®23-induced IgM titers *in vivo*. Furthermore, B-1 cell-intrinsic defects of IL-5Rα expression were shown to contribute to reduced IgM release in response to IL-5 stimulation. Finally, we proved that these defective B-1 cells were the source of the observed impaired IgM titers following vaccination of TG animals. These results reveal SLy2 as an important immuno-inhibitory adaptor protein for B-1 cell-mediated humoral immune responses following BCR-independent activation, and thus, strongly propose the IL-5Rα to be essential for proper responses to Pneumovax®23 vaccine.

4.2 Regulation of IL-5Rα expression by SLy2

Having shown that SLy2 regulates the transcription of the *IL-5Rα* in B-1 cells, the next presented experiments aimed to clarify the biochemical mechanisms behind. SLy2 is an adaptor protein, which is localized in the cytoplasm as well as in the nucleus. Both compartments may harbor potential interacting proteins. Candidate factors were those involved in controlling *IL-5Rα* transcription in B-1 cells. Literature searches identified the transcription factor OCT2 as an interesting candidate, since it was shown to promote *IL-5Rα* expression exclusively in B-1 cells [27]. This feature was important since we and others did not observe any population shifts in IL-5Rα-positive eosinophils in mice globally missing *SLy2* (data not shown and [97]). Therefore, the transcription factor OCT2 was selected for a more detailed biochemical characterization related to the presented immuno-regulatory process.

4.2.1 Co-precipitation of SLy2 with the transcription factor OCT2

In a first approach, constitutive binding of SLy2 to the transcription factor OCT2 was examined. To this end, primary splenic B cells from TG mice were purified and protein lysates were prepared. As the transgenic SLy2 is HA-tagged, SLy2 was easily precipitated with anti-HA antibodies. Following precipitation, lysates were analyzed by Western blotting and checked for co-precipitation of OCT2. In parallel, buffer was used as a negative input control (*Fig. 23*, lanes "HA"). Similarly, OCT2 was precipitated from B cell lysates and checked for SLy2-HA co-precipitation (*Fig. 23*, lanes "Oct2"). However, Western blots showed no constitutive co-precipitation in both cases, suggesting that OCT2 and SLy2 did not constitutively co-precipitate in unstimulated splenic B cells.

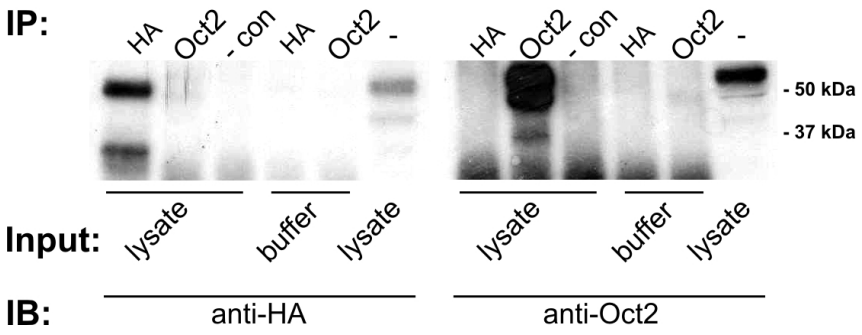

Figure 23: **Co-precipitation of SLy2 and OCT2.** Immunoblot (IB) analysis shows protein content of HA-tagged SLy2 (left panel) or OCT2 (right panel) following immunoprecipitation (IP) from stated inputs with either anti-HA or anti-OCT2 antibodies. Negative control (-con): precipitation without antibodies. Input control (-): lysate without precipitation.

4.2.2 Global Serine phosphorylation of OCT2 in presence of SLy2

Basically, the activity of transcription factors is strongly dependent on post-translational modifications, such as phosphorylation or acetylation. For OCT2 in particular, differential phosphorylation at N-terminal and C-terminal Ser-phosphorylation sites was reported to control its activity [88]. In general, the strength of Ser-phosphorylation positively correlates with OCT2 transcriptional activity [88]. Having shown that SLy2 does not constitutively bind to OCT2, we suggested a more complex relationship that finally results in reduced transcriptional activity of OCT2. Due to technical limitations in analyzing time- and stimulation-dependent phosphorylation of 50 kDa proteins in primary B cells, a cell culture-based approach was used for the following investigation. To this end, HEK293T cells were transiently transfected with plasmid constructs to over-express OCT2, or were co-transfected with myc-tagged SLy2 (*Fig. 24* A, left blots). OCT2 was precipitated of these protein lysates, and analyzed for the amount of global Ser-phosphorylation by Western blotting (*Fig. 24* A, right blots). Quantification of Western blots was performed by normalizing phospho-Serine (pSer) bands to those of precipitated OCT2. Mean values revealed a significant 17.7 % reduction of phosphorylated Serine following SLy2 co-precipitation, when compared to OCT2 transfected controls (*Fig. 24* B), indicating that the presence of SLy2 leads to an inhibition of global OCT2 Ser-phosphorylation.

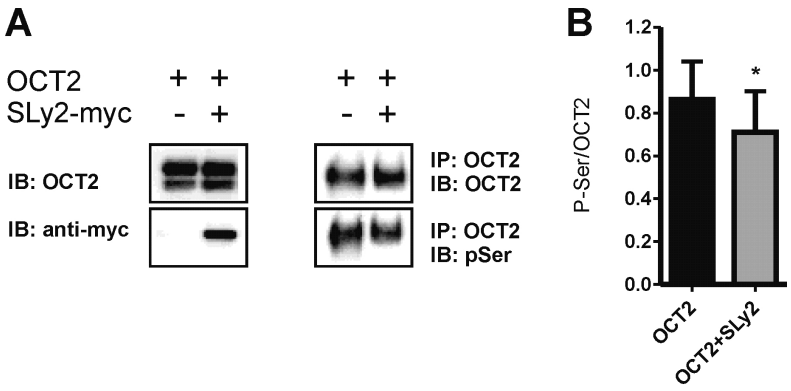

Figure 24: **Phosphorylation of OCT2 in transfected HEK293T cells. (A)** Left blots: Immunoblot (IB) analysis of protein lysates transfected with either OCT2 alone, or in combination with myc-tagged SLy2. Right blots: IB analysis of immunoprecipitated (IP) OCT2 for global pSer. **(B)** Quantification of bands. Pixel density was measured for pSer and normalized to OCT2. Bars represent the means + SEM of three independent experiments. Asterisk indicates statistical significance (* $p < 0.05$; Student's *t*-test).

In summary, these initial findings from biochemical analyses revealed that SLy2 reduces global phosphorylation of the transcription factor OCT2 in a cell culture-based approach. As mentioned before, it is well-known that OCT2 transcriptional activity depends on its Ser-phosphorylation status [88]. This strongly supports our hypothesis that SLy2 reduces OCT2 transcriptional activity, which is followed by an impaired *IL-5R*α expression particularly in B-1 cells, leading to the presented immuno-inhibitory phenotype of TG mice.

Fig. 25 A schematically illustrates the signal transduction in B-1 cells, leading to IL-5Rα expression, which subsequently facilitates IL-5-dependent self-replenishment or differentiation of B-1 cells into specific IgM-producing B-1 plasma cells. According to our findings presented in this work, we propose this immuno-regulatory process to contribute to B-1 cell self-replenishment as well as to the production of pPS-specific antibodies following vaccination with Pneumovax®23. The involvement of the adaptor protein SLy2 is demonstrated in *Fig. 25* B, which illustrates the identical process for SLy2 over-expressing B-1 cells.

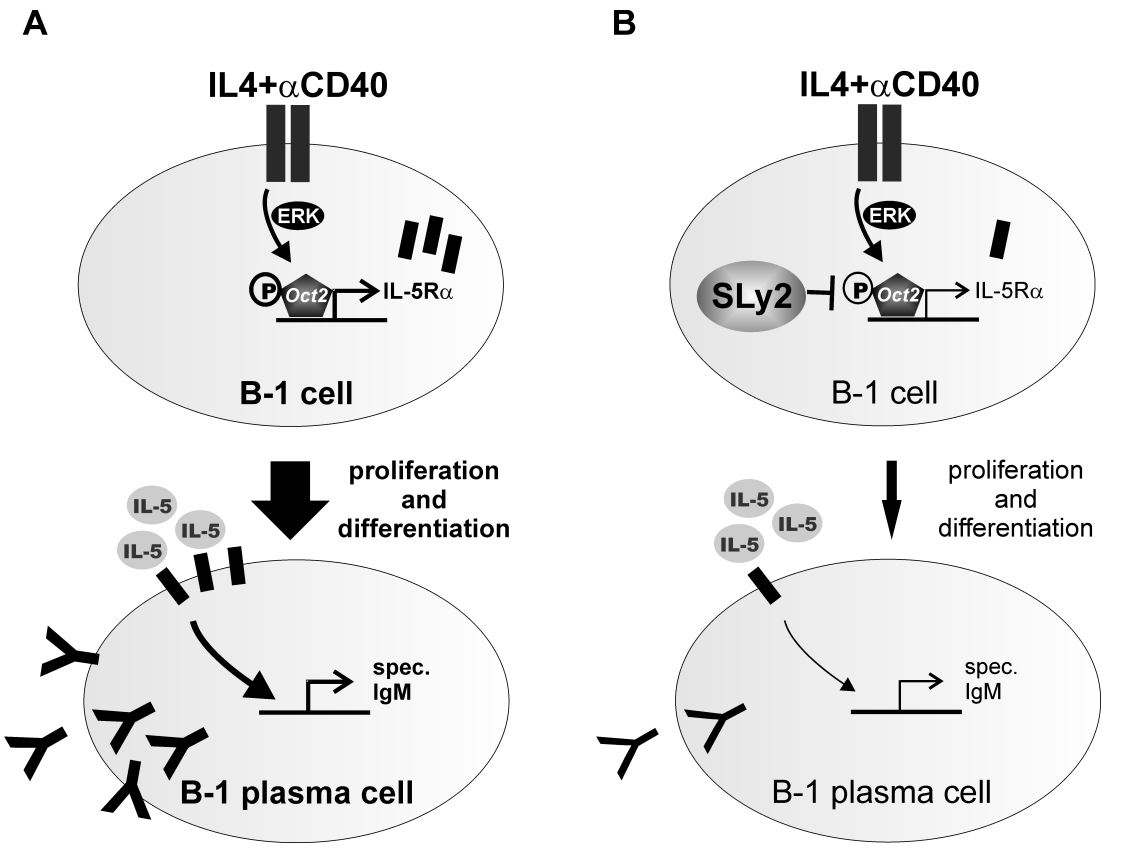

Figure 25: **Schematic illustration of the role of SLy2 in B-1 cells.** **(A)** IL4 and anti-CD40 signal *via* ERK and result in OCT2-activating phosphorylation. This ends up in increased IL-5Rα expression in B-1 cells. The IL-5Rα subsequently gets activated by T cell-derived IL-5 and induces B-1 cell self-replenishment under resting conditions, or B-1 cell differentiation into IgM producing plasma cells under stimulated conditions, for example following Pneumovax®23 immunization. **(B)** Inhibitory effects of SLy2 are visualized by lighter lines and arrows, and less IL-5Rα and IgMs.

4.3 Improved immune responses through decreased *SLy2* expression

The previous sections demonstrated that SLy2 plays an important immuno-inhibitory role in pPS-specific humoral immune responses through an IL-5Rα-dependent mechanism in B-1 cells. Due to the relevance of pneumococcal infections in DS patients, and the fact that *SLy2* is over-expressed in the latter, suitability of the adaptor protein as a target for immunomodulatory strategies comes into account. The so far presented data were based on *SLy2* over-expessing model organisms, which showed inhibited pPS-specific immune responses, as similarly observed in DS patients [67]. In turn, to improve immunity to *S. pneumoniae* in human DS patients, the therapeutic aim would be to down-regulate the immuno-inhibitory function of SLy2. This issue was concerned in the subsequently presented experiments, which were based on the characterization of a *SLy2*$^{-/-}$ (KO) mouse model, recently generated by Max von Holleben [94]. Moreover, BALB/c mice were partially analyzed in parallel, since a previous publication showed that BALB/c mice were resistant to infections with *S. pneumoniae* [31]. The major goal of the next presented experiments was to validate the findings from TG animals, and to bring out SLy2 as a novel potential host genetic factor controlling susceptibility to pneumococcal infections.

4.3.1 Expression of *SLy2* in BALB/c and *SLy2*$^{-/-}$ mice

As mentioned above, BALB/c mice were reported to be resistant to infections with *S. pneumoniae* [31]. Hence, the question came up whether SLy2 was involved in this phenotype. With regard to this issue *SLy2* mRNA expression levels were quantified by RT-PCR in purified splenic B cells of BALB/c mice and compared to those of cells from C57BL/6 mice. C57BL/6 mice were used as controls, as these mice represent the genetic background of SLy2-TG and KO mice. Analysis of RT-PCR data revealed a dramatically reduced expression level of *SLy2* in BALB/c mice (*Fig. 26* A). Concomitantly, purified splenic B and T cells from KO mice were analyzed for *SLy2* expression levels. Both cell types showed a significant reduction of 99.9 % by mean (*Fig. 26* B).

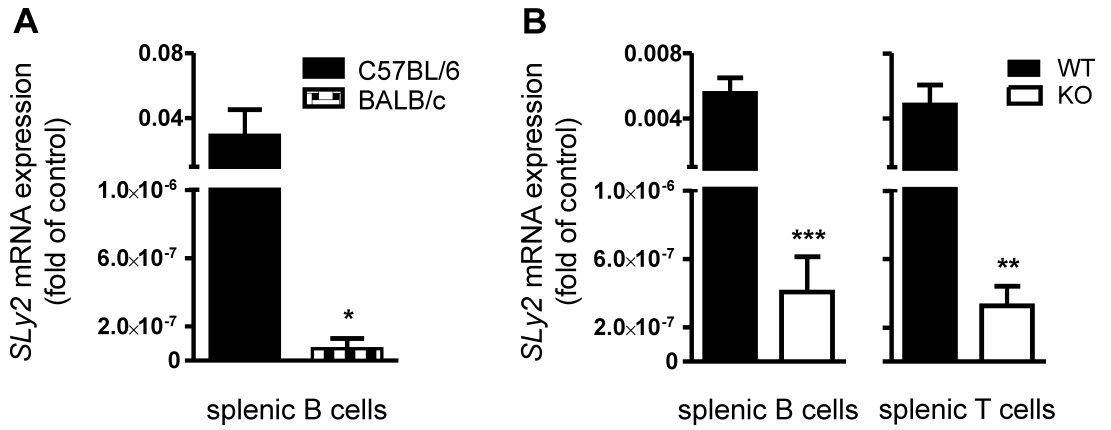

***Figure 26: SLy2* mRNA expression in BALB/c and KO mice. (A)** RT-PCR analysis of *SLy2* mRNA levels in purified splenic B cells from C57BL/6 and BALB/c mice. Bars represent the mean + SEM of n = 5 mice per genotype, presented as fold of an internal positive control. Asterisk indicates statistical significance (* $p < 0.05$; Student's t-test). **(B)** RT-PCR analysis of *SLy2* mRNA levels in purified splenic B and T cells from WT and KO mice. Bars represent the mean + SEM of n = 5-6 mice per genotype, presented as fold of an internal positive control. Asterisks indicate statistical significance (** $p < 0.01$; *** $p < 0.001$; Student's t-test).

4.3.2 Basal IgM levels in BALB/c and *SLy2*$^{-/-}$ mice

Investigations using TG mice clearly showed that *SLy2* over-expression decreases natural serum IgM levels. In contrast, analyses of serum IgM and splenic IgM levels in C57BL/6 and BALB/c mice revealed highly significantly increased titers for BALB/c mice, which were 2.1-fold higher by mean in the serum (*Fig. 27* A, left panel), and 2.4-fold higher by mean in the spleens (*Fig. 27* A, right panel). In KO mice, a similar phenotype was observed, showing average 1.5-fold higher IgM levels in the serum, and 1.9-fold higher IgM levels in the spleens (*Fig. 27* B, left panel and middle panel). Supernatants from peritoneal wash-outs of WT and KO mice were additionally assessed, and revealed slightly increased IgM levels in KO mice, although differences to WT mice were statistically not significant (*Fig. 27* B, right panel). Together, these results demonstrate that mice expressing less *SLy2* in B cells, yielded the opposite basal IgM phenotypes of *SLy2* over-expressing TG mice, and support the idea of a potential correlation between *SLy2* expression and immunity to infections with *S. pneumoniae*.

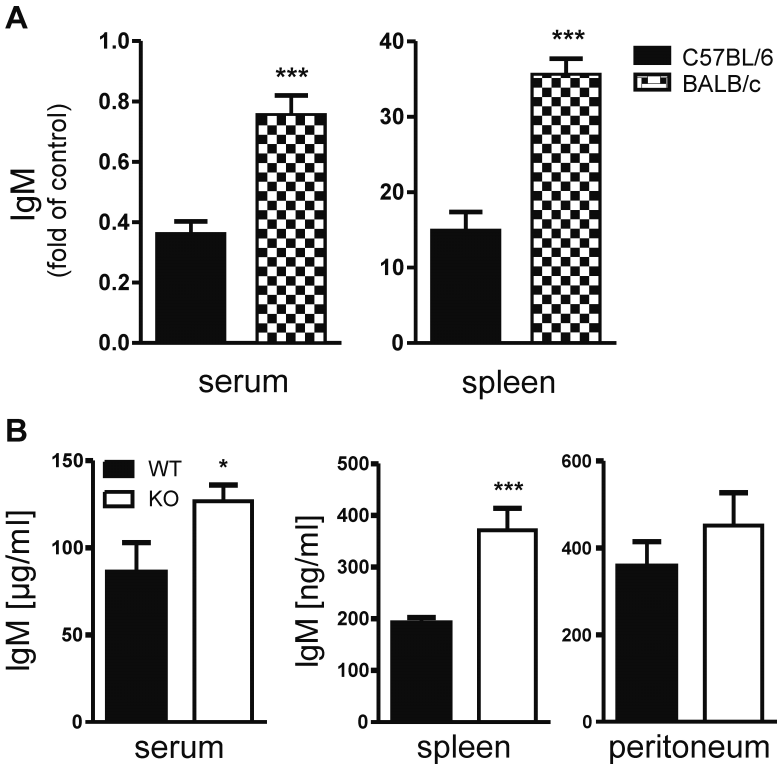

Figure 27: **Basal IgM levels in BALB/c and KO mice. (A)** ELISA of total natural IgM in the serum and supernatants from spleens of C57BL/6 and BALB/c mice. Bars represent the means + SEM from n = 6 sera per genotype, and n = 4 splenic supernatants per genotype, calculated from OD_{450}, presented as fold of an internal positive control. Asterisks indicate statistical significance (*** $p < 0.001$; Student's t-test). **(B)** ELISA of total natural IgM concentrations in the serum and supernatants from spleens and peritoneal wash-outs of WT and KO mice. Bars represent the means + SEM from n = 7-8 sera per genotype, and n = 8 splenic supernatants per genotype, and n = 6 peritoneal supernatants per genotype. Asterisks indicate statistical significance (* $p < 0.05$; *** $p < 0.001$; Student's t-test).

4.3.3 Immunoglobuline responses to Pneumovax® vaccine

The characteristic phenotype of *SLy2* over-expressing TG mice was a significantly impaired immune response to vaccination with Pneumovax®23. Additionally, WT and KO mice were immunized according to the identical protocol, in order to monitor specific IgM courses. Pneumovax®-specific IgM titers (P23) were measured in the sera of immunized WT and KO mice. ELISAs revealed that KO mice exhibited improved antibody responses compared to WT animals. Statistically significant differences were calculated at day 7 (*Fig. 28*, left plot). In addition to total P23-specific IgM production, courses of the single polysaccharide-specific IgMs were assessed for pPS4, pPS6B, and pPS19F (*Fig. 28*, from left to right). Obviously, pPS4-specific IgM responses were significantly higher in KO mice at day 7, which was comparable to total P23-specific IgMs. Moreover, pPS6B-specific IgM was overall moderately increased, whereas no significant differences were observed between WT and KO animals for pPS19F-specific IgM levels. These findings clearly show reverse phenotypes as they

were observed for TG animals, although effects were less pronounced. Nevertheless, these data support the hypothesis that SLy2 essentially controls the humoral immune response to pneumococcal polysaccharides, and foregrounds the basic necessity of investigating the role of *SLy2* over-expression and down-regulation during infections with *S. pneumoniae*.

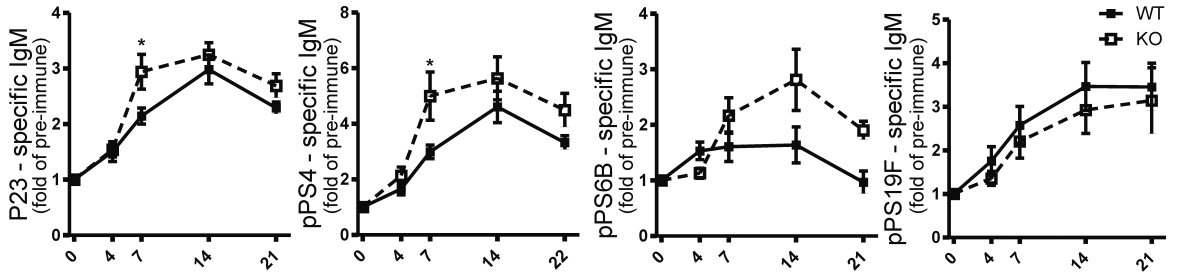

Figure 28: **Pneumovax®23-induced immune responses in KO mice.** From left to right: P23, pPS4, pPS6B,and pPS19F-specific serum IgM levels of WT and KO mice, followed over 21 days after intraperitoneal immunization. Mean values ± SEM, presented as fold of pre-immune titers of n = 7-8 mice per genotype from two independent experiments. Asterisks indicate statistical significance (* $p < 0.05$; ANOVA; Bonferroni posttests).

4.3.4 Peritoneal and splenic B-1 cell populations in BALB/c and *SLy2*$^{-/-}$ mice

As a final confirmatory experiment, B-1 cell abundances in the peritoneal cavities and the spleens of BALB/c and KO mice were measured by flow cytometry. Interestingly, when comparing the sizes of B-1 cell pools in C57BL/6 mice with age-matched BALB/c mice, significantly increased abundance of peritoneal B-1a as well as B-1b cells was found (*Fig. 29*, left panels), confirming recently published data [44]. B-1a cell pools were on average 1.9-fold increased, and B-1b cell pools were 1.8-fold increased by mean in BALB/c mice, giving an explanation for the significantly higher basal IgM titers. However, B-1a and B-1b cell abundances were significantly reduced by 29.4 % and 23.5 % in the spleens of BALB/c mice (*Fig. 29*, right panels), indicating that genetic variances, other than the marginal *SLy2* expression, also significantly control B-1 cell numbers in BALB/c mice.

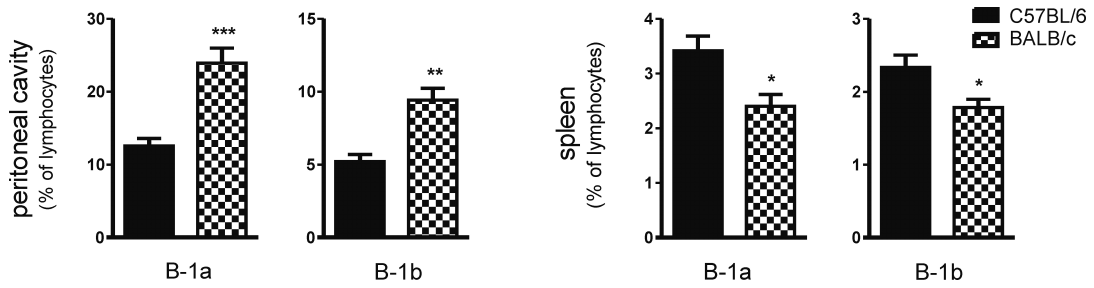

Figure 29: **B-1 cell abundance in C57BL/6 and BALB/c mice.** Flow cytometry analysis of peritoneal and splenic B-1a and B-1b cells of C57BL/6 and BALB/c mice. Bars represent the means ± SEM of n = 6 mice per genotype from two independent experiments, presented as relative abundance within singlet lymphocytes. Asterisks indicate statistical significance (* $p < 0.05$; ** $p < 0.01$; *** $p < 0.001$; Student's t-test).

Furthermore, analyses of B-1 cells in the peritoneal cavities and spleens of WT and KO animals revealed overall increased abundance of both, $CD5^{int}IgM^{hi}$ B-1a cells, and $CD5^{-}IgM^{hi}$ B-1b cells (*Fig. 30* A), which confirms and extends previously published data [97]. Evaluation of flow cytometry measurements yielded a significant 1.2-fold increase of peritoneal B-1a cells in KO mice (*Fig. 30* B, left panel). Peritoneal B-1b cells were also increased, however, these differences were statistically not significant. Moreover, splenic B-1a cells were 1.6-fold increased and B-1b cells 1.5-fold (*Fig. 30* B, right panel).

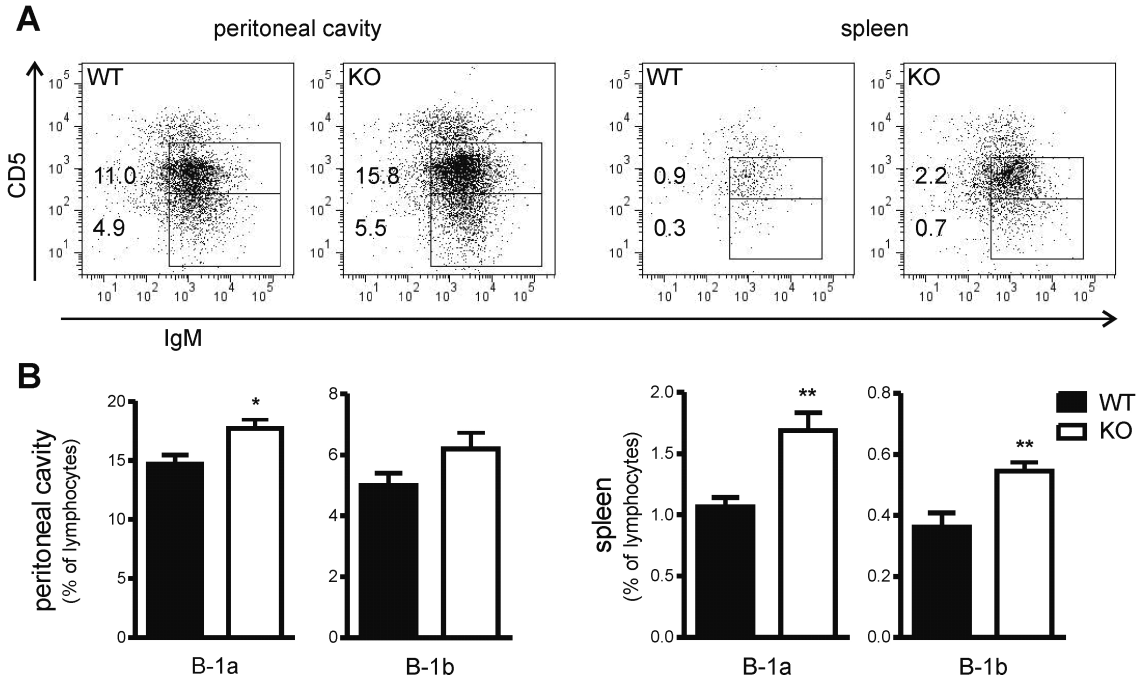

Figure 30: **B-1 cell abundance in KO mice.** **(A)** Flow cytometry analysis of peritoneal and splenic B-1a ($CD19^{+}CD43^{+}IgM^{hi}CD5^{int}$) and B-1b cells ($CD19^{+}CD43^{+}IgM^{hi}CD5^{-}$) of WT and KO mice. FACS plots represent the abundance of B-1 cells of one individual per genotype. **(B)** Analysis of flow cytometry data. Bars represent the means ± SEM of n = 8-10 mice per genotype from three independent experiments, presented as relative abundance within singlet lymphocytes. Asterisks indicate statistical significance (* $p < 0.05$; ** $p < 0.01$; Student's t-test).

Together, investigations using BALB/c and KO mice, provided evidence, that *SLy2* down-regulation basically caused the opposite phenotypes of TG mice. Noting that BALB/c mice were resistant to pneumococcal infections [31] and humoral immune responses to pneumococcal vaccine were improved in KO mice, the presented study strongly proposes a critical role for the adaptor protein SLy2 in immunity to *S. pneumoniae*.

Further investigations using WT, KO, and TG mice during pneumococcal infections will clarify the relevance of the presented novel immuno-regulatory mechanism *in vivo*. Moreover, these studies will be required to highlight the significance in human immunologic disorders, as they are present in DS patients.

CHAPTER 5

DISCUSSION

5.1 Expression of SLy2 in human diseases

The genetic location of *SLy2* on human chromosome 21q11.2 contributes to its significance in DS, which is resulting from a complete or segmental trisomy 21. Interestingly, trisomy 21 is not stringently followed by a triplication of gene expression. In fact, the analysis of lymphoblastoid cell lines from DS patients revealed that the expression of most of the chromosome 21 transcripts was not altered. Only a fraction of 22 % of all transcripts (30 genes) were over-expressed according to the gene-dosage effect and a minority of 7 % (9 genes) were identified to be additionally amplified [3], as schematically illustrated below (*Fig. 31*).

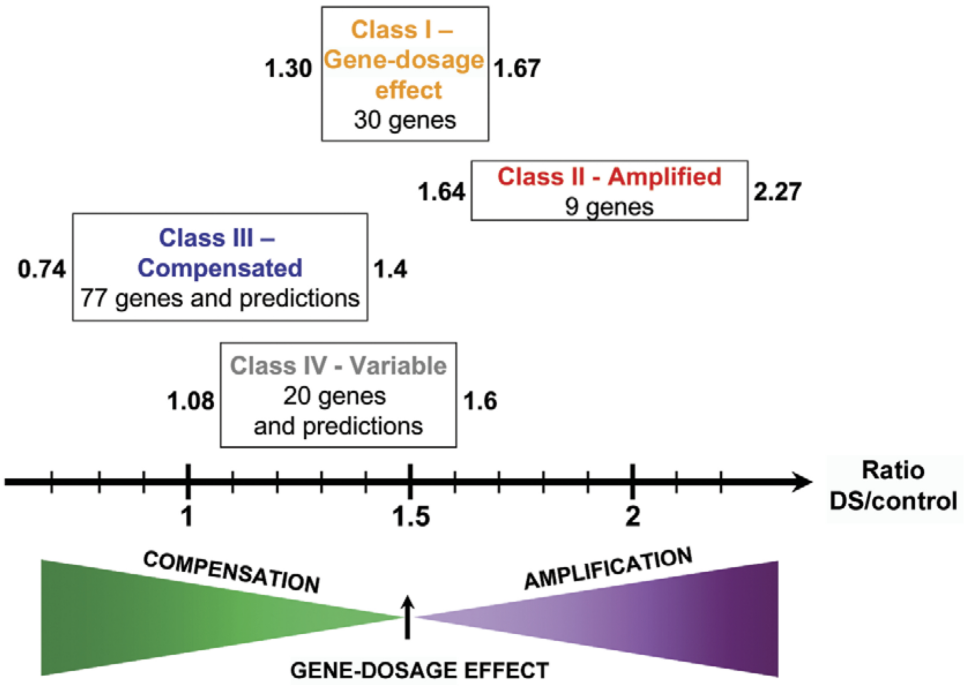

Figure 31: **Gene expression analysis of human lymphoblastoid cells.** Class I genes were amplified about 1.5-fold, according to the gene-dosage effect. Class II genes were more than 1.5-fold amplified. Class III genes were compensated, and class IV genes were variably expressed and not grouped into one specific category (adapted from [3]).

The nine class II genes, amongst which *SLy2* was identified, were considered to determine DS phenotypes, and thus, were of special interest to elucidate genotype-phenotype correlations. The identified amplified genes might also represent interesting targets with regard to all secondary malignancies along with DS. In the present work this microarray data was confirmed and validated by RT-PCR analysis of *SLy2* expression in individual peripheral blood samples.

5.1.1 Potential implications of SLy2 on Down syndrome phenotypes

Two relevant secondary malignancies along with DS represent leukemia and Alzheimer's disease [45, 52, 77]. In particular, the incidence of acute myeloid leukemia (AML) is increased with DS [77], and also Alzheimer's disease (AD) typically occurs in DS patients [52]. Notably, *SLy2* was found to be over-expressed in an AML-derived cell line, named KG-1a, as well as in peripheral blood of AML patients [18]. Similarly, SLy2 was identified amongst a subset of markers associated with AD. Therefore, it is tempting to speculate that SLy2 has indeed a significant impact on AML development and AD, and this becomes apparent with human trisomy 21. Moreover, due to SLy2 expression in heart and brain [18] it is conceivable that the adaptor protein has a certain importance in other non-immunological DS phenotypes, such as congenital heart defects and mental retardation, which results from a multitude of defects in the brain (reviewed in [24]). Previous work reported that SLy2 affects actin remodeling [95], which represents a basic mechanism underlying the formation of neuronal synapses as well as muscle contraction [94]. Thus, investigations of SLy2 in heart and brain represent eligible future fields of research, regarding the significance in human trisomy 21. An adequate murine model organism to study these genotype-phenotype correlations, represents a previously published DS mouse model, in which *SLy2* over-expression was found in whole embryo RNAs [68]. Yet, the present study focused on the investigation of SLy2 in the immune system, given that DS is accompanied with a severely increased susceptibility to infections.

5.2 Murine model organisms for immunological investigations

The immune system is a complex integrative system composed of cellular as well as a multitude of non-cellular components. To examine cell biology of immune cells, it is therefore essential to keep them in their natural environment. Hence, for immunologists, the mouse represents the experimental tool of choice to exemplarily study human biology. However, there are significant limitations of such models, which need to be considered before extrapolating data from mice to men [59]. Some important differences and general specifications of the herein used mouse models are outlined in the subsequent paragraphs.

5.2.1 Tg-*SLy2* and *SLy2*$^{-/-}$ mouse lines

In the present work, TG mice were used to investigate the significance of *SLy2* over-expression in lymphocyte biology. The TG mouse is a valid model to study the role of SLy2 in T and B cells, however, other cell types do not over-express *SLy2* and were therefore not considered for detailed functional analysis in this work. Hence, the TG animals represent a simplified model to study the functional consequences of *SLy2* over-expression in T and B lymphocytes, in an otherwise wild-type-like environment.
On the contrary, KO animals lack *SLy2* expression globally, and thus, do not represent a true counterpart to TG mice. Immune cells other than lymphocytes might additionally contribute to altered lymphocyte functionality in KO mice, complicating the analysis of cell type-specific defects. However, the significance of the adaptor protein in the whole organism and in tissues other than the hematopoietic system could be studied with the help of these animal models. Altogether, these basic limitations of the utilized model organisms need to be minded when interpreting the presented results.

5.3 Humoral immune responses in mice and men

With the help of TG animals, basal IgM levels as well as TI and TD immune responses were assessed within this work. Significant differences were found in basal IgM levels and IgM courses following Pneumovax®23 vaccination. This corroborates with former publications that reported reduced basal serum IgM levels in DS patients, and an impaired response to pPS [1, 67]. Accordingly, generally reduced basal serum IgM titers were herein observed in a random cohort of hospitalized DS children, confirming these earlier studies. However, the limited number of test persons recruited in the present work did not allow to calculate potential correlations with *SLy2* expression levels. Moreover, three out of ten patients had IgM levels within the reference range for healthy individuals, slightly weakening the value.

5.3.1 Hospitalized patients versus SPF mice

A major limitation of the values obtained from human samples, represents their existing health status. In fact, test persons were all hospitalized patients whose immune system might be activated by in-house antigens or by any pre-existing malignancies. IgM represents a sensitive parameter, which rapidly increases with small extrinsic or intrinsic immunological activators. Therefore, the measured basal IgM levels might represent more or less biased values. Large-scaled assessment of IgM levels and *SLy2* mRNA expression in DS patients and control subjects, under consideration of the pre-existing health status, would be of importance to finally clarify a potential correlation between these two parameters. The data obtained from TG mice are comparatively less influenced, due to the SPF housing conditions, which ensure a low-grade pathogenic environment. Moreover, only healthy WT and TG animals were used for experiments, thus preventing unwanted malignancy-induced immunological alterations. Together, the differences between WT and TG mice obtained from murine studies are explained by different *SLy2* expression only, whereas values from human individuals might be the result of differences other than *SLy2* expression.

5.4 Cell population shifts in mice and men

Changes in humoral immune responses are indicative of either functionally defective cells or general alterations in the sizes of specific cell populations. Interestingly, in TG mice, exclusively B-1 cells were changed in numbers whereas other hematopoietic subpopulations remained unaltered. Due to the fact that B-1 cells mainly determine basal IgM titers and contribute to pPS-specific immune responses [10, 35], these cells in particular were assigned a crucial role in the present investigations. However, in DS patients it is well-known that a variety of T lymphocyte subpopulations as well as certain B cell subpopulations were significantly reduced in comparison to non-DS control subjects [23, 93]. Hence, the impaired humoral immune responses can't be simply attributed to one particular cell population in these patients. It remains therefore speculative, whether altered B-1 cells alone contribute to this immunological deficit.

5.4.1 Unequivocal identification of murine B-1 cells

The moderate differences in B-1 cell numbers of WT and TG mice do not adequately explain the strongly reduced IgM response following vaccination. Therefore, functional examinations of WT and TG B-1 cells were performed to elucidate potential B-1 cell-intrinsic defects. Yet, such functional studies require the unequivocal identification of cell types. Although development, functionality, and the phenotype of murine B-1 cells are quite well characterized, it remains challenging to examine B-1 cells *in vivo*, owing to their low abundance and the lack

of a specific surface marker. For FACS analyses, B-1 cells have to be defined through a panel of surface markers, which are all shared by other cell types [8]. Functionally, constitutive production of natural IgM, and specific IgM production following TI antigen stimulation represent the hallmark features of B-1 cells (reviewed in [8]). However, also MZ B cells participate in antibody production to TI antigens [58]. Thus, B-1 cell identification by serum IgM levels alone, likewise persists insufficient. Therefore, to unequivocally identify a true involvement of B-1 cells in the phenotype of any mouse models, adoptive transfer experiments represent the most significant approach. In the present work, no such adoptive transfer experiments were performed. However, application of FACS analyses in combination with a set of functional studies allowed to localize the source of the characteristic phenotype to the subset of B-1 cells. Moreover, the IL-5Rα is a relatively secure marker of B-1 cells, which is otherwise expressed on a minority of only 2-4 % of splenic conventional B-2 cells [40] and eosinophils, that can be easily distinguished from B-1 cells. Nevertheless, these difficulties in B-1 cell identification and distinction from other cell types might indeed influence the significance of experiments, and could be responsible for attenuated read-outs or stronger variances. To further highlight the specific involvement of B-1 cells in the present study, functional studies on T and B cell signaling and cytokine releases were performed. The experiments clearly indicated that the examined pathways remained unaffected and strengthened the hypothesis that SLy2 regulates B-1 cell functionality. Nevertheless, it remains uncertain whether SLy2 is additionally involved in the function and behavior of cell types other than lymphocytes, for example in IL-5Rα-expressing eosinophils. This will have to be terminally clarified in future studies.

Tissue-distribution of B-1 cells in the mouse

Beside the characteristic functions in humoral immune responses, another feature of B-1 cells is their preferred residence in the pleural and peritoneal cavities. The relative distribution of B-1 cells in the steady state is given below (*Fig. 32*).

Tissue	B-1 cell frequency (% of $CD19^+$ B cells)	Spontaneous antibody secretion?
Pleural and peritoneal cavities	35–70%	No*
Blood	0.3–0.5%	Unknown
Spleen	1–2%	IgM
Bone marrow	0.1–0.2%	IgM
Lymph nodes	0.1–0.3%	No
Intestinal lamina propria	Up to 50% of IgA^+ cells	IgA
Lung parenchyma	0.4–0.6%	IgM and IgA

Figure 32: **Distribution of B-1 cells under steady state conditions.** (Adapted from [8]).

According to this typical distribution, it appears plausible to examine B-1 cells primarily in the peritoneal cavity. On the other hand, the low absolute cell number in the cavity again limits the availability of B-1 cells. Furthermore, whenever B-1 cells are activated, they leave the peritoneal cavity and migrate to the spleen and peripheral lymph nodes to become APCs [34, 64, 66]. Therefore, identification of B-1 cells *in vivo* also requires a sensible selection of immunologic tissues which are being analyzed. Hence, in this work B-1 cells were examined in the peritoneal cavity as well as in the spleen, whenever possible. Overall, under consideration of these technical limitations for an unequivocal identification of primary murine B-1 cells, the presented data strongly support a B-1 cell-specific function for SLy2, although a definite proof by adoptive transfer experiments was not provided.

5.4.2 The ambiguity of human B-1 cells

As outlined above, murine B-1 cells are well-described in function, phenotype, and location. However, in humans, the existence of B-1 cell analogs remains a matter of debate. In 2011, $CD20^+CD27^+CD43^+CD70^-$-expressing cells were found in human adult peripheral blood and umbilical cord blood [32]. According to their capacity to produce natural IgM and their skewed antibody repertoire, they were claimed to represent the counterpart of murine B-1 cells. Moreover, these cells were then reported to produce pPS-specific antibodies following vaccination with Pneumovax®23 [92]. Nevertheless, another group proposed the identified cells of rather being activated B cells on their way to plasma cell differentiation, instead of being an eligible B-1 cell analog. This was further propagated by another study, which positioned the predicted human B-1 cells somewhere between plasmablasts and memory B cells, showing a pre-plasmablast-like phenotype rather than a B-1 cell phenotype [21]. Until now, this is not fully clarified and the two groups still debate about the true human B-1 cell counterparts.

Recently, a study with common variable immune deficiency (CVID) patients reported that the proposed B-1 cells were reduced and this correlated with serum IgM levels [54], supporting the B-1 cell-like phenotype for these cells. In the present work, the relative abundances of predicted B-1 cells, memory B cells, and pre-plasmablasts were exemplarily analyzed in peripheral blood samples of one DS patient and one control subject. Interestingly, all subpopulations were reduced in the DS patient, which could be explained by the concomitant reduction of naive and total $CD19^+$ B cells [93]. Of course, the significance of this experiment is very low, and much more patients will have to be recruited to confirm the reduced B cell subsets, that phenotypically resemble murine B-1 cells. Moreover, still there are no studies concerning the functionality of B-1 cells in DS patients, and owing to the ambiguity of human B-1 cells it is arguable whether the presented murine studies on B-1 cell functionality can simply be transferred across species.

5.5 Molecular connection between OCT2 and SLy2

In B cells, the transcription factor OCT2 was initially predicted to induce the expression of Ig genes [19]. Later on, a variety of other target genes were identified in the lymphoid lineage, demonstrating an important role for OCT2 during B cell differentiation [72]. The IL-5Rα represents one target in B cells, mainly B-1 cells, which significantly governs IL-5-induced B cell differentiation to ASCs [27]. In this work, SLy2 was demonstrated to be involved in the transcriptional regulation of *IL-5R*α expression in B-1 cells, suggesting that SLy2 is functionally linked to the transcription factor OCT2. Moreover, *Oct2* null mice and *IL-5R*$\alpha^{-/-}$ mice had in part similar phenotypes as observed in TG mice, including reduced serum IgM levels and reduced B-1 cell numbers [42, 102], which further suggests a molecular link between these proteins. Nevertheless, the preliminary data from biochemical approaches into the molecular connection did not reveal a direct constitutive co-precipitation in primary B cells.
At this point it is important to note that immunoprecipitation (IP) of OCT2 from primary B cells was challenging due to its molecular weight of about 50 kDa, which is identical to the weight of the Ig heavy chain. To reduce the unspecific signals from the Ig heavy chain of native Igs from B cells or from the antibody used for precipitation, conformation-specific secondary reagents were used in Western blots. This successfully worked for the examination of total proteins, however, when analyzing Ser-phosphorylation, the unspecific background was still prevailing. To completely circumvent this problem, we therefore decided to use a cell-line based approach for these purposes. The advantages were an easier handling, owing to the unlimited availability of cells, and an improved precipitation of OCT2 from lysates of transfected cells, as compared to primary cells. Yet, the apparent disadvantage of this approach represents the reduced validity for primary cells. Furthermore, the plasmid constructs expressing *SLy2*, as used in the present study, encoded the murine protein, whereas HEK293T cells represent a human cell line. Thus, it remains uncertain whether the murine

SLy2 was unrestrictedly functional in this human environment.
In future, appropriate biochemical approaches will have to be conducted to clarify the potential molecular connection between OCT2 and SLy2. For example, mass spectrometric analyses of OCT2 post-translational modifications in primary B cells from WT and TG mice will be of value in order to elucidate whether SLy2 influences OCT2 transcriptional activity. Interestingly, several candidate Ser-residues that account for transactivation or repression of the transcription factor were identified within the OCT2 protein [2]. In conclusion, the presented data might be indicatory for a potential interaction of SLy2 and OCT2, resulting in reduced OCT2 Ser-phosphorylation, however, the consequent transcriptional activity was not tested and remains to be investigated in future studies. Moreover, the presence and activity of OCT2 co-activating factors, such as the B cell-specific co-activator OBF1 [33], will have to be examined next. Altogether, a substantial biochemical analysis of the predicted connection between SLy2 and OCT2 remains to be conducted in future experiments.

5.5.1 B cell-specific OCT2 target gene expression

Apart from IL-5Rα, other B cell-specific OCT2 target genes, such as the gene encoding the scavenger receptor CD36, were formerly described [72]. In a first approach to address OCT2 transcriptional activity in isolated B cells, *CD36* mRNA expression was found to be significantly reduced by 36.3 % on average in cells from TG mice, when compared to WT cells (*Fig. 33*). With regard to the discussion of whether SLy2 and OCT2 are functionally linked, this finding, further strengthens the hypothesis that SLy2 exerts its effects through an interaction with the transcription factor OCT2 in murine B cells. Nevertheless, for the differential regulation of *CD36* mRNA expression, no functional effects on the immune system were examined within this work. It is however important to mention that CD36 can recognize amyloid fibrils, which may contribute to AD, as well as phosphocholine residues of pneumococcal lipoteichoic acid, thereby reducing inflammation [80, 82].
Given that OCT2 has additional effects in other cell types as well, cell-specificity of the proposed OCT2-SLy2 interaction represents indeed an interesting task. In T cells for example, OCT2 contributes to the expression of *IL-5* [78], which represents a major growth factor for B-1 cells as well as for eosinophils. Yet, no population shifts in eosinophils were observed in the TG mice, and resting, as well as anti-CD3-stimulated T cells did not show any different *IL-5* mRNA expression and IL-5 release. Therefore, a critical role for SLy2 in T cells is not supported by the present data and SLy2 is rather suggested to be important for B cell-specific OCT2 target gene expression.

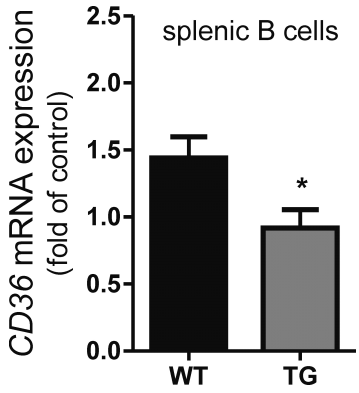

***Figure 33: CD36* mRNA expression in B cells.** RT-PCR analysis of *CD36* mRNA levels in purified splenic B cells from WT and TG animals. Bars represent the means + SEM of $n = 7$ mice per genotype, presented as fold of an internal positive control. Asterisk indicates statistical significance (* $p < 0.05$; Student's *t*-test).

5.5.2 OCT2 expression in the central nervous system

Regarding the relevance of *SLy2* in DS patients, the question arises whether the predicted interaction could be of value in cell types outside the hematopoietic system. As mentioned in the introduction, SLy2 was found to be expressed in the brain [18]. Interestingly, also OCT2 was found to be expressed in the central nervous system (CNS), especially in the cerebellar cortex [57]. Moreover, OCT2 was reported to contribute to CNS development and neuronal differentiation [87, 89]. Noting that mental disability in DS is mainly due to defective neonatal neuronal development, it is tempting to speculate that SLy2 is partially involved through the hypothetical interaction with OCT2, which in turn brings out an interesting future field of research.

5.6 A question of relevance and future perspectives

In summary, the present work describes a function for SLy2 in the inhibition of IL-5Rα expression on B-1 cells. As the IL-5Rα is important for B-1 cell proliferation as well as differentiation to ASCs, SLy2 is suggested to regulate B-1 cell self-replenishment and IgM production through this mechanism. This would explain the observed phenotypes in TG mice, which were reduced B-1 cell numbers and reduced basal as well as specific IgM levels following Pneumovax®23 immunization. As these phenotypes were similar to those observed in DS patients, and *SLy2* was significantly amplified in the latter, a relevance for human disease was assumed from the present work. However, as discussed before, it remains uncertain whether murine data can uncritically be translated to humans. Moreover, the issue of B-1 cells and their identification *in vivo*, requests further studies with other mouse models to ensure the presented novel molecular link between the IL-5Rα and pPS-specific IgM production. In particular, the importance of IL-5Rα expression for Pneumovax®23-induced IgM responses could be additionally examined in *IL-5R$\alpha^{-/-}$* mice. The here described findings would be of great value, if SLy2 was investigated as an adaptor protein that down-regulates the immune response to infections with *S. pneumoniae*. Then, SLy2 would represent an interesting target for immuno-modulatory therapies, especially for immuno-compromised individuals, like DS patients.
Furthermore, the investigation of SLy2 in cells outside of the immune system would be of great value for DS patients, when considering the promising constellation of SLy2 and OCT2 expression in the brain. However, this in turn requires a fundamental revealing of the definite molecular link between SLy2 and OCT2.
The data presented in the last part of this work, using BALB/c and KO mice, were conducted in preparation of the future investigation of SLy2 during infections with *S. pneumoniae*, in order to clarify the relevance of SLy2 for pneumococcal diseases. KO mice showed improved responses to Pneumovax®23 immunization, further supporting an immuno-inhibitory role for SLy2. A previous publication already suggested SLy2 to be a useful target for immune suppression therapy, according to their analyses of *Hacs$^{-/-}$* mice [97]. The authors showed that mice lacking functional SLy2 had an increased peritoneal B-1a cell pool, increased B cell proliferation following BCR stimulation, as well as improved Ficoll-specific IgM and IgG3 responses, when compared to WT controls. Moreover, Th1 and Th2 responses were reported to be significantly stronger in *Hacs$^{-/-}$* mice [97]. Altogether, a multitude of immunological phenotypes were examined in this study showing overall immuno-inhibitory effects for SLy2, however, neither a concrete immunological context, nor fundamental biochemical approaches were provided by this article. Therefore, the proper investigation of SLy2 in coherence of infections remains to be addressed in future studies.

5.6.1 Susceptibility to *S. pneumoniae* infections

A recent study compared the survival of different mouse strains following *S. pneumoniae* infections [31]. As a result, BALB/c mice were identified to be resistant to these bacterial infections. Interestingly, *SLy2* mRNA expression in purified splenic B cells was much lower in BALB/c, when compared to C57BL/6 mice, as demonstrated in this work. The hypothesis, that *SLy2* amplification contributes to susceptibility to *S. pneumoniae* was supported by the data obtained from KO mice, which showed a largely reverse phenotype to TG mice, and which shared some phenotypes with BALB/c mice, including an increased number of B-1 cells and increased IgM levels. In turn, for KO mice an increased survival for *S. pneumoniae* infections would be expected when extrapolating these findings. However, phenotypes were not consistently comparable between BALB/c and KO mice. For example, B-1 cell abundance was increased in the peritoneal cavity of BALB/c mice, which confirms recent data [44], however a significantly reduced abundance was found in the spleen, when compared to C57BL/6 mice. At this point it is important to mention that *SLy2* was observed to be significantly reduced in splenic B cells from BALB/c mice, however, expression levels in thymocytes were significantly increased (data not shown), and further cell types were not analyzed in these mice at all. In KO mice on the contrary, a lack of *SLy2* expression was demonstrated in splenic T cells and otherwise expected for all cell types [94]. Hence, to bring out SLy2 as a host genetic factor for controlling susceptibility to pneumococcal infections, the establishment of an infection model represents the subsequent approach with KO and TG mice. The results will shed light on whether SLy2 plays a relevant role in human DS patients, who suffer from recurrent pneumococcal infections.

5.6.2 Targeting SLy2 - A key to novel therapeutic strategies?

Speculating that SLy2 represents a newly identified host genetic factor that accounts for an increased susceptibility to pneumococcal infections, when amplified in DS patients, the development of novel therapeutic strategies might represent a promising approach to improve their health status and thus, to prolong their general life span. Also other patients, who suffer from reduced pneumococcal-specific immunity, like patients with selective polysaccharide antibody deficiency, could benefit from therapies that aim to down-regulate SLy2. It is important to notice that a global knock-out of *SLy2* in mice did not affect the viability of these animals, but rather improved their overall adaptive immunity, as reported recently [97]. Hence, with regard to unpredicted side-effects, the targeting strategy does not necessarily have to be cell type-specific, which might facilitate the development of the latter.

RNAi-based approaches - a future perspective

Down-regulation of mRNA and protein of specific targets can be easily achieved in cultured cells by transient transfection of exogenous siRNA. In recent years, the suitability of this mechanism for therapeutic uses was more and more investigated. However, the major challenge still represents the delivery of exogenous siRNA into the body. Problems which have to be overcome are the efficient introduction into specific tissues and the circumvention of immune reactions. Moreover, siRNA is a very unstable molecule, which is rapidly degraded by serum nucleases. A quite promising approach to successfully deliver siRNA represents the use of self-exosomes [83]. Exosomes are endogenous nanovesicles responsible for cell-to-cell transports of mRNA and proteins, and thus, they are able to cross biological barriers, such as cell membranes or the blood-brain-barrier. Due to their feature of being host-derived structures, immunogenicity following re-introduction is strongly reduced as compared to chemically engineered transport vesicles. Interestingly, a recent study provided evidence that the delivery of siRNA was achieved with the help of exosomes derived from dendritic cells [5]. The authors demonstrated that siRNA was efficiently delivered into the murine brain, where a knockdown of about 60 % at mRNA and protein levels was achieved in neurons, microglia, and oligodendrocytes following intravenous injection of self-exosomes, that had been packed with exogenous siRNA by electroporation. Moreover, another group showed that exogenous siRNA was successfully delivered into human blood cells by using plasma exosomes [96].
In conclusion, such therapeutic approaches could represent future strategies to efficiently knock-down target genes in a tissue-specific manner, which might be of great value for the therapy of genetic diseases. In due consideration of the multi-faceted phenotypes along with trisomy 21, basic investigations on genotype-phenotype correlations might bring out potential target genes for these therapeutic strategies. Finally, the present work suggests *SLy2* as an interesting candidate to be investigated as a potential future therapeutic target to improve the outcome of pneumococcal infections in immuno-compromised patients.

BIBLIOGRAPHY

[1] M. Adinolfi, B. Gardner, and W. Martin. Observationson the levels of gG, gA, and gM globulins, anti-A and anti-B agglutinins, and antibodies to *Escherichia coli* on Down's anomaly. *Journal of Clinical Pathology*, 20:860–864, Oct. 1967.

[2] I. Ahmad. Oct-2 DNA binding transcription factor: functional consequences of phosphorylation and glycosylation. *Nucleic Acids Research*, 34:175–184, Jan. 2006.

[3] E. Ait Yahya-Graison, J. Aubert, L. Dauphinot, I. Rivals, M. Prieur, G. Golfier, J. Rossier, L. Personnaz, N. Créau, H. Bléhaut, Robert-Koch-Institut, J. M. Delabar, and M.-C. Potier. Classification of Human Chromosome 21 Gene-Expression Variations in Down Syndrome: Impact on Disease Phenotypes. *The American Journal of Human Genetics*, 81:475–491, Sept. 2007.

[4] K. C. Allison, W. Strober, and G. R. Harriman. Induction of IL-5 Receptors on Normal B Cells by Cross-linking Surface Ig with Anti-Ig-Dextran. *The Journal of Immunology*, 146(12):4197–4203, June 1991.

[5] L. Alvarez-Erviti, Y. Seow, H. Yin, C. Betts, S. Lakhal, and M. J. A. Wood. nbt.1807. *Nature Biotechnology*, 29(4):341–345, Apr. 2011.

[6] A. Annweiler, S. Zwilling, and T. Wirth. Functional differences between the Oct2 transactivation domains determine the transactivation potential of individual Oct2 isoforms. *Nucleic Acids Research*, 22:4250–4258, Jan. 1994.

[7] E. Arana, A. Vehlow, N. E. Harwood, E. Vigorito, R. Henderson, M. Turner, V. L. J. Tybulewicz, and F. D. Batista. Activation of the Small GTPase Rac2 via the B Cell Receptor Regulates B Cell Adhesion and Immunological-Synapse Formation. *Immunity*, 28(1):88–99, Jan. 2008.

[8] N. Baumgarth. The double life of a B-1 cell: self-reactivity selects for protective effector functions. *Nature Reviews Immunology*, 11(1):34–46, Dec. 2010.

[9] N. Baumgarth, O. C. Herman, G. C. Jager, L. E. Brown, L. A. Herzenberg, and J. Chen. B-1 and B-2 Cell-derived Immunoglobulin M Antibodies Are Nonredundant Components of the Protective Response to Influenza Virus Infection. *The Journal of Experimental Medicine*, 192(2):271–280, July 2000.

[10] N. Baumgarth, O. C. Herman, G. C. Jager, L. E. Brown, L. A. Herzenberg, and L. A. Herzenberg. Innate and acquired humoral immunities to influenza virus are mediated by distinct arms of the immune system. *PNAS*, 96:2250–2255, Mar. 1999.

[11] S. Beer, T. Scheikl, B. Reis, N. Hüser, K. Pfeffer, and B. Holzmann. Impaired immune responses and prolonged allograft survival in Sly1 mutant mice. *Molecular and Cellular Biology*, 25(21):9646–9660, Nov. 2005.

[12] S. Beer, A. B. Simins, A. Schuster, and B. Holzmann. Molecular cloning and characterization of a novel SH3 protein (SLY) preferentially expressed in lymphoid cells. *Biochimica et Biophysica Acta*, 1520:89–93, 2001.

[13] M. Boes, C. Esau, M. B. Fischer, T. Schmidt, M. Carroll, and J. Chen. Enhanced B-1 Cell Development, But Impaired IgG Antibody Responses in Mice Deficient in Secreted IgM. *The Journal of Immunology*, 160:4776–4787, Apr. 1998.

[14] S. Brandt, K. Ellwanger, C. Beuter-Gunia, M. Schuster, A. Hausser, I. Schmitz, and S. Beer-Hammer. SLy2 targets the nuclear SAP30/HDAC1 complex. *International Journal of Biochemistry and Cell Biology*, 42(9):1472–1481, Sept. 2010.

[15] M. C. Brouwer, J. de Gans, S. G. Heckenberg, A. H. Zwinderman, T. van der Poll, and D. van de Beek. Host genetic susceptibility to pneumococcal and meningococcal disease: a systematic review and meta-analysis. *The Lancet Infectious Diseases*, 9(1):31–44, Jan. 2009.

[16] Y. S. Choi and N. Baumgarth. Dual role for B-1a cells in immunity to influenza virus infection. *The Journal of Experimental Medicine*, 205(13):3053–3064, Dec. 2008.

[17] Y. S. Choi, J. A. Dieter, K. Rothaeusler, Z. Luo, and N. Baumgarth. B-1 cells in the bone marrow are a significant source of natural IgM. *European Journal of Immunology*, 42(1):120–129, Nov. 2011.

[18] J. O. Claudio, Y. X. Zhu, S. J. Benn, A. H. Shukla, C. J. McGlade, N. Falcioni, and A. K. Stewart. HACS1 encodes a novel SH3-SAM adaptor protein differentially expressed in normal and malignant hematopoietic cells. *Oncogene*, 20(38):5373–5377, Aug. 2001.

[19] L. M. Corcoran and M. Karvelas. Oct-2 Is Required Early in T Cell-Independent B Cell Activation for G1 Progression and for Proliferation. *Immunity*, 1:635–645, Nov. 1994.

[20] L. M. Corcoran, F. Koentgen, W. Dietrich, M. Veale, and P. O. Humbert. All Known In Vivo Functions of the Oct-2 Transcription Factor Require the C-Terminal Protein Domain. *The Journal of Immunology*, 172:2962–2969, Feb. 2004.

[21] K. Covens, B. Verbinnen, N. Geukens, I. Meyts, F. Schuit, L. Van Lommel, M. Jacquemin, and X. Bossuyt. Characterization of proposed human B-1 cells reveals pre-plasmablast phenotype. *Blood*, 121(26):5176–5183, June 2013.

[22] M. Crisby, L. Henareh, and S. Agewall. Relationship Between Oxidized LDL, IgM, and IgG Autoantibodies to ox-LDL Levels With Recurrent Cardiovascular Events in Swedish Patients With Previous Myocardial Infarction. *Angiology*, Nov. 2013.

[23] Y. C. M. de Hingh, P. W. van der Vossen, E. F. A. Gemen, A. B. Mulder, W. C. J. Hop, F. Brus, and E. de Vries. Intrinsic Abnormalities of Lymphocyte Counts in Children with Down Syndrome. *The Journal of Pediatrics*, 147(6):744–747, Dec. 2005.

[24] M. Dierssen. Down syndrome: the brain intrisomic mode. *Nature Reviews Neuroscience*, 13(12):844–858, Dec. 2012.

[25] K. Dorshkind and E. Montecino-Rodriguez. Fetal B-cell lymphopoiesis and the emergence of B-1-cell potential. *Nature Reviews Immunology*, 7(3):213–219, Mar. 2007.

[26] M. R. Ehrenstein and C. A. Notley. The importance of natural IgM: scavenger, protector and regulator. *Nature Reviews Immunology*, 10(11):778–786, Oct. 2010.

[27] D. Emslie, K. D'Costa, J. Hasbold, D. Metcalf, K. Takatsu, P. O. Hodgkin, and L. M. Corcoran. oct2 enhances antibody-secreting cell differentiation through regulation of IL-5 receptor a chain expression on activated B cells. *The Journal of Experimental Medicine*, 205(2):409–421, Feb. 2008.

[28] A. Englund, B. Jonsson, C. S. Zander, J. Gustafsson, and G. Annerén. Changes in mortality and causes of death in the Swedish Down syndrome population. *American Journal of Medical Genetics Part A*, 161A:642–649, Mar. 2013.

[29] W. Fiskus, S. Sharma, B. Shah, B. P. Portier, S. G. T. Devaraj, K. Liu, S. P. Iyer, D. Bearss, and K. N. Bhalla. Highly effective combination of LSD1 (KDM1A) antagonistand pan-histone deacetylase inhibitor against human AML cells. *Leukemia*, Apr. 2014.

[30] E. E. B. Ghosn, P. Sadate-Ngatchou, Y. Yang, L. A. Herzenberg, and L. A. Herzenberg. Distinct progenitors for B-1 and B-2 cells are present in adult mouse spleen. *PNAS*, 108(7):2879–2884, Feb. 2011.

[31] N. A. Gingles, J. E. Alexander, A. Kadioglu, P. W. Andrew, A. Kerr, T. J. Mitchell, E. Hopes, P. Denny, S. Brown, H. B. Jones, S. Little, G. C. Booth, and W. L. McPheat. Role of Genetic Resistance in Invasive Pneumococcal Infection: Identification and Study of Susceptibility and Resistance in Inbred Mouse Strains. *Infection and Immunity*, 69(1):426–434, Jan. 2001.

[32] D. O. Griffin, N. E. Holodick, and T. L. Rothstein. Human B1 cells in umbilical cord and adult peripheral blood express the novel phenotype $CD20^{+}CD27^{+}CD43^{+}CD70^{-}$. *The Journal of Experimental Medicine*, 208(1):67–80, Jan. 2011.

[33] M. Gstaiger, L. Knoepfel, O. Georgiev, W. Schaffner, and C. M. Hovens. A B-cell coactivator of octamer-binding transcription factors. *Nature*, 373:360–362, Jan. 1995.

[34] S.-a. Ha, M. Tsuji, K. Suzuki, B. Meek, N. Yasuda, T. Kaisho, and S. Fagarasan. Regulation of B1 cell migration by signals through Toll-like receptors. *The Journal of Experimental Medicine*, 203(11):2541–2550, Oct. 2006.

[35] K. M. Haas, J. C. Poe, D. A. Steeber, and T. F. Tedder. B-1a and B-1b Cells Exhibit Distinct Developmental Requirements and Have Unique Functional Roles in Innate and Adaptive Immunity to *S.pneumoniae*. *Immunity*, 23:7–18, July 2005.

[36] W. D. Hastings, J. R. Tumang, T. W. Behrens, and T. L. Rothstein. Peritoneal B-2 cells comprise a distinct B-2 cell population with B-1b-like characteristics. *European Journal of Immunology*, 36:114–1123, Apr. 2006.

[37] K. Hayakawa, R. R. Hardy, L. A. Herzenberg, and L. A. Herzenberg. Progenitors for Ly-1 B cells are distinct from progenitors for other B cells. *The Journal of Experimental Medicine*, 161:1554–1568, June 1985.

[38] K. Hayakawa, R. R. Hardy, D. R. Parks, and L. A. Herzenberg. The "Ly-1 B" Cell Subpopulation in Normal, Immunodefective, and Autoimmune Mice. *The Journal of Experimental Medicine*, 157:202–218, Jan. 1983.

[39] L. A. Herzenberg. B-1 cells: the lineage question revisited. *Immunological Reviews*, 175:9–22, June 2000.

[40] Y. Hitoshi, N. Yamaguchi, S. Mita, E. Sonoda, S. Takaki, A. Tominaga, and K. Takatsu. Distribution of IL-5 Receptor-Positive B Cells. Expression of IL-5 Receptor on Ly-1(CD5)$^+$B Cells. *The Journal of Immunology*, 144:4218–4225, June 1990.

[41] A. Hoffmann, S. Kerr, J. Jellusova, J. Zhang, F. Weisel, U. Wellmann, T. H. Winkler, N. Kneitz, P. R. Crocker, and L. Nitschke. Siglec-G is a B1 cell-inhibitory receptor that controls expansion and calcium signaling of the B1 cell population. *Nature Immunology*, 8(7):695–704, July 2007.

[42] P. O. Humbert and L. M. Corcoran. oct-2 Gene Disruption Eliminates the Peritoneal B-1 Lymphocyte Lineage and Attenuates B-1 Cell Maturation and Function. *The Journal of Immunology*, 159:5273–5284, Aug. 1997.

[43] M. M. Huston, J. P. Moore, H. J. Mettes, G. Tavana, and D. P. Huston. Human B Cells Express IL-5 Receptor Messenger Ribonucleic Acid and Respond to IL-5 with Enhanced IgM Production After Mitogenic Stimulation with *Moraxella catarrhalis*. *The Journal of Immunology*, 156:1392–1401, Jan. 1996.

[44] A. Itakura, Y. Kikuchi, T. Kuoro, M. Ikutani, S. Takaki, P. W. Askenase, and K. Takatsu. Interleukin 5 Plays an Essential Role in Elicitation of Contact Sensitivity through Dual Effects on Eosinophils and B-1 Cells. *International Archieves of Allergy and Immunology*, 140:8–16, June 2006.

[45] S. Izraeli. Down's syndrome as a model of a pre-leukemic condition. *Haematologica*, 91(11):1448–1452, Nov. 2006.

[46] A. Jeurissen, A. D. Billiau, L. Moens, L. Shengqiao, W. Landuyt, G. Wuyts, L. Boon, M. Waer, J. L. Ceuppens, and X. Bossuyt. CD4+ T Lymphocytes Expressing CD40 Ligand Help the IgM Antibody Response to Soluble Pneumococcal Polysaccharides via an Intermediate Cell Type. *The Journal of Immunology*, 176:529–536, Dec. 2006.

[47] A. Jeurissen, G. Wuyts, A. Kasran, S. Ramdien-Murli, N. Blanckaert, L. Boon, J. L. Ceuppens, and X. Bossuyt. The human antibody response to pneumococcal capsular polysaccharides is dependent on the CD40-CD40 ligand interaction. *European Journal of Immunology*, 34(3):850–858, Mar. 2004.

[48] A. Jeurissen, M. Wuyts, A. Kasran, S. Ramdien-Murli, L. Boon, J. L. Ceuppens, and X. Bossuyt. Essential Role for CD40 Ligand Interactions in T Lymphocyte-Mediated Modulation of the Murine Immune Response to Pneumococcal Capsular Polysaccharides. *The Journal of Immunology*, 168:2773–2781, Feb. 2002.

[49] M. S. Jonczyk, M. Simon, S. Kumar, V. E. Fernandes, N. Sylvius, A.-M. Mallon, P. Denny, and P. W. Andrew. Genetic Factors Regulating Lung Vasculature and Immune Cell Functions Associate with Resistance to Pneumococcal Infection. *PLoS ONE*, 9(3):e89831, Mar. 2014.

[50] A. B. Kantor. The development and repertoire of B-1 cells (CD5 B cells). *Immunology Today*, 12(11):389–391, May 1991.

[51] A. B. Kantor, A. M. Stall, S. Adams, L. A. Herzenberg, and L. A. Herzenberg. Differential development of progenitor activity for three B-cell lineages. *PNAS*, 89:3320–3324, Apr. 1992.

[52] R. Kimura, K. Kamino, M. Yamamoto, A. Nuripa, T. Kida, H. Kazui, R. Hashimoto, T. Tanaka, T. Kudo, H. Yamagata, Y. Tabara, T. Miki, H. Akatsu, K. Kosaka, E. Funakoshi, K. Nishitomi, G. Sakaguchi, A. Kato, H. Hattori, T. Uema, and M. Takeda. The DYRK1A gene, encoded in chromosome 21 Down syndrome critical region, bridges between β-amyloid production and tau phosphorylation in Alzheimer disease. *Human Molecular Genetics*, 16(1):15–23, Nov. 2007.

[53] M. Kopf, F. Brombacher, P. O. Hodgkin, A. J. Ramsay, E. A. Milbourne, W. J. Dai, K. S. Ovington, C. A. Behm, G. Köhler, I. G. Young, and K. I. Matthaei. IL-5-Deficient Mice Have a Developmental Defect in CD5+ B-1 Cells and Lack Eosinophilia but Have Normal Antibody and Cytotoxic T Cell Responses. *Immunity*, 4:15–24, Jan. 1996.

[54] K. Kraljevic, S. Wong, and D. A. Fulcher. Circulating phenotypic B-1 cells are decreased in common variable immunodeficiency and correlate with immunoglobulin M levels. *Clinical and Experimental Immunology*, 171:278–282, Feb. 2012.

[55] T. Kurosaki. Regulation of B-cell signal transduction by adaptor proteins. *Nature Reviews Immunology*, 2(5):354–363, May 2002.

[56] P. I. Lobo, A. Bajwa, K. H. Schlegel, J. Vengal, S. J. Lee, L. Huang, H. Ye, U. Deshmukh, T. Wang, H. Pei, and M. D. Okusa. Natural IgM Anti-Leukocyte Autoantibodies Attenuate Excess Inflammation Mediated by Innate and Adaptive Immune Mechanisms Involving Th-17. *The Journal of Immunology*, 188(4):1675–1685, Feb. 2012.

[57] E. Lopez-Bayghen, I. Cruz-Solis, M. Corona, A. M. Lopez-Colome, and A. Ortega. Glutamate-induced octamer DNA binding and transcriptional control in cultured radial glia cells. *Journal of Neurochemistry*, 98(3):851–859, Aug. 2006.

[58] F. Martin, A. M. Oliver, and J. F. Kearney. Marginal Zone and B1 B Cells Unite in the Early Response against T-Independent Blood-Borne Particulate Antigens. *Immunity*, 14:617–629, May 2001.

[59] J. Mestas and C. C. W. Hughes. Of Mice and Not Men: Differences between Mouse and Human Immunology. *The Journal of Immunology*, 172(5):2731–2738, Feb. 2004.

[60] S. Mithraprabhu, T. Khong, and A. Spencer. Overcoming inherent resistance to histone deacetylase inhibitors in multiple myeloma cells by targeting pathways integral to the actin cytoskeleton. *Cell Death and Disease*, 5(3):e1134–12, Mar. 2014.

[61] J. J. Mond, A. Lees, and C. M. Snapper. T cell-independent antigens type 2. *Annual Reviews of Immunology*, 13:655–692, Aug. 1995.

[62] E. Montecino-Rodriguez, H. Leathers, and K. Dorshkind. Identification of a B-1 cell-specified progenitor. *Nature Immunology*, 7(3):293–301, Jan. 2006.

[63] B.-g. Moon, S. Takaki, K. Miyake, and K. Takatsu. The Role of IL-5 for Mature B-1 Cells in Homeostatic Proliferation, Cell Survival, and Ig Production. *The Journal of Immunology*, 172:6020–6029, Apr. 2004.

[64] M. Murakami, K. Nakajima, K.-i. Yamazaki, T. Muraguchi, T. Serikawa, and T. Honjo. Effects of Breeding Environments on Generation and Activation of Autoreactive B-1 Cells in Anti-red Blood Cell Autoantibody Transgenic Mice. *The Journal of Experimental Medicine*, 185(4):791–794, Feb. 1997.

[65] I. B. P. Ni, N. C. Ching, C. K. Meng, and Z. Zakaria. Translocation t(11;14) (q13;q32) and genomic imbalances in multi-ethnic multiple myeloma patients: a Malaysian study. *Hematology Reports*, 4(e9):60–65, Sept. 2012.

[66] S. Nisitani, T. Tsubata, M. Murakami, and T. Honjo. Administration of interleukin-5 or -10 activates peritoneal B-1 cells and induces autoimmune hemolytic anemia in anti-erythrocyte autoantibody-transgenic mice. *European Journal of Immunology*, 25:3047–3052, Oct. 1995.

[67] T. Nurmi, M. Leinonen, V.-M. Häivä, A. Tiilikainen, and K. Kouvalainen. Antibody response to pneumococcal vaccine in patients with trisomy-21 (Down's syndrome). *Clinical and Experimental Immunology*, 48:485–490, June 1982.

[68] A. O'Doherty, S. Ruf, C. Mulligan, V. Hildreth, M. L. Errington, S. Cooke, A. Sesay, S. Modino, L. Vanes, D. Hernandez, J. M. Linehan, P. T. Sharpe, S. Brandner, T. V. P. Bliss, D. J. Henderson, D. Nizetic, V. L. J. Tybulewicz, and E. M. C. Fisher. An Aneuploid Mouse StrainCarrying Human Chromosome 21with Down Syndrome Phenotypes. *Science*, 309:2033–2037, Mar. 2005.

[69] A. O'Garra, R. Chang, N. Go, R. Hastings, G. Haughton, and M. Howard. Ly-1 B (B-1) cells are the main source of B cell-derived interleukin 10. *European Journal of Immunology*, 22:711–717, Nov. 1992.

[70] S. A. Oracki, J. A. Walker, M. L. Hibbs, L. M. Corcoran, and D. M. Tarlinton. Plasma cell development and survival. *Immunological Reviews*, 237:140–159, Aug. 2010.

[71] E. J. Peterson, J. L. Clements, N. Fang, and G. A. Koretzky. Adaptor proteins in lymphocyte antigen-receptor signaling. *Current Opinion in Immunology*, 10:337–344, Jan. 1998.

[72] P. Pfisterer, J. Hess, and T. Wirth. Identification of Target Genes of the Lymphoid-Specific Transcription Factor Oct2. *Immunobiology*, 198(1-3):217–226, Dec. 1997.

[73] A. J. Pollard, K. P. Perrett, and P. C. Beverley. Maintaining protection against invasive bacteria with protein– polysaccharide conjugate vaccines. *Nature Reviews Immunology*, 9:213–220, Feb. 2009.

[74] H.-H. S. K. Potula, Z. Xu, L. Zeumer, A. Sang, B. P. Croker, and L. Morel. Cyclin-Dependent Kinase Inhibitor Cdkn2c Deficiency Promotes B1a Cell Expansion and Autoimmunity in a Mouse Model of Lupus. *The Journal of Immunology*, 189:2931–2940, Aug. 2012.

[75] B. Reis, K. Pfeffer, and S. Beer-Hammer. The orphan adaptor protein SLY1 as a novel anti-apoptotic protein required for thymocyte development. *BMC Immunology*, 10(38):1471–2172, July 2009.

[76] Robert-Koch-Institut. Epidemiologisches Bulletin. Technical Report 34, Aug. 2013.

[77] J. A. Ross, L. G. Spector, L. L. Robison, and A. F. Olshan. Epidemiology of leukemia in children with Down syndrome. *Pediatr. Blood Cancer*, 44(1):8–12, 2004.

[78] M. S. Salerno, G. T. F. Schwenger, C. J. Sanderson, and V. A. Mordvinov. Binding of Octamer Factors to the Murine IL-5 CLE0 in Primary T-Cells and a T-Cell Line. *Cytokine*, 15(1):4–9, July 2001.

[79] T. Scheikl, B. Reis, K. Pfeffer, B. Holzmann, and S. Beer. Reduced notch activity is associated with an impaired marginal zone B cell development and function in *Sly1* mutant mice. *Molecular Immunology*, 46:969–977, Feb. 2009.

[80] O. Sharif, U. Matt, S. Saluzzo, K. Lakovits, I. Haslinger, T. Furtner, B. Doninger, and S. Knapp. The Scavenger Receptor CD36 Downmodulates the Early Inflammatory

Response while Enhancing Bacterial Phagocytosis during Pneumococcal Pneumonia. *The Journal of Immunology*, 190:5640–5648, Apr. 2013.

[81] A. S. Shaw and E. L. Filbert. Scaffold proteins and immune-cell signalling. *Nature Reviews Immunology*, 9(1):47–56, Jan. 2009.

[82] F. J. Sheedy, A. Grebe, K. J. Rayner, P. Kalantari, B. Ramkhelawon, S. B. Carpenter, C. E. Becker, H. N. Ediriweera, A. E. Mullik, D. T. Golenbock, L. M. Stuart, E. Latz, K. A. Fitzgerald, and K. J. Moore. CD36 coordinates NLRP3 inflammasome activation by facilitating intracellular nucleation of soluble ligands into particulate ligands in sterile inflammation. *Nature Immunology*, 14(8):812–822, July 2013.

[83] T. A. Shtam, R. A. Kovalev, E. Y. Vafolomeeva, E. M. Makarov, Y. V. Kil, and M. V. Filatov. Exosomes are natural carriers of exogenous siRNA to human cells *in vitro*. *Cell Communication and Signaling*, 11(88):1–10, Dec. 2013.

[84] K. Siepmann, G. Wohlleben, and D. Gray. CD40-mediated regulation of interleukin-4 signaling pathways in B lymphocytes. *European Journal of Immunology*, 26:1544–1552, May 1996.

[85] J. Slack, G. P. Der-Balian, M. H. Nahm, and J. M. Davie. Subclass Restriction of Murine Antibodies II. The IgG Plaque-forming Cell Response to Thymus-independent Type 1 and Type 2 Antigens in Normal Mice and Mice Expressing an X-linked Immunodeficiency. *The Journal of Experimental Medicine*, 151:853–862, May 1980.

[86] N. Solvason, W. Wei Wu, D. Parry, D. Mahony, E. W.-F. Lam, J. Glassford, G. G. B. Klaus, P. Sicinski, R. Weinberg, Y. Jun Liu, M. Howard, and E. Lees. Cyclin D2 is essential for BCR-mediated proliferation and CD5 B cell development. *International Immunology*, 12(5):631–638, Apr. 2000.

[87] A. S. Stoykova, S. Sterrer, J. R. Erselius, A. K. Hatzopoulos, and P. Gruss. Mini-Oct and Oct-2c: Two Novel, Functionally Diverse Murine *Oct-2* Gene Products Are Differentially Expressed in the CNS. *Neuron*, 8:541–558, Sept. 1992.

[88] M. Tanaka and W. Herr. Differential Transcriptional Activation by Oct-1 and Oct-2: Interdependent Activation Domains Induce Oct-2 Phosphorylation. *Cell*, 60:375–386, Feb. 1990.

[89] E. Theodorou, G. Dalembert, C. Heffelfinger, E. White, S. Weissman, L. Corcoran, and M. Snyder. A high throughput embryonic stem cell screen identifies Oct-2 as a bifunctional regulator of neuronal differentiation. *Genes & Development*, 23(5):575–588, Mar. 2009.

[90] A. Tominaga, S. Takaki, N. Koyama, S. Katoh, R. Matsumoto, M. Migita, Y. Hitoshi, J.-I. Miyazaki, G. Usuku, K.-I. Yamamura, and K. Takatsu. Transgenic Mice Expressing a B Cell Growth and Differentiation Factor Gene (Interleukin 5) Develop Eosinophilia and

Autoantibody Production. *The Journal of Experimental Medicine*, 173:429–437, Feb. 1991.

[91] T. Uchida, A. Nakao, N. Nakano, A. Kuramasu, H. Saito, K. Okumura, and H. Ogawa. Identification of Nash1, a Novel Protein Containing a Nuclear Localization Signal, a Sterile α Motif, and an SH3 Domain Preferentially Expressed in Mast Cells. *Biochemical and Biophysical Research Communications*, 288(1):137–141, Oct. 2001.

[92] B. Verbinnen, K. Covens, L. Moens, I. Meyts, and X. Bossuyt. Human CD20+CD43+CD27+CD5- B cells generate antibodies to capsular polysaccharides of Streptococcus pneumoniae. *Journal of Allergy and Clinical Immunology*, 130(1):272–275, July 2012.

[93] R. H. J. Verstegen, M. A. A. Kusters, E. F. A. Gemen, and E. de Vries. Down Syndrome B-Lymphocyte Subpopulations, Intrinsic Defect or Decreased T-Lymphocyte Help. *Pediatric Research*, 67(5):563–569, Apr. 2010.

[94] M. von Holleben. *Functional characterisation of SLy2 as a novel regulator of the actin cytoskeleton*. PhD thesis, Albert-Magnus University, Cologne, Dec. 2008.

[95] M. von Holleben, A. Gohla, K.-P. Janssen, B. M. Iritani, and S. Beer-Hammer. The Immunoinhibitory Adapter Protein Src Homology Domain 3 Lymphocyte Protein 2 (SLy2) Regulates Actin Dynamics and B Cell Spreading. *The Journal of Biological Chemistry*, 286(15):13489–13501, Apr. 2011.

[96] J. Wahlgren, T. D. L. Karlson, M. Brisslert, F. Vaziri Sani, E. Telemo, P. Sunnerhagen, and H. Valadi. Plasma exosomes can deliver exogenous short interfering RNA to monocytes and lymphocytes. *Nucleic Acids Research*, 40(17):e130–e130, Sept. 2012.

[97] D. Wang, A. K. Stewart, L. Zhuang, Y. Zhu, Y. Wang, C. Shi, A. Keating, A. Slutsky, H. Zhang, and X.-Y. Wen. Enhanced adaptive immunity in mice lacking the immunoinhibitory adaptor Hacs1. *The FASEB Journal*, 24:1–10, Feb. 2010.

[98] J. D. Weber, P. C. Isakson, and J. M. Purkerson. IL-5 Receptor Expression and Ig Secretion from Murine B Lymphocytes Requires Coordinated Signaling by Membrane Ig, IL-4, and IL-5. *The Journal of Immunology*, 157:4428–4435, Feb. 1996.

[99] T. Wirth, P. Pfisterer, A. Annweiler, S. Zwilling, and H. König. Molecular Principles of Oct2-Mediated Gene Activation in B Cells. *Immunobiology*, 193(2-4):161–170, July 1995.

[100] K. Wu, X. Zhang, J. Shi, N. Li, D. Li, M. Luo, J. Cao, N. Yin, H. Wang, W. Xu, Y. He, and Y. Yin. Immunization with a Combination of Three Pneumococcal Proteins Confers Additive and Broad Protection against *Streptococcus pneumoniae* Infections in Mice. *Infection and Immunity*, 78(3):1276–1283, Mar. 2010.

[101] Y. Yang, J. W. Tung, E. E. B. Ghosn, L. A. Herzenberg, and L. A. Herzenberg. Division and differentiation of natural antibody- producing cells in mouse spleen. *PNAS*, 104(11):4542–4546, Mar. 2007.

[102] T. Yoshida, K. Ikuta, H. Sugaya, K. Maki, M. Takagi, H. Kanazawa, S. Sunaga, T. Kinashi, K. Yoshimura, J.-I. Miyazaki, S. Takaki, and K. Takatsu. Defective B-1 Cell Development and Impaired Immunity against Angiostrongylus cantonensis in IL-5Ra-Deficient Mice. *Immunity*, 4:483–494, May 1996.

[103] C. Zeller, B. Hinzmann, S. Seitz, H. Prokoph, E. Burkhard-Goettges, J. Fischer, B. Jandrig, L.-E. Schwarz, A. Rosenthal, and S. Scherneck. SASH1: a candidate tumor suppressor gene on chromosome 6q24.3 is downregulated in breast cancer. *Oncogene*, 22(19):2972–2983, May 2003.

[104] Y. X. Zhu, S. Benn, Z. H. Li, E. Wei, E. Masih-Khan, Y. Trieu, M. Bali, C. J. McGlade, J. O. Claudio, and A. K. Steward. The SH3-SAM Adaptor HACS1 is Up-regulated in B Cell Activation Signaling Cascades. *Journal of Experimental Medicine*, 200(6):737–747, Sept. 2004.

DANKE

Hiermit möchte ich mich ganz herzlich bei allen bedanken, die zum erfolgreichen Abschluss dieser Arbeit einen wesentlichen Beitrag geleistet haben.

An erster Stelle geht mein ganz besonderer Dank an PD Dr. Sandra Beer-Hammer. Die kontinuierliche Betreuung und Beratung und die vertrauensvolle Zusammenarbeit haben ein sehr eigenständiges wissenschaftliches Arbeiten und zielstrebiges Vorankommen ermöglicht.

Ebenfalls möchte ich mich bei Prof. Dr. Dr. Bernd Nürnberg bedanken, dass ich diese Arbeit am Institut für Pharmakologie und Toxikologie, des Uniklinikums Tübingen anfertigen durfte.

Bei Prof. Dr. Hans-Georg Rammensee bedanke ich mich für seine Beratung und bereitwillige Unterstützung als zweiter Berichterstatter.

Weiterhin bedanke ich mich bei Prof. Dr. Hanspeter A. Mallot für die Gutachtertätigkeit von Seiten der Mathematisch-Naturwissenschaftlichen Fakultät, sowie für seine Unterstützung bei der Annahme als Doktorandin im Fachbereich Biologie.

Prof. Dr. Dominik Hartl, sowie Dr. Andreas Hector möchte ich ganz herzlich danken für die Organisation der humanen Down Syndrom Blutproben und ihre Unterstützung bei der Anfertigung der Publikation.

Ein ganz herzliches Dankeschön geht an alle Mitarbeiter des Instituts für Pharmakologie und Toxikologie für die Hilfsbereitschaft und freundliche Zusammenarbeit.
Ganz besonders bedanke ich mich bei Dr. Kirsten Bucher und Daniel Schäll für die sehr hilfreichen Diskussionen und tatkräftige Unterstützung bei den Experimenten, Claudia Müller für ihre ausgezeichnete technische Assistenz, sowie den wissenschaftlichen Hilfskräften des Instituts für die Unterstützung bei der Genotypisierung.
Klaudia Buljovcic danke ich für die Durchführung der RT-PCR Analysen zur Quantifizierung von *SLy2* in TG Mäusen.

Zu guter Letzt, DANKE an meine liebe Familie für die wohltuende seelische Pflege.

DECLARATION

Ich erkläre hiermit, dass ich die zur Promotion eingereichte Arbeit mit dem Titel: ”The immuno-inhibitory adaptor protein SLy2 - A potential therapeutic target for pneumococcal infections” selbständig verfasst, nur die angegebenen Quellen und Hilfsmittel benutzt und wörtlich oder inhaltlich übernommene Zitate als solche gekennzeichnet habe. Ich erkläre, dass die Richtlinien zur Sicherung guter wissenschatflicher Praxis der Universität Tübingen beachtet wurden. Ich versichere an Eides statt, dass diese Angaben wahr sind und dass ich nichts verschwiegen habe. Mir ist bekannt, dass die falsche Angabe einer Versicherung an Eides statt mit Freiheitsstrafe bis zu drei Jahren oder mit Geldstrafe bestraft wird.

Tübingen, 13.08.2014

Fee Schmitt

PUBLICATIONS

Journal articles

Schmitt, F., Schäll, D., Bucher, K., Schindler, T., Hector, A., Biedermann, T., Zemlin, M., Hartl, D., and Beer-Hammer, S. (2014) SLy2 controls the antibody response to pneumococcal vaccine through an IL-5Rα-dependent mechanism in B-1 cells. *European Journal of Immunology* DOI: 10.1002/eji.201444882

Schmitt, F., Nguyen, P.-H., Gupta N., and Mayer, D. (2013) Eph receptor B4 is a regulator of estrogen receptor alpha in breast cancer cells. *Journal of Receptors and Signal Transduction* 33, 244-248.

Gupta, N., **Schmitt, F.**, Grebhardt, S., and Mayer, D. (2010) β-Catenin is a positive regulator of estrogen receptor-α function in breast cancer cells. *Cancers* 2, 1-13.

Abstracts

Schmitt, F., Schäll, D., Bucher, K., Hector, A., Hartl, D., and Beer-Hammer, S. (2014) The adaptor protein SLy2 inhibits humoral immune responses to pneumococcal vaccine - 44th Annual Meeting of the German Society of Immunology, Bonn. Oral presentation.

Schmitt, F., Schäll, D., Bucher, K., and Beer-Hammer, S. (2013) The adaptor protein SLy2 modulates B-1 cell functionality - 43th Annual Meeting of the German Society of Immunology, Mainz. Poster presentation.

Schmitt, F., Bucher, K., Beer-Hammer, S. (2012) The role of SLy2 *in vivo* - Regulators of the Humoral Immune Response, Erlangen. Poster presentation.

Schmitt, F., Bucher, K., and Beer-Hammer, S. (2012) The role of SLy2 *in vivo* - Forschungskolloquium, Tübingen. Poster presentation.

Schmitt, F. (2011) The nucleo-cytoplasmic adaptor protein SLy2 *in vivo* - 3rd Autumn School, Current Concepts in Immunology, Bad Schandau. Oral presentation.

Schmitt, F., Brandt, S., von Holleben, M., and Beer-Hammer, S. (2011) The nucleo-cytoplasmic adaptor protein SLy2 - STS Meeting, Weimar. Poster presentation.

Schmitt, F., Brandt, S., von Holleben, M., and Beer-Hammer, S. (2011) The Immunoinhibitory Adaptor Protein SLy2 - SIICA and DGfI, Joint Annual Meeting, Riccione, Italy. Poster presentation.